



TECHNICAL UNIVERSITY
OF CRETE

SCHOOL OF MINERAL
RESOURCES

DIPLOMA THESIS

Well Placement Optimization in a given
Reservoir and Production Data History
Matching

Author:

Ioannis
KARYTINOS

Supervisor:

Dr. Christos
CHANTZICHRISTOS

January 15, 2018

In memoriam of my friend Andreas

Acknowledgements

I want to thank *NCSR Demokritos* for providing an excellent working environment, *INRASTES* personnel for their assistance and eagerness for supporting either in academic or personal aspect. I deeply thank *Juicy Grill* burger house for the support provided (both literal and emotional) throughout the time that the current diploma thesis was carried out.

Abstract

The current diploma thesis project focuses in utilizing the *ECLIPSE* reservoir simulation software to optimize the well placement processes in a given reservoir and the history matching processes of the simulation model data with the history data that accompany the simulation model. The optimization processes mentioned above will be conducted on the simulation model built for a block that is part of *Gullfaks* reservoir in the North Sea, Norway.

PlanOpt and *SimOpt* are modules of *ECLIPSE* reservoir simulation software, *PlanOpt* is used to optimize the well placement processes and *SimOpt* is used to optimize the history matching processes of the simulation model data with the history data that accompany the simulation model.

As far as well placement optimization is concerned, the already existing production wells of the simulation model will be discarded and by utilizing the well placement optimization software, *PlanOpt*, a less or equal number of production wells will be placed on the simulation model and will be scheduled to operate for the same simulation period that the initial simulation model is operating, aiming finally to achieve equal or higher cumulative oil production than the initial simulation model at the end of the simulation period.

SimOpt will be used to reduce the mismatch between the production data of the simulation model and the real production data that were reported during the operation of the wells on the field. Several reservoir parameters will be set to vary within a range and at the end of the optimization processes *SimOpt* will calculate the values of the parameters chosen which produce the least possible mismatch between the real production data and the data resulted from the simulation model. Since there are different types production data that are going to be matched, a study will be conducted of whether the type of production data which are going to be matched in each different simulation run of *SimOpt*, affect the resulted matching at the end of each optimization run.

Contents

Acknowledgements	5
Abstract	7
1 Reservoir Simulation Software	13
1.1 Formulation of the Equations of <i>ECLIPSE 100</i> Reservoir Simulator	13
1.1.1 Description of Equations	13
1.1.2 Variable Set	14
1.1.3 Flow	16
1.1.4 Reservoir Densities	17
1.1.5 Newton Iterations of the Non-Linear Residual	18
1.2 Solution of the System of Linear Equations	19
1.2.1 Nested Factorization Preconditioning	19
1.2.2 Initialization for Nested Factorization Preconditioning	22
1.2.3 Solution Procedure for Nested Factorization	22
1.2.4 Orthomin	22
1.2.5 Convergence Criteria	23
1.2.6 Treatment of Wells	23
1.3 <i>PlanOpt</i>	25
1.3.1 Phase 1	25
1.3.2 Phase 2 (Static Screening)	25
1.3.3 Optimization	25
1.4 <i>SimOpt</i>	27
1.4.1 Observed Data, Prior Information and Objective Function	27
1.4.2 Gradients and <i>RMS</i>	30
1.4.3 Prior Regression Operations	31

1.4.4	Regression Mode	33
2	Initial Model Production Data and Details	35
2.1	Reservoir	35
2.2	Geometry	35
2.3	Well Topology	36
2.4	Field Data	38
2.5	Well Production/Injection Data	40
2.6	Well Observed Production Data	45
3	Well Placement Optimization aided by PlanOpt	49
3.1	Model Setup Prior to Optimization Process	49
3.1.1	Pre-existing Production Wells	49
3.1.2	Injection/Production Wells Management	49
3.2	Optimization Setup Processes	51
3.2.1	Exclusion Zones	51
3.2.2	Phase-1	52
3.2.3	Phase-2	53
3.2.4	Limits-Constraints	54
3.2.5	Target Number of Wells - Well Reduction	57
3.2.6	Optimization	57
3.3	Oil Production Maximization	58
3.4	Optimal Simulation Model Analysis	65
3.4.1	Field Data	66
3.4.2	Well Production Data	69
4	Production Data History Matching aided by SimOpt	73
4.1	Observed Production Data	73
4.2	Parameters	74
4.3	Optimization	76
4.3.1	Evaluation Run	76
4.3.2	Gradient Run	77
4.3.3	Regression Run	78
4.4	History Matching Optimization	79

5 Conclusion	91
5.1 Well Placement Optimization	91
5.2 History Matching Optimization	92
Appendix A Well Position on Initial Simulation Model	95
Appendix B Optimal Simulation Model Well Reduction	99
Appendix C Well Position on Optimal Simulation Model	111
Bibliography	113

Chapter 1

Reservoir Simulation Software

The current diploma thesis utilizes *Schlumberger ECLIPSE Reservoir Simulation Software* 2010.1 version [1]. The software features which were used are:

- *ECLIPSE 100*, a black-oil reservoir simulator
- *FloViz*, a 3D visualization tool used to display reservoir simulation model data
- *PlanOpt*, a well placement tool assisting in choosing the locations of vertical production wells [2]
- *SimOpt*, an interactive computer program assisting in history matching between *ECLIPSE* simulation model and the corresponding observed data [3]

The equations incorporated by the reservoir simulation software will be described in the sections below.

1.1 Formulation of the Equations of *ECLIPSE 100* Reservoir Simulator

As mentioned above, *ECLIPSE 100* is a black-oil reservoir simulator that recognizes three phases, can model reservoirs in three dimensions, incorporates equations in fully-implicit approach allowing the option of having large time steps during the simulation period [4].

1.1.1 Description of Equations

R_{fl} is the non-linear residual for each fluid component in each cell at each time step.

$$R_{fl} = \frac{dM}{dt} + F + Q \quad (1.1)$$

where

dM : is the mass -per unit surface density- accumulated during the current time step dt

F : is the net flow rate into neighboring grid blocks

Q : is the net flow rate into wells during the time step

The non-linear residual, R_{fl} , is defined for each grid block and each fluid in the study. In the black-oil model case the fluids are oil, water and gas.

1.1.2 Variable Set

A set of solution variables is required in order to solve the residual equation. Furthermore, to utilize Newton's Method it is required that the number of independent variables should be equal to the number of residual conditions.

For a three phase black-oil study (oil, water, gas), the primary solution variables X are pressure P and two saturation variables. Water saturation S_w and either S_g , R_s or R_v are chosen to complete the set of primary solution variable set. The residual R and the solution X are three component vectors in each cell.

$$R = \begin{bmatrix} R_o \\ R_w \\ R_g \end{bmatrix}, \quad X = \begin{bmatrix} P_o \\ S_w \\ S_g \text{ or } R_s \text{ or } R_v \end{bmatrix} \quad (1.2)$$

Jacobian $J = \frac{dR}{dX}$ has the form shown below:

$$J = \frac{dR_i}{dX_j} = \begin{bmatrix} \frac{dR_o}{dP_o} & \frac{dR_o}{dS_w} & \frac{dR_o}{dS_g} \\ \frac{dR_w}{dP_o} & \frac{dR_w}{dS_w} & \frac{dR_w}{dS_g} \\ \frac{dR_g}{dP_o} & \frac{dR_g}{dS_w} & \frac{dR_g}{dS_g} \end{bmatrix} \quad (1.3)$$

The mass change during each time step dt is then proportional to the quantity $dM = dM_{t+\delta t}^{-2.5} - dM_t$, with:

$$M = PV \begin{bmatrix} \frac{S_o}{B_o} + \frac{R_v S_g}{B_g} \\ \frac{S_w}{B_w} \\ \frac{S_g}{B_g} + \frac{R_s S_o}{B_o} \end{bmatrix} \quad (1.4)$$

where

PV : is the pore volume

$B_{o,w,g}$: are the oil, water, gas formation volume factors

R_s : is the solution gas/oil ratio

R_v : is the vapor oil/gas ratio

Based on the type of the reservoir (gas or oil) there are two options for the solution variables. While the reservoir oil remains under-saturated ($S_g = 0$), then solution variable becomes R_s and while the reservoir gas remains under-saturated ($S_o = 0$), then solution variable becomes R_v . As a result Jacobian is also

adjusted in accordance with the change of variable. Finally, no approximation is being carried out while calculating Jacobian in order to ensure the quadratic convergence of the Newton's Method.

The hydrocarbon states are:

- *State 1*: Gas only ($R_s = 0, S_g = 1 - S_w$),
Variables: P_o, S_w, R_v
- *State 2*: Gas and oil ($R_v = R_{v,sat}, R_s = R_{s,sat}$),
Variables: P_o, S_w, S_g
- *State 3*: Oil only ($R_v = 0, S_g = 0$),
Variables: P_o, S_w, R_s

ECLIPSE 100 treats a cell that is almost full of water as being in *state 2*. Therefore the solution variable is by default ($R_s = R_{s,sat}$). However, if a transition occurs in the cell to *state 3* (influx of under-saturated oil) then the R_s value is limited not to exceed the average GOR of inflow from neighboring cells as this will be a better estimate than $R_{s,sat}$.

In order to solve the non-linear residual equations $R(X) = 0$, Newton's method is being used. It might require several iterations until the residuals are reduced to a *sufficient small* value. In *ECLIPSE 100* there are two measures which are used in order to define the above mentioned *sufficient small* value : material balance error and maximum saturation normalized residual.

Material Balance Error

When residuals are summed over all grid cells in the reservoir, the flow term is canceled since the flow out of one grid cell is always equal and opposite in sign to the corresponding flow into its neighboring grid cells. As a result, the sum of the residuals for each phase corresponds to the net mass accumulation within the reservoir less the net influx through the wells. This is the material balance error and its equations are presented below for a three phase system:

$$\begin{aligned} \sum_i (R_o)_i &= \sum_i \left(\frac{dM_o}{dt} \right)_i + \sum_i (Q_o)_i \\ \sum_i (R_w)_i &= \sum_i \left(\frac{dM_w}{dt} \right)_i + \sum_i (Q_w)_i \\ \sum_i (R_g)_i &= \sum_i \left(\frac{dM_g}{dt} \right)_i + \sum_i (Q_g)_i \end{aligned} \tag{1.5}$$

where

\sum_i : is the sum over all reservoir grid blocks

$(R_{o,w,g})_i$: are the oil, water, gas residuals in grid block i

In *ECLIPSE 100* the material balance errors are converted to meaningful, problem independent numbers by scaling to equivalent field saturation values as shown in the equation below:

$$\begin{aligned}
 MB_o &= \bar{B}_o dt \left\{ \left[\sum_i (R_o)_i \right] / \left[\sum_i (PV)_i \right] \right\} \\
 MB_w &= \bar{B}_w dt \left\{ \left[\sum_i (R_w)_i \right] / \left[\sum_i (PV)_i \right] \right\} \\
 MB_g &= \bar{B}_g dt \left\{ \left[\sum_i (R_g)_i \right] / \left[\sum_i (PV)_i \right] \right\}
 \end{aligned} \tag{1.6}$$

where

$\bar{B}_{o,w,g}$: are the average oil, water, gas formation volume factors

$MB_{o,w,g}$ are computed for each Newton iteration and the material balance errors are considered to be *sufficiently small* if they are less than 10^{-7} .

Maximum Saturation Normalized Residual

Apart from the material balance error that should be small as stated in the section above, another test is required in order to have a sufficiently rigorous test of convergence. The second test is obtained by computing the maximum saturation normalized residuals as shown below:

$$\begin{aligned}
 CNV_o &= \bar{B}_o dt MAX_i \left| \frac{(R_o)_i}{(PV)_i} \right| \\
 CNV_w &= \bar{B}_w dt MAX_i \left| \frac{(R_w)_i}{(PV)_i} \right| \\
 CNV_g &= \bar{B}_g dt MAX_i \left| \frac{(R_g)_i}{(PV)_i} \right|
 \end{aligned} \tag{1.7}$$

where

MAX_i : is the maximum value over all grid blocks of the reservoir

By converting each convergence error to an equivalent saturation value, CNV numbers (which are considered to have converged when their values are less than 0.001) are being attached with sensible limits.

1.1.3 Flow

The flowrate into cell i from a neighboring cell n , F_{ni} is:

$$F_{ni} = T_{ni} \begin{bmatrix} \frac{k_{ro}}{B_o \mu_o} & 0 & \frac{R_v k_{rg}}{B_g \mu_g} \\ 0 & \frac{k_{rw}}{B_w \mu_w} & 0 \\ \frac{R_s k_{ro}}{B_o \mu_o} & 0 & \frac{k_{rg}}{B_g \mu_g} \end{bmatrix}_u \times \begin{bmatrix} dP_{oni} \\ dP_{uni} \\ dP_{gni} \end{bmatrix} \tag{1.8}$$

where

$$dP_{oni} = P_{on} - P_{oi} - \rho_{oni}G(D_n - D_i)$$

$$\begin{aligned} dP_{wni} &= P_{wn} - P_{wi} - \rho_{wni}G(D_n - D_i) \\ &= P_{on} - P_{oi} - \rho_{wni}G(D_n - D_i) - P_{cown} + P_{cowi} \end{aligned}$$

$$\begin{aligned} dP_{gni} &= P_{gn} - P_{gi} - \rho_{gni}G(D_n - D_i) \\ &= P_{on} - P_{oi} - \rho_{gni}G(D_n - D_i) + P_{cogn} - P_{cogi} \end{aligned}$$

T_{ni} : is the transmissibility between cell n and i

k_r : is the relative permeability of each phase

μ : is the viscosity of each phase

dP : is the potential difference of each phase

ρ : is the fluid density

G : is the gravity acceleration

D : is the cell center depth

The subscript u denotes that each fluid mobility is to be evaluated in the upstream cell (cell n if dP_{ni} is positive). The upstream calculation applies separately for each equation (oil, water, gas) so that e.g. oil may flow from cell i to cell n while water from cell n to cell i .

The net flowrate from cell i into neighboring cells is:

$$F_i = \sum_n F_{ni} \quad (1.9)$$

The rate of flow into a production well from cell i is:

$$Q_i = -T_{wi} (P_{oi} - H_{iw} - P_{bh}) \begin{bmatrix} \frac{k_{ro}}{B_o \mu_o} + \frac{R_v k_{rg}}{B_g \mu_g} \\ \frac{k_{rw}}{B_w \mu_w} \\ \frac{k_{rg}}{B_g \mu_g} + \frac{R_s k_{ro}}{B_o \mu_o} \end{bmatrix}_i \quad (1.10)$$

where

T_{wi} : is the well connection transmissibility factor

H : is the hydrostatic head correction

P_{bh} : is the bottom hole pressure

1.1.4 Reservoir Densities

In the black oil case, reservoir densities (ρ) of oil and gas are computed from surface densities (ρ_s) using:

$$\begin{aligned}\varrho_o &= (\varrho_{so} + C R_s \varrho_{sg}) / B_o \\ \varrho_g &= (C \varrho_{sg} + R_v \varrho_{so}) / B_g\end{aligned}\tag{1.11}$$

with $C = 1$ for metric and lab units and $C = 178.1076$ for field units.

The reservoir density at the interface between cells n and i is computed as the average of the reservoir densities in cells i and n :

$$\begin{aligned}\varrho_{oni} &= (\varrho_{on} + \varrho_{oi}) / 2 \\ \varrho_{gni} &= (\varrho_{gn} + \varrho_{gi}) / 2\end{aligned}\tag{1.12}$$

1.1.5 Newton Iterations of the Non-Linear Residual

Given the non-linear residual $R = R_{fl}$ and the solution variables X , the equation that is needed to be solved is $R_{fl}(X) = 0$. In each iteration of the non-linear equations the sequence of operations is:

1. Given the solution X , $R(X)$ is obtained, then a correction Δx have to be found such that $R(X + \Delta x) - R(X) + J\Delta x = 0$, where J is the Jacobian $\frac{d}{dX}R(X)$
2. For Δx to be calculated, the linear equation $J\Delta x = R(X) \iff \Delta x = J^{-1}R(X)$ needs to be solved
3. Update the solution vector, $X \rightarrow X + \Delta x$. If some measure of convergence has been achieved then the equation is considered solved, else proceed to the next iteration until convergence is achieved

In the fully implicit case the equations above may be solved for X , using the linear solver to give:

$$\Delta x = J^{-1}R'_{fl}\tag{1.13}$$

The diagonal and band terms of J^{-1} for a three phase oil, water, gas system are presented below:

$$J'_D = \begin{array}{c} \\ \\ \\ \end{array} \begin{array}{ccc} P & S_w & X_3 \\ \left[\begin{array}{ccc} x & x & 0 \\ x & 0 & x \\ x & 0 & x \end{array} \right] \\ \end{array}, \quad J'_B = \begin{array}{c} \\ \\ \\ \end{array} \begin{array}{ccc} P & S_w & X_3 \\ \left[\begin{array}{ccc} x & 0 & 0 \\ x & 0 & 0 \\ x & 0 & 0 \end{array} \right] \\ \end{array}\tag{1.14}$$

1.2 Solution of the System of Linear Equations

By utilizing Newton's method the complex non-linear residual equations can be solved with an iterative way which only needs the solution of systems of linear equations [5]. The linear equations are also solved iteratively using *Orthomin* [6]. *Orthomin* is a linear solver preconditioned by nested factorization. At each iteration *Orthomin* minimizes the sum of the squares of the residuals by orthogonalizing each new search direction to the existing search directions. To carry out these orthogonalizations, each search direction must be stored. Usually, only the last few search directions are restricted. The number of stored search directions should be less or equal to the total number of linear iterations. Each search direction consists of pressures, saturations and residuals for each cell in an *ECLIPSE 100* black-oil run which means that 6 double-precision numbers will be stored per cell for a three phase black oil run.

Material Balance

At each Newton iteration the equation $Ax = b$ needs to be solved, where A is the Jacobian matrix $\left(\frac{dR}{dX}\right)$ and b is the non-linear residual of the prior Newton iteration:

$$b = R = \frac{dM}{dt} + F + Q \quad (1.15)$$

If the elements of b are summed over all cells in the reservoir then the flow terms, F , will cancel and the sum corresponds to the rate of mass accumulation in the reservoir. *ECLIPSE 100* computes an initial approximate solution, y , by solving an approximate equation, $By = b$. The material balance error (the error in the mass accumulation rate) corresponding to y is obtained by summing the elements of the residual r :

$$r = b - Ay = (B - A)y, \quad \text{sum} = \sum_{i=1}^{n \text{ cells}} r_i \quad (1.16)$$

This sum is zero if B is chosen such that $\text{colsum}(B) = \text{colsum}(A)$, where $\text{colsum}(A)$ is the diagonal matrix formed by summing A in columns.

The above *colsum* constraint is obeyed independently for each component by *ECLIPSE 100*. The *colsum* constraint is appropriate to obtain fast convergence for fully implicit black-oil cases because of the material balance constraint.

1.2.1 Nested Factorization Preconditioning

A simple $3 \times 2 \times 3$ grid is used as an example as shown on the figure presented below:

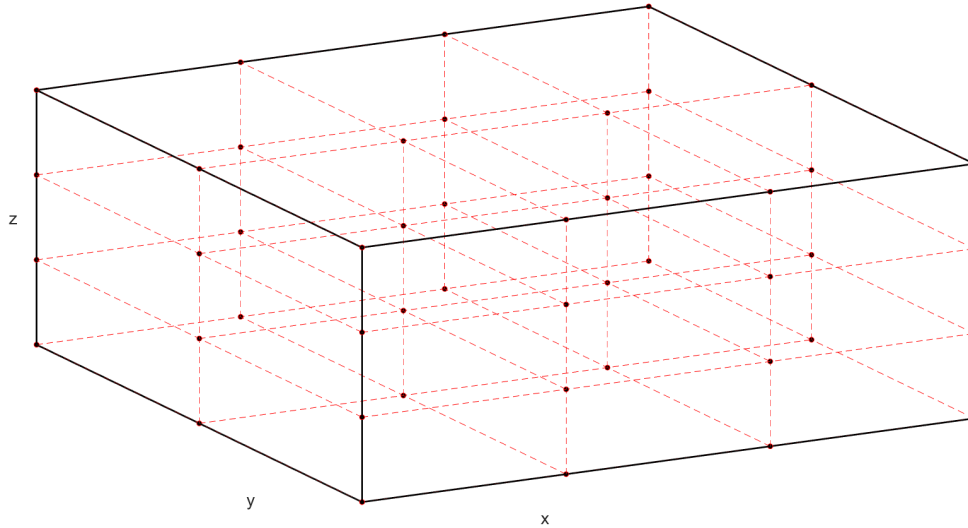


Figure 1.1: Mesh box of a $3 \times 2 \times 3$ grid

where

$N_i = 3$: is the number of grid blocks in the x direction

$N_j = 2$: is the number of grid blocks in the y direction

$N_k = 3$: is the number of grid blocks in the z direction

The structure of the Jacobian matrix for the $3 \times 2 \times 3$ problem above is shown below:

$$A = \begin{bmatrix}
 D & U1 & 0 & U2 & 0 & 0 & U3 & 0 & 0 & 0 & 0 & 0 & 0 & 0 & 0 & 0 & 0 \\
 L1 & D & U1 & 0 & U2 & 0 & 0 & U3 & 0 & 0 & 0 & 0 & 0 & 0 & 0 & 0 & 0 \\
 0 & L1 & D & 0 & 0 & U2 & 0 & 0 & U3 & 0 & 0 & 0 & 0 & 0 & 0 & 0 & 0 \\
 L2 & 0 & 0 & D & U1 & 0 & 0 & 0 & 0 & U3 & 0 & 0 & 0 & 0 & 0 & 0 & 0 \\
 0 & L2 & 0 & L1 & D & U1 & 0 & 0 & 0 & 0 & U3 & 0 & 0 & 0 & 0 & 0 & 0 \\
 0 & 0 & L2 & 0 & L1 & D & 0 & 0 & 0 & 0 & 0 & U3 & 0 & 0 & 0 & 0 & 0 \\
 L3 & 0 & 0 & 0 & 0 & 0 & D & U1 & 0 & U2 & 0 & 0 & U3 & 0 & 0 & 0 & 0 \\
 0 & L3 & 0 & 0 & 0 & 0 & L1 & D & U1 & 0 & U2 & 0 & 0 & U3 & 0 & 0 & 0 \\
 0 & 0 & L3 & 0 & 0 & 0 & 0 & L1 & D & U1 & 0 & U2 & 0 & 0 & U3 & 0 & 0 \\
 0 & 0 & 0 & L3 & 0 & 0 & L2 & 0 & L1 & D & U1 & 0 & 0 & 0 & 0 & U3 & 0 \\
 0 & 0 & 0 & 0 & L3 & 0 & 0 & L2 & 0 & L1 & D & 0 & 0 & 0 & 0 & 0 & U3 \\
 0 & 0 & 0 & 0 & 0 & L3 & 0 & 0 & 0 & 0 & 0 & D & U1 & 0 & U2 & 0 & 0 \\
 0 & 0 & 0 & 0 & 0 & 0 & 0 & L3 & 0 & 0 & 0 & 0 & L1 & D & U1 & 0 & U2 \\
 0 & 0 & 0 & 0 & 0 & 0 & 0 & 0 & L3 & 0 & 0 & 0 & 0 & L1 & D & 0 & 0 & U2 \\
 0 & 0 & 0 & 0 & 0 & 0 & 0 & 0 & 0 & L3 & 0 & 0 & L2 & 0 & 0 & D & U1 & 0 \\
 0 & 0 & 0 & 0 & 0 & 0 & 0 & 0 & 0 & 0 & L3 & 0 & 0 & L2 & 0 & L1 & D & U1 \\
 0 & 0 & 0 & 0 & 0 & 0 & 0 & 0 & 0 & 0 & 0 & L3 & 0 & 0 & L2 & 0 & L1 & D
 \end{bmatrix} \quad (1.17)$$

ECLIPSE 100 chooses direction 1 automatically to correspond to the direction of highest transmissibility (usually the Z-direction). Thus, $L1$, $U1$ usually correspond to derivatives of flow between cells in the Z-direction.

Three dimensional finite difference systems give rise to sparse linear equations with banded matrices, such as:

$$A = D + L1 + U1 + L2 + U2 + L3 + U3 \quad (1.18)$$

where

D : is a diagonal matrix

$L1, L2, L3$: are the lower bands

$U1, U2, U3$: are the upper bands

The elements of $D, U1, U2, U3, L1, L2, L3$ are 2×2 matrices for implicit two-phase systems (oil/water, oil/gas, gas/water) and 3×3 matrices for implicit three-phase systems.

$L2$ and $U2$ connect cells in the second direction and the third direction is connected with the help of $L3$ and $U3$. In nested factorization [7], an approximation, B , is constructed by the following nested sequence of factorizations:

$$\begin{aligned} B &= (P + L3) P^{-1} (P + U3) = P + L3 + U3 + L3P^{-1}U3 \\ B &= (T + L2) T^{-1} (T + U2) = T + L2 + U2 + L2T^{-1}U2 \\ B &= (G + L1) G^{-1} (G + U1) = G + L1 + U1 + L1G^{-1}U1 \end{aligned} \quad (1.19)$$

where

G : is a diagonal matrix

P^{-1} : is the inverse of P

T^{-1} : is the inverse of T

G^{-1} : is the inverse of G

It follows that:

$$\begin{aligned} B &= G + L1 + U1 + L2 + U2 + L3 + U3 + L1G^{-1}U1 + L2T^{-1}U2 + L3P^{-1}U3 \\ &= A + G - D + L1G^{-1}U1 + L2T^{-1}U2 + L3P^{-1}U3 \end{aligned} \quad (1.20)$$

The diagonal matrix is computed using:

$$0 = G - D + L1G^{-1}U1 + \text{colsum}(L2T^{-1}U2 + L3P^{-1}U3) \quad (1.21)$$

This choice of G ensures that $\text{colsum}(B) = \text{colsum}(A)$ which, in turn, ensures that there are no material balance errors in the solution of the linear equation.

Off-band elements -not belonging on the above mentioned bands $U1, U2, U3, L1, L2, L3$ - which are possibly corresponding to non-neighboring connections, arising in the treatment of faults, local grid refinement (LGR) or completing the circle in a three dimensional radial study, may destroy the simple structure of the bands above. However, these off-band elements can be easily incorporated in the nested factorization procedure by simply generalizing the definition of the band.

1.2.2 Initialization for Nested Factorization Preconditioning

Before iterations begins the diagonal matrix G must be computed. *ECLIPSE 100* computes and stores G^{-1} rather than G as this is more efficient in subsequent calculations. To conserve material balance, using the *colsum* variant on the preconditioner it holds:

$$G = D - L1G^{-1}U1 - \text{colsum}(L2T^{-1}U2) - \text{colsum}(L3P^{-1}U3) \quad (1.22)$$

Calculation proceeds one cell at a time, thus:

1. when G^{-1} is known for a cell, then the contribution of $L1G^{-1}U1$ to the value of G in the next cell can be calculated
2. when G^{-1} is known for a line, then the contribution of $L2T^{-1}U2$ to the value of G in the next line can be calculated
3. when G is known for a plane, then the contribution of $L3P^{-1}U3$ to the value of G in the next plane can be calculated

1.2.3 Solution Procedure for Nested Factorization

To compute a new search direction *ECLIPSE 100* solves the equation $By = r$ by the following hierarchical procedure. At the outermost level the equation below is solved:

$$(P + L3)(I + P^{-1}U3)y = ry = P^{-1}(r - L3y)y = y - P^{-1}U3y \quad (1.23)$$

The equations above are solved one plane at a time, starting with the first plane and progressing forward until y is known on each plane. The equation is explicit since the quantity $L3y$ involves the known solution, y , on the previous plane.

During the solution of the equation above $z = P^{-1}q$ must be computed on each plane. This involves solving the equation below:

$$(T + L2)(I + T^{-1}U2)z = qz = T^{-1}(q - L2z)z = z - T^{-1}U2z \quad (1.24)$$

The equations above are solved by sweeping backwards one line at a time.

Finally, during the solution of the equations above must be noted that the vector of the form $w = T^{-1}q$ must be computed on each plane. This involves solving the tridiagonal equation below:

$$(G + L1)(I + G^{-1}U1)w = vw = G^{-1}(v - L1w)w = w - G^{-1}U1w \quad (1.25)$$

The equations above are solved by sweeping first forward, then backward through the cells in a line. This may be solved as a block tridiagonal in the intermediate nesting if a method exists of inverting the line tridiagonal equations.

1.2.4 Orthomin

The *Orthomin* procedure used by *ECLIPSE 100* can be summarized in the steps below:

1. Compute the initial solution: $y = B^{-1}b$, $x \rightarrow y$
2. Compute the initial residual: $r = b - Ay$, (if the *colsum* constraint is used, the sum of the elements of r is now zero)
3. Test for convergence and escape if converged else find a new search direction, $y = B^{-1}b$
4. Orthogonalize γ to the stack of previous search directions (z):

$$y = y - \frac{(yz)}{(zz)}z \quad (1.26)$$

5. Find the optimum step length, s , which minimizes the saturation normalized sum of the squares of the residuals (rr):

$$s = \frac{(rq)}{(qq)} \quad (1.27)$$

$$q = Ay \quad (1.28)$$

6. Update the solution ($x \rightarrow x + sy$), the residual ($r \rightarrow r - sq$) and the stack $z = (z, y)$ (if not converged, return to step 5)

1.2.5 Convergence Criteria

The convergence criterion in *ECLIPSE 100* is based on the maximum residuals for each phase. As noted in [section 1.1.2](#) these are normalized to represent effective saturation normalized residuals so that the convergence criteria are physically meaningful in terms of saturation changes.

The *Orthomin* procedure is set to minimize the saturation normalized root mean square residuals. Residual sums (material balance errors) should be zero to within rounding error, while absolute maximum saturation normalized residual is used to test for convergence. The standard convergence criterion is that the maximum saturation normalized residual, $|r|_{max}$, be less than 0.0001. Convergence is also assumed if $|r|_{max}$ is less than $MIN(0.1|b|_{max}, 0.001r_{top}, 0.001)$. $|b|_{max}$ is the largest saturation normalized input residual and r_{top} is the greatest saturation normalized residual to occur at any stage of the procedure. r_{top} may be much larger than $|b|_{max}$ since the *colsum* constraint makes the initial residual quite large.

1.2.6 Treatment of Wells

The strongly coupled fully implicit treatment of wells in *ECLIPSE 100* extends the linear equations to include the well variables, w , corresponding to the bottom hole flowing pressure and wellbore fractions. Thus, each well, like each cell, has three variables in the three phase case. Including the well terms, the linear equations now become:

$$Ax + Cw = r \quad (1.29)$$

$$Rx + Dw = u$$

where

u : is the well residuals

If there are N grid blocks and L wells then:

A : is a band $N \times N$ matrix

C : is a sparse $N \times L$ matrix

R : is a sparse $L \times N$ matrix

D : is a sparse $L \times L$ matrix

Usually, D is lower triangular and easily inverted, allowing the well terms to be eliminated. Thus the equation for x becomes:

$$(A - CD^{-1}R)x = r - CD^{-1}u \quad (1.30)$$

which is easily solved by preconditioned *Orthomin*.

1.3 *PlanOpt*

PlanOpt is part of *ECLIPSE* reservoir simulation software which targets in assisting in choosing the locations of vertical production wells. The vertical wells are completed in each column of cells that satisfies specific criteria. After the *ECLIPSE* reservoir model is loaded in *PlanOpt* software several steps should be followed in order to achieve the best well placement according to the specified criteria and constraints.

1.3.1 Phase 1

At first an initial distribution of vertical producing wells should be generated based on minimum exclusion zones for pre-existing production and injection wells, mobile saturations of grid blocks, the existence of other wells and layer or depth of the wells to be created. Based on these information *PlanOpt* conducts a scan to determine qualifying grid blocks which hold true to the above restrictions. Finally, it is important that the new wells created surely are not placed in the vicinity of pre-existing wells according to the minimum exclusion zones that have been also predefined.

1.3.2 Phase 2 (Static Screening)

Phase 2 is an optional step very helpful though since it can aid in rejecting a lot of wells found during the operations of phase 1 and so make the optimization procedure run for shorter period of time. *PlanOpt* runs the simulation for a nominal period of time (e.g. 1 day) and so minimum and maximum values for the *PI*, *GOR*, *GLR*, *Water-cut*, *Kh* and the number of open connections are calculated for the new wells. Then user may specify the minimum and maximum allowable ranges for the above values resulting in "screening" wells which do not comply with the allowable range that the user have defined.

Furthermore, it should be noted that when there are lots of wells next to each other, there might be interference between them when simulating, causing chopping. By using the *Well Distance* option wells are ranked based on *PI*, *GOR*, *GLR*, *Water - cut*, *Kh* and the number of open connections and then disabled based on rank and the number of wells that happen to exist in the specific distance defined by the user.

1.3.3 Optimization

The optimization phase of the *PlanOpt* software involves iteratively "screening" the well configuration according to results obtained from a full simulation run of the initial model together with the additional constraints and limits that have been added by the user with the *PlanOpt* software. Screening operation involves the ranking of all wells according to their value.

The equation below shows the objective function at the k 'th iteration:

$$OF = \sum_i (a_o \Delta Q_{oi} + a_g \Delta Q_{gi} + a_w \Delta Q_{wi}) / (1 - DF)^j \quad (1.31)$$

where

i : is the number of cycles over the wells present at the current k 'th iteration

$a_{o,w,g}$: are the objective function coefficients for oil, water and gas

$Q_{o,w,g}$: are the oil, water, gas production or $WOPT$ for oil, $WWPT$ for water and $WGPT$ for gas for well i over time

DF : is the discount factor

j : is the number of days since start to date divided by 365

The objective function equation can also be written in the form below:

$$\begin{aligned}
 OF &= \frac{WOPT(2^{nd}date) - WOPT(Initial\ Date)}{(1 + DF)^{(\#\ of\ days\ since\ start\ until\ 2^{nd}\ date / 365)}} + \\
 &+ \frac{WOPT(3^{rd}date) - WOPT(2^{nd}date)}{(1 + DF)^{(\#\ of\ days\ since\ start\ until\ 3^{rd}\ date / 365)}} + \\
 &+ \dots + \frac{WOPT(N^{th}date) - WOPT((N - 1)^{th}\ date)}{(1 + DF)^{(\#\ of\ days\ since\ start\ until\ end\ date / 365)}}
 \end{aligned} \tag{1.32}$$

where

$WOPT(Initial\ Date) = 0$

number of days of period $k =$ number of days corresponding to time interval $[Initial\ Date, k + 1date]$

If $DF = 0$, then $OF = WOPT(Last\ Date)$

Finally, an alternative well objective function can be used as shown below:

$$(User\ OF) = \left\{ b \times \sum_i [O.F.(i)] \right\} - (B \times N) \tag{1.33}$$

where

i : is the number of cycles over the wells present at the current k 'th iteration

$O.F.(i)$: is the well (discounted) objective function as defined above for well i

b, B : are the user assigned coefficients

N : is the number of wells present in the k 'th iteration

Default values: $b = 1$ and $B = 0$

1.4 *SimOpt*

SimOpt is part of *ECLIPSE* reservoir simulation software which targets on aiding all aspects concerning history matching processes. It incorporates the full field reservoir model together with observed data collected during the actual operation of the reservoir through time. Since there might be a mismatch between the observed and the simulation model data there is a need to modify several parameters of the simulation model (porosity, permeability, transmissibility, etc) so that the simulation model data will have a better match with the observed data. After the parameters are chosen the software operations will indicate which of them will have the greatest impact on the matching process. Finally, when the correct parameters are chosen as the software indicates a regression process will follow that will calculate the values of the parameters with which the best possible matching occurs. The basic work flow and operations of the software is described below.

1.4.1 Observed Data, Prior Information and Objective Function

Observed Data

The observed data are split into two categories the observed production data (bottom hole pressure, fluid production rates, etc) and survey production data (fluid saturations or acoustic impedance to pressure waves etc).

The observed data are of the form of measurement data sets which also should be accompanied with their corresponding measurement error values. If specific data sets are deemed to be of more importance then weight factors can be assigned to the whole data set so that during the matching process will have a more precise match.

The simulated and observed data are compared point to point so in the case that no simulated value exists for an observed data time, a linear interpolation is conducted.

Prior Information

Based on geological surveys that might be conducted, several statistical information are collected through the life span of the reservoir. So the parameters that are chosen to vary during matching should acquire values that are reasonable and consistent. The prior information is a measure of the uncertainty of reservoir parameters and specifies how parameter modifiers are expected to vary. During the regression process prior information is used to normalize the parameter modifier which leads to improved convergence and finally is used to modify the objective function so that the parameter modifiers try to match the statistical information as well as the observed data.

There are two types of distributions:

- Normal: Allows small range of variations
- Log-Normal: Variation with order of magnitude

A mean value of 1 for normal distribution or 0 for log-normal distribution for parameter modifier indicates that the imported simulation model is treated as the most likely value of the parameter modifier value. Any changes away from the imported model will be penalized by the prior term in the objective function.

Standard deviation of a parameter modifier distribution indicates the amount of variation away from the mean value in the parameter modifier.

Prior weight is given to each property parameter modified in the prior term of the objective function. By default the prior weights are 0 meaning that there is no contribution from the prior term in the objective function.

The normalization of a parameter modifier reflects the mean value and amount of variation expected in the modifier and depends on the distribution type.

- Normal: $r = \frac{\lambda - \bar{\lambda}}{\sigma}$
- Log-Normal: $r = \frac{\log_{10}(\lambda) - \bar{\lambda}}{\sigma}$

where

$\lambda, \bar{\lambda}$: are the value and mean value of the parameter modifier distribution respectively

σ : is the standard deviation of the parameter modifier distribution

Objective Function

The objective function which have to be minimized to achieve the matching between the observed and the simulation model production data is presented below:

$$f = \frac{\alpha}{2} \mathbf{r}^T \mathbf{r} + \frac{\beta}{2} \mathbf{s}^T \mathbf{C}_s^{-1} \mathbf{s} + \gamma f_{prior} \quad (1.34)$$

where

α, β, γ : are the overall weights for production, survey and prior terms

\mathbf{r} : is the vector of residuals for the observed production data

\mathbf{s} : is the vector of residuals for the observed survey data

\mathbf{C}_s : is the matrix of correlation between observed survey data residuals

f_{prior} : is the objective function for the prior term

$$f_{prior} = \frac{1}{2} \mathbf{v}^T \mathbf{B}^T \mathbf{C}_{prior}^{-1} \mathbf{B} \mathbf{v} \quad (1.35)$$

where

\mathbf{v} : is the vector of normalized parameter modifiers

\mathbf{B} : is the diagonal matrix of parameter modifier prior weights

\mathbf{C}_{prior} : is the parameter modifier prior correlation matrix

subscript T denotes the transpose of the matrix or vector

Each element, r_i , in the vector of residuals for the observed production data is the normalized and weighted difference between an observed production value and the corresponding simulated value. The equation is shown below:

$$r_i = w_d w_i \frac{(o_i - c_i)}{\sigma_d} \quad (1.36)$$

where

d : references one set of observed production data of a given type, at a given well or group of connection

i : references an individual data point in the d 'th item of observed production data

o_i and c_i : are the observed and calculated (that is simulation) production values respectively

σ_d : is the measurement error for the d 'th production data set

w_d : is an overall weighting for the d 'th production data set

w_i : is a weighting for the i 'th production data point

As mentioned in the beginning of the section the weighting factors may be used to "filter out" bad or unreliable production data, and/or reduce the importance of suspect measurements. Different values of w_d can be used to express particular interest in certain production data sets, while zero or low values of w_i can be used to indicate a low level of confidence in production data at a given time.

In the formulation of the production term in the objective function, there is an inherent assumption that there is no correlation between the production residuals. Studies have shown, that the temporal correlation length for typical production data is less than a month, while this data is usually specified at monthly intervals meaning that this assumption is reasonable. However, it is important that when preparing history match data the sampling frequency should be longer than the correlation length.

Each element, s_i , in the vector of residuals for the observed survey data is the normalized and weighted difference between an observed survey value and the corresponding simulated value. The equation is shown below:

$$s_i = w_d \frac{(o_i - c_i)}{\sigma_i} \quad (1.37)$$

where

d : references one set of observed survey data of a given type at a given time

i : references an individual grid block data point in the d 'th item of observed survey data

o_i and c_i : are the observed and calculated (that is simulation) survey values respectively

σ_i : is the square root of the variance associated with the observed survey residual value (the error in the observed survey value)

w_d : is an overall weighting for the d 'th data set

It is quite common for the information contained in the observed survey residuals to have correlation lengths that are greater than the size of the simulation model grid blocks. Hence it is necessary to specify the correlation between the observed survey residuals in order to ensure that the correct weighting is applied within each observed survey data set. In *SimOpt* Software this is done by specifying a correlation model and correlation lengths (L_x , L_y and L_z) for each observed survey data set.

There are three correlation models available in *SimOpt*:

1. No correlation - in which the correlation matrix is simply the identity matrix
2. Exponential correlation - in which the correlation matrix entries are given by:

$$C_{s,ij} = e^{-3h} \quad (1.38)$$

3. Spherical correlation - in which the correlation matrix entries are given by:

$$C_{s,ij} = 1 - \frac{3h}{2} + \frac{h^3}{2} \quad (h \leq 1) \quad , \quad C_{s,ij} = 0 \quad (h > 1) \quad (1.39)$$

where, for both the exponential and the spherical correlation models,

$$h = \sqrt{\left(\frac{\Delta x_{ij}}{L_x}\right)^2 + \left(\frac{\Delta y_{ij}}{L_y}\right)^2 + \left(\frac{\Delta z_{ij}}{L_z}\right)^2} \quad (1.40)$$

and Δx_{ij} , Δy_{ij} and Δz_{ij} are the distances between the i^{th} and the j^{th} grid blocks in the x , y and z directions respectively.

As there may be a large number of observed grid block survey values, the correlation matrix can be very large and it would take too much space to store. Hence, a correlation cut-off value can be specified. If a value generated by the exponential or spherical models is below this cut-off, then it is treated as zero.

1.4.2 Gradients and RMS

Gradients

First derivative of the objective function:

$$\begin{aligned} \nabla f &= \alpha (\nabla \mathbf{r})^T \mathbf{r} + \beta (\nabla \mathbf{s})^T C_s^{-1} \mathbf{s} + \nabla f_{prior} \\ [\nabla \mathbf{r}]_{ij} &= \frac{dr_i}{dv_j} = -\frac{w_d w_i}{\sigma_d} \left(\frac{dc_i}{dv_i} \right), \quad [\nabla \mathbf{s}]_{ij} = \frac{ds_i}{dv_j} = -\frac{w_d}{\sigma_i} \left(\frac{dc_i}{dv_i} \right) \end{aligned} \quad (1.41)$$

Second derivative of the objective function:

$$\nabla^2 f = \alpha \left[(\nabla^2 \mathbf{r})^T \mathbf{r} + (\nabla \mathbf{r})^T (\nabla \mathbf{r}) \right] + \beta \left[(\nabla^2 \mathbf{s})^T C_s^{-1} \mathbf{s} + (\nabla \mathbf{s})^T C_s^{-1} (\nabla \mathbf{s}) \right] + \gamma \nabla^2 f_{prior} \quad (1.42)$$

According to the *Gauss-Newton* approximation the terms involving second derivatives of the simulated values can be ignored since their values are very small compared to the first term. Also it is pre-multiplied by the residual term which is small near the solution although the approximation is used even when away from the solution.

So, the equation above can be written also:

$$\nabla^2 f \simeq \alpha (\nabla \mathbf{r})^T (\nabla \mathbf{r}) + \beta (\nabla \mathbf{s})^T C_s^{-1} (\nabla \mathbf{s}) + \gamma \nabla^2 f_{prior} \quad (1.43)$$

It is important to note that the first and second derivative of the objective function can be generated using only the first derivatives of the simulated quantity with respect to the parameter.

RMS Values

The overall measure of a history matching process is expressed as a Root Mean Square (*RMS*) index which provides an average value of the deviation between simulated and observed data:

$$RMS = \sqrt{\frac{2f}{m}} \quad (1.44)$$

where

f : is the objective function

m : is the total number of observations over which the index is formed and consists of:

- data points in active observed production data that have non-zero point weight w_i
- active observed survey data points
- active prior terms (parameters with non-zero prior weight specified)

RMS index is also calculated for each different group/well/connection/survey data set separately.

RMS Sensitivities

The partial derivatives of the RMS with respect to each of the parameters modifiers are called RMS sensitivities which are indication of the most sensitive parameters for the history matching.

$$\nabla (RMS) = \frac{\nabla f}{m \times RMS} \quad (1.45)$$

with respect to normalized or un-normalized parameters.

1.4.3 Prior Regression Operations

Before running the *Regression Mode* of *SimOpt* which will modify the chosen parameters in order to achieve the best possible match between observed and simulation model data, *Evaluation Mode* or *Base Run* and *Gradient Mode* can be utilized. These modes can be used -after choosing the reservoir parameters- to clarify whether a reservoir parameter that is chosen to vary will have high or negligible impact on the matching process during the operations of regression mode.

Evaluation Mode

After running the *Evaluation Mode*, the RMS between observed and simulated model data is calculated. The RMS tables that are produced point the sensitivity of changing the parameters on the RMS matching. Depending on the mismatches, parameters should be chosen to be change and improve the match. The parameters chosen will affect the simulated values meaning that the magnitude and the sense of change should comply with the geological information that exist for the reservoir. Finally, it is common that parameters may exist that will produce similar effects or act on the opposite direction with each other or even be totally dependent.

Gradient Mode

During the operations of the *Gradient Mode* each of the parameters chosen will change at a time so that the gradient of required simulation value with respect to each parameter is calculated. The calculated gradients are in fact the sensitivities of the RMS to changes in each of the parameters which will aid in

determining the order of magnitude of the modifier of each parameter. In order to achieve the best quality of the *Regression Mode* (fast and firm convergence), it is also extremely important to chose parameters which are either uncorrelated with each other or have no contradictions. With the aid of the gradients that were calculated *Hessian* matrix, *Covariance* Matrix and *Correlation* Matrix are produced.

Hessian Matrix

The *Hessian* matrix elements are the second derivatives of the objective function with respect to the parameters that have been chosen, see [equation \(1.42\)](#). *Hessian* matrix aids to examine the conditioning of the regression problem.

It is preferable to have a *Hessian* matrix whose diagonal elements dominate and are roughly equal in size. *SimOpt* measures the quality of each parameter's row/column with:

- Diagonal dominance

$$\frac{\sum_{i \neq j} |H_{ij}|}{H_{ii}} \quad (1.46)$$

- Normalized maximum off-diagonal

$$\frac{\max_{(i \neq j)} |H_{ij}|}{H_{ii}} \quad (1.47)$$

where

$|H_{ij}|$: is the element of the i 'th row and j 'th column corresponding to the second derivative of the objective function with respect to parameter i and j

Parameters with small values of the measurements above will perform better during regression. An ill-conditioned *Hessian* matrix may result in slow convergence of regression procedure and should be remedied by removing redundant parameters and reducing interdependence between parameters as will be discussed below.

Covariance Matrix

The parameter *Covariance* matrix is calculated as the inverse of the *Hessian* matrix and may be utilized to determine how well determined are the parameters for the current match.

The diagonal elements of the matrix are, approximately, the parameter variances. The parameter variances are the square of the standard deviation of the parameter value probability distribution function. Larger variances are associated with less well-determined parameters. The off-diagonal elements represent the parameter covariances. These can be loosely considered as a measure of how well one known given that the others were known exactly.

Correlation Matrix

The parameter correlation matrix is calculated from the covariance matrix as shown below:

$$\text{Correlation}(i, j) = \frac{\text{Covariance}(i, j)}{\sqrt{\text{Covariance}(i, i) \times \text{Covariance}(j, j)}} \quad (1.48)$$

The matrix above indicates the degree of association between changes in one parameter i with changes in another parameter j . Correlation values range from -1 to $+1$. A value of zero indicates that the effect on the history match of changing one of the parameters does not interfere with the effect on the history match of changing the other meaning that they are independent of one another.

The correlation of a parameter with itself is clearly always $+1$ and so the leading diagonal of the correlation matrix is always filled with values of $+1$.

In general, the correlation between pairs of parameters is not -1 , $+1$ or zero, but some values in between.

Regression operations work best when the parameters are independent. When designing a set of parameters for regression operations it is useful then to perform a run with the *Gradient Mode* first to ensure that the correlations between parameters are not too strong (that is close to $+1$ or -1).

Redundant Parameters

There are two types of redundant parameters:

1. Parameters whose gradients are identical. Such parameters will lead to a *Hessian* matrix that is non-invertible (no correlation matrix)
2. Parameters whose gradients are exactly opposite will have the same effect on *Hessian* matrix like above making it non-invertible

If during the operations above redundant parameters appear, either one of the parameters have to be rejected or set to semi-active mode meaning that it will not contribute during the operations of the *Regression Mode*.

Interdependent Parameters

There are two types of interdependent parameters:

1. Strongly anti-correlated parameters: Two parameters with similar gradients leading to a correlation matrix entry for these parameters close to -1 . Effect of increasing one parameter is canceled by the effect of decreasing the other parameter. Such parameters can be merged to a single parameter for regression to converge quicker
2. Strongly correlated parameters: Two parameters with almost similar gradients leading to a correlation matrix entry for these parameters close to $+1$. Effect of increasing one parameter is canceled by the effect of increasing the other parameter. In such a case either reject one of the parameters or make one parameter semi-active

When one parameter of a pair of redundant or strongly correlated parameters have to be rejected then in order to chose which will be rejected the measurements of diagonal dominance or normalized maximum off-diagonal as discussed on [chapter 1.4.3](#) can be used.

1.4.4 Regression Mode

During the operations of *Regression* mode the objective function that will have been formed based on the parameters chosen, needs to be minimized in order to achieve the best possible match of observed and simulation model data. There is a variety of regression algorithms which will optimize an objective function like the [equation \(1.34\)](#).

Levenberg-Marquardt Algorithm

SimOpt uses the *Levenberg-Marquardt* algorithm which is a combination of the *Newton* method and a *steepest descent* scheme. Denoting the vector of current parameter normalized modifier values as v^k , then the algorithm estimates the step, $dv^k(\mu)$, required to minimize the objective below:

$$dv^k(\mu) = (H + \mu I)^{-1} \nabla f(\mu^k) \quad (1.49)$$

where

H : is the *Hessian* matrix of second derivatives of f

I : is the identity matrix

The parameter μ is free and is varied so that, away from solution where the quadratic *Newton* model may have less validity, it takes large values and so the bias of the step is towards the *steepest descent* direction. Whilst near the solution, it takes small values to make the best possible use of the fast quadratic convergence rate of the *Newton* step.

If the input data measurement errors are close to being normally distributed, the inverse of the *Hessian* matrix approximates the parameter covariance matrix. This can be used to estimate the parameter squared standard errors.

Model Trust Region

A refinement on the *Levenberg-Marquardt* method used in the program is to vary not the parameter μ , but instead to vary the length of the step dv^k and adjust μ accordingly.

The degree of freedom thus becomes the size of the region in which the regression step is being constrained and so can be set to reflect the confidence in the quadratic model's ability to represent the actual objective function. This region is called the Model Trust Region and the allowable step length, the trust region radius, TRR .

The following equations are used to determine the value of the parameter μ . For:

$$\left\| dv^k(0) \right\|_2 \leq TRR \quad \rightarrow \quad \mu = 0 \quad (1.50)$$

(i.e. a pure *Gauss-Newton* step), otherwise μ is calculated so that,

$$\left\| dv^k(\mu) \right\|_2 = TRR \quad (1.51)$$

The trust region radius is set to an initial conservative value at the start of a regression. This initial trust region radius can be specified manually or it can be calculated using the length of the *Cauchy* step given by:

$$TRR_0 = \frac{\left\| \nabla f(v^0) \right\|_2^3}{\{\nabla f(v^0)\}^T H \{\nabla f(v^0)\}} \quad (1.52)$$

The trust region radius is then updated, subject to preset upper and lower bounds, after each iteration of the minimization procedure, according to the degree to which the change in the objective function was correctly modeled.

Chapter 2

Initial Model Production Data and Details

The software packages of *PlanOpt* and *SimOpt* are going to be used in order to optimize the well placement and achieve history matching on a reservoir block of *Gullfaks*. On this chapter basic information about geometry, topology of existing producing and injecting wells, field data, well production data of the simulation model and well production observed data are going to be presented.

By utilizing the *FloViz* package from *ECLIPSE* Reservoir Simulation software, 3D figures of the reservoir simulation model are going to be presented in order to understand and visualize the information mentioned above.

2.1 Reservoir

The reservoir block that is incorporated in the current diploma thesis is part of the *Gullfaks* oil field [8]. *Gullfaks* is an oil and gas field in the Norwegian sector of the North sea. It was discovered in 1978 in block 34/10 at a water depth range of 130 – 230 meters. The first production platform of *Gullfaks* started producing in 1986. Two additional production platforms were built in 1988 and 1989.

The reservoir consists of delta sandstones from Middle Jurassic Brent Group, shallow-marine Lower Jurassic Cook Formation sandstones and the fluvial-channel and delta-plain Lower Jurassic Statfjord Formation.

2.2 Geometry

The simulation model of *Gullfaks* oil field block part is $20 \times 40 \times 13$ grid blocks. The whole 13'th layer and several other grid cells in other layers of the reservoir were set as inactive since no contribution from these regions is wanted on the specific block.

The figure below shows the whole reservoir simulation model with both the active grid cells (red color) and inactive grid cells (blue color):

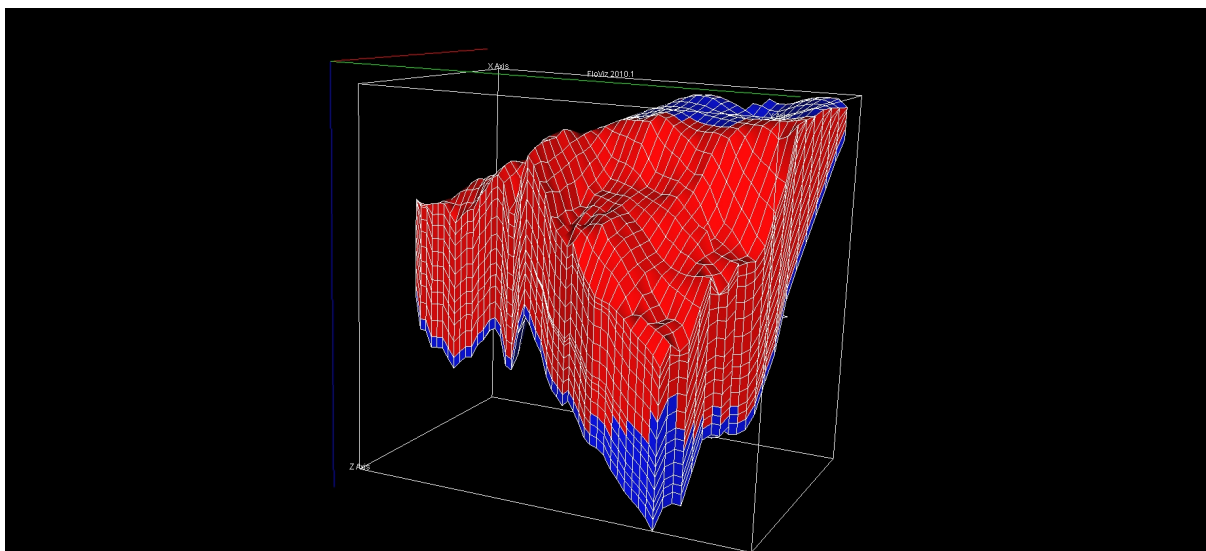


Figure 2.1: *Gullfaks* block $20 \times 40 \times 13$ grid blocks simulation model

The depth range of the specific reservoir block part of *Gullfaks* is shown on the figure below:

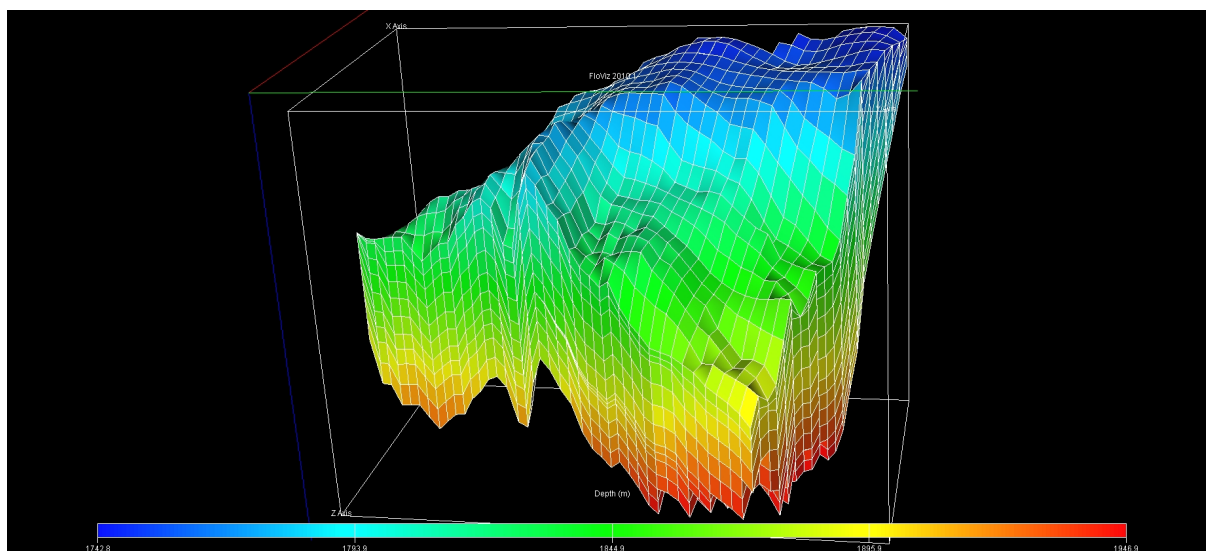


Figure 2.2: *Gullfaks* block depth of active grid cells in meters (m)

By looking on the figure above it can be deduced that the shallowest part of the reservoir simulation model is set at 1742.8 meters below sea bottom, the deepest part at 1946.9 meters below sea bottom and so the maximum pay-zone thickness is 204.1 meters.

2.3 Well Topology

The figures below shows the injection and production wells topology of the simulation model.

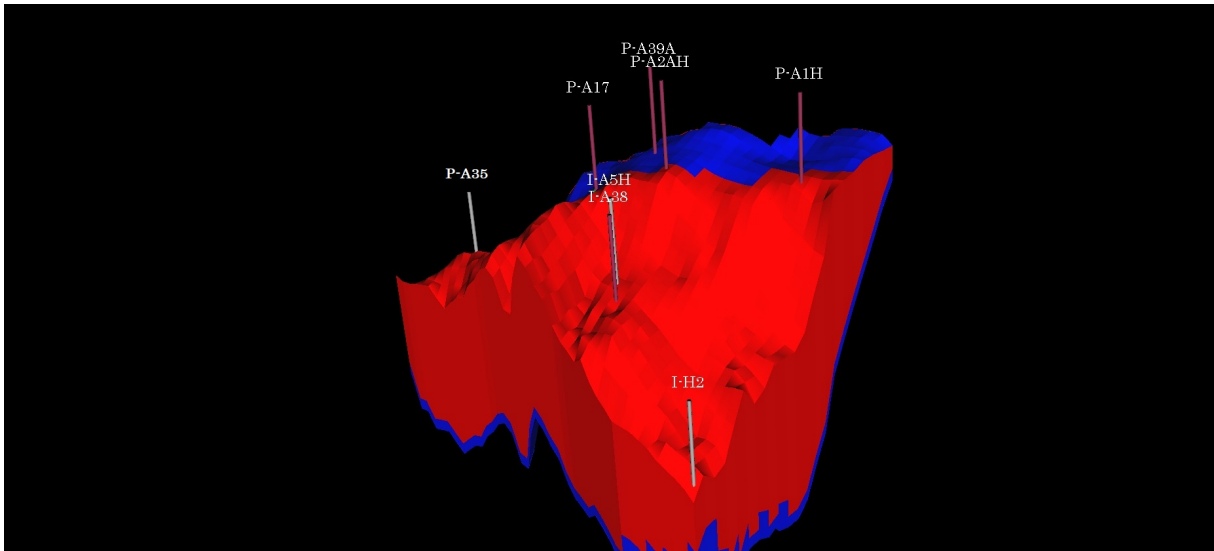


Figure 2.3: Gullfaks block well topology

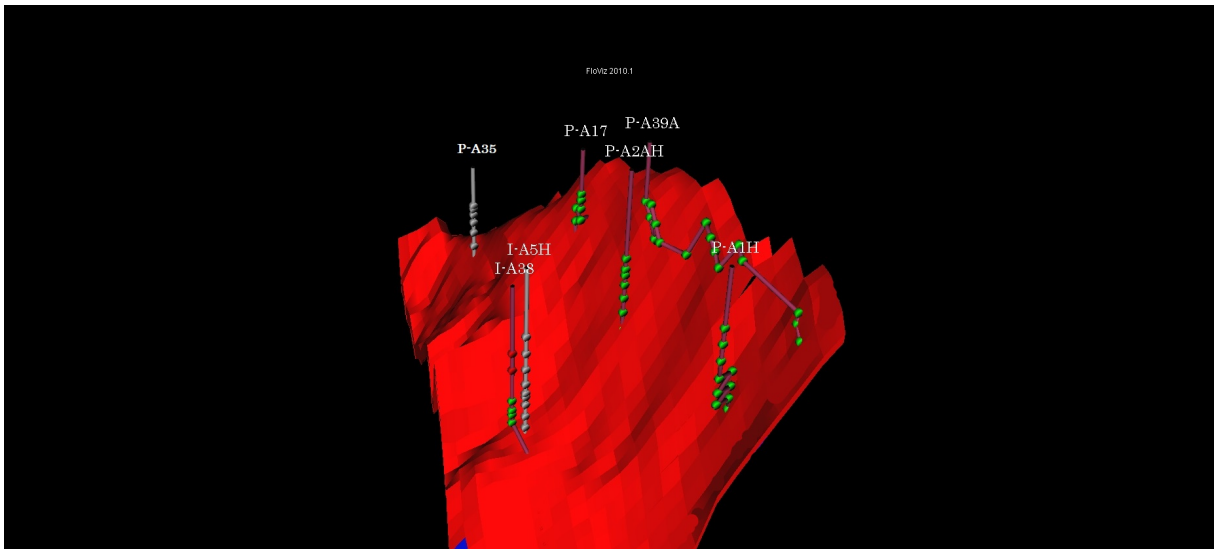


Figure 2.4: Gullfaks block 12'th layer well topology

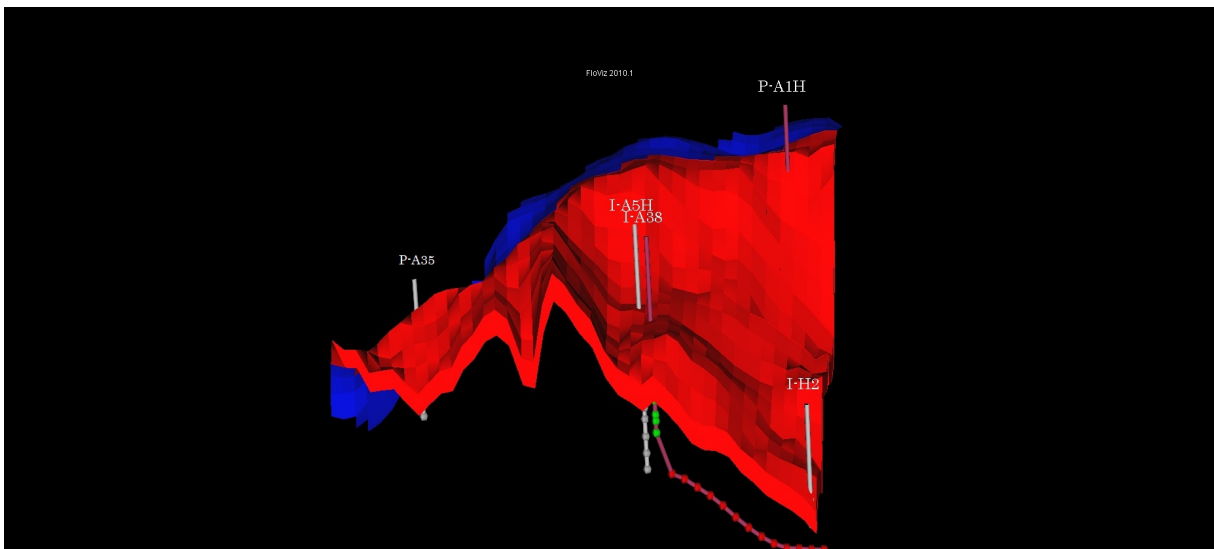


Figure 2.5: Gullfaks block 3'rd layer well topology

There are five production wells completed on the reservoir:

- Well *P-A1H*: Vertical well with small deviations after the 4'th completed connection. First connection is completed at the 4'th layer of the reservoir and last connection is completed at the 12'th layer of the reservoir
- Well *P-A2AH*: Vertical well. First connection at the 6'th layer and last connection at the 12'th layer
- Well *P-A17*: Vertical well with small deviations after the 3'rd completed connection. First connection at the 5'th layer and last connection at the 12'th layer
- Well *P-A35*: Vertical well. First connection at the 3'rd layer and last connection at the 12'th layer
- Well *P-A39A*: Deviated-Horizontal well. First connections at the 10'th layer and last connections at the 12'th layer

There are two injection wells completed on the reservoir:

- Well *I-A5H*: Vertical well. First connection at the 3'rd layer and last connection at the 12'th layer
- Well *I-A38*: Vertical/Horizontal well. First connection at the 3'rd layer and last connection at the 12'th layer. Well becomes horizontal at the 12'th layer of the reservoir

Injection well *I-H2* is not a real completed well. It simulates a water influx caused by an adjacent aquifer.

Production wells *P-A35* and *P-A17* are drilled through layers (7'th and 8'th) with grid cells that are marked as inactive cells.

2.4 Field Data

Several important field data are presented on the figures below:

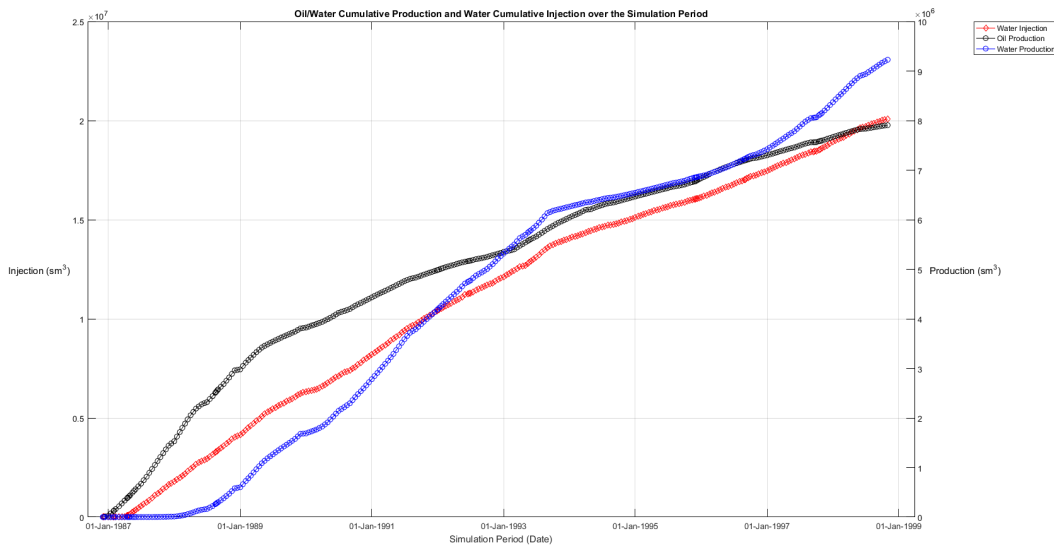


Figure 2.6: Field cumulative oil/water production (Black/Blue curves, Right y-axis) and water injection (Red curve, Left y-axis) over time

After running the simulation of the initial model provided for the current diploma thesis the original oil in place was measured to be $24.18 \times 10^6 \text{ sm}^3$. The residual oil saturation of the reservoir model was set at 20% meaning the original mobile oil in place of the reservoir is $19.344 \times 10^6 \text{ sm}^3$.

The simulation model runs for a certain period of time (1st December 1986 until 1st November 1998) and provides field simulation results along the whole simulation period.

By observing [figure \(2.6\)](#), it can be derived that the cumulative oil and water production at the end of the simulation period are $7.91 \times 10^6 \text{ sm}^3$ and $7.23 \times 10^6 \text{ sm}^3$ respectively. The cumulative water injected in the reservoir at the end of the simulation period is $20.10 \times 10^6 \text{ sm}^3$.

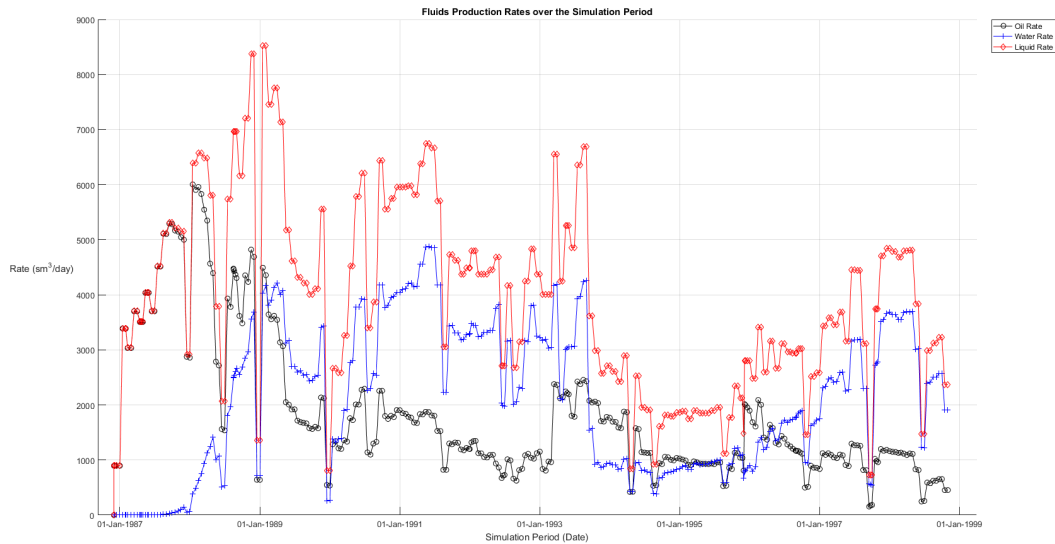


Figure 2.7: Field oil/water/liquid production rate (Black/Blue/Red curves, Left y-axis) over time

The figure above shows the daily production of oil, water and their sum -the liquid daily production rate- of the whole field.

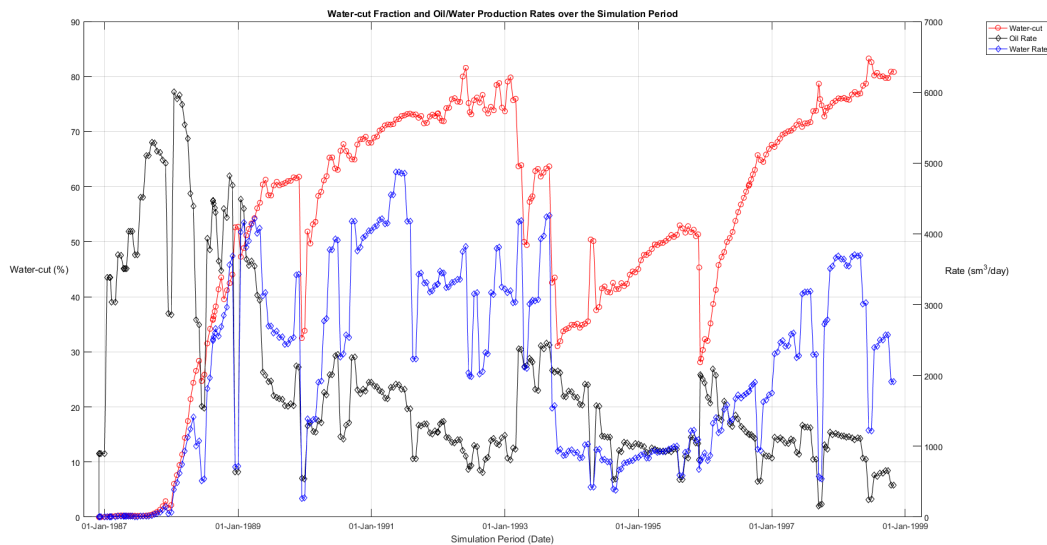


Figure 2.8: Field oil/water production rate (Black/Blue curves, Right y-axis) and water-cut fraction (Red curve, Left y-axis) over time

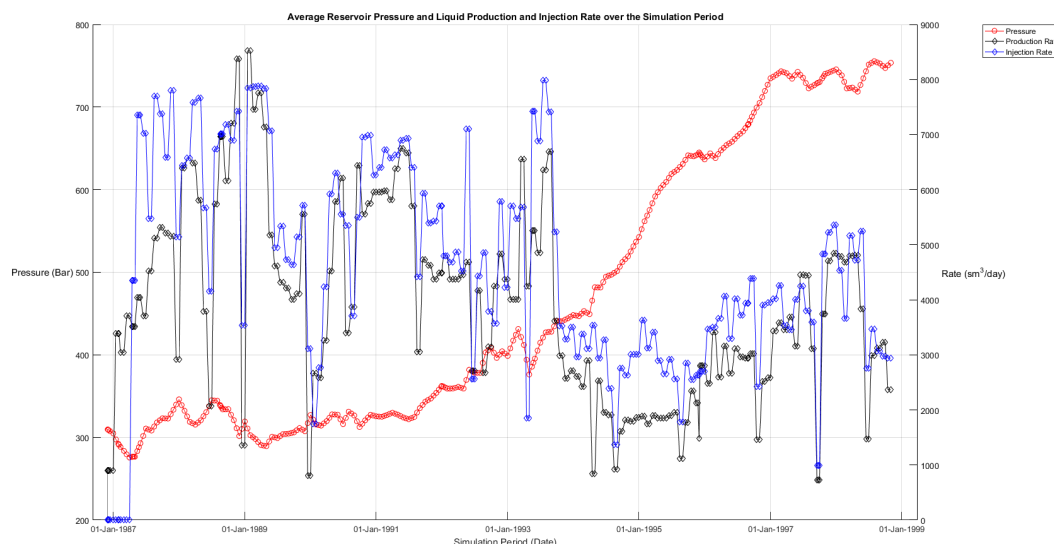


Figure 2.9: Field liquid production rate (Black curve, Right y-axis), water injection rate (Blue curve, Right y-axis) and average reservoir pressure (Red curve, Left y-axis) over time

Reservoir pressure is highly related to the total liquid production and water injection rates. The pressure profile of the figure above shows a continuous increase after one year of production since after that time the water injection rate is continuously higher than the total liquid production rate of the reservoir. Furthermore, as liquid production and water injection continues, water covers more space than oil used to occupy, the pore volume available due to the compressibility of oil is waning resulting in an even more abrupt increase of the average reservoir pressure curve.

2.5 Well Production/Injection Data

On this chapter well production data are going to be presented for all producing and injecting wells. As far as production wells are concerned oil and water production rates (Black/Blue curves, Right y-axis) and water-cut (Red curve, Left y-axis) will be presented. For the injection wells the water injection rate (Blue curve, Left y-axis) is going to be presented.

Together with the above mentioned data that is going to be presented below, information will be printed for all wells about the percentage of:

- oil cumulative production of each production well on the field cumulative oil production
- water cumulative production of each production well on the field cumulative water production
- water cumulative injection of each injection well on the field cumulative water injection

The above mentioned information are vital in order to understand which production well contributes more during the simulation period which also indicates the regions that are capable of producing higher quantity of oil. The water production data for each well together with their corresponding water-cut values and the injection profiles of injecting wells will aid in understanding which wells and finally which regions will have early water breakthrough during production.

During the optimization processes that are going to be discussed on [chapter 3](#) the information mentioned above will aid on choosing and setting up variables, constrains and limits of the objective function.

Production Well P-A1H

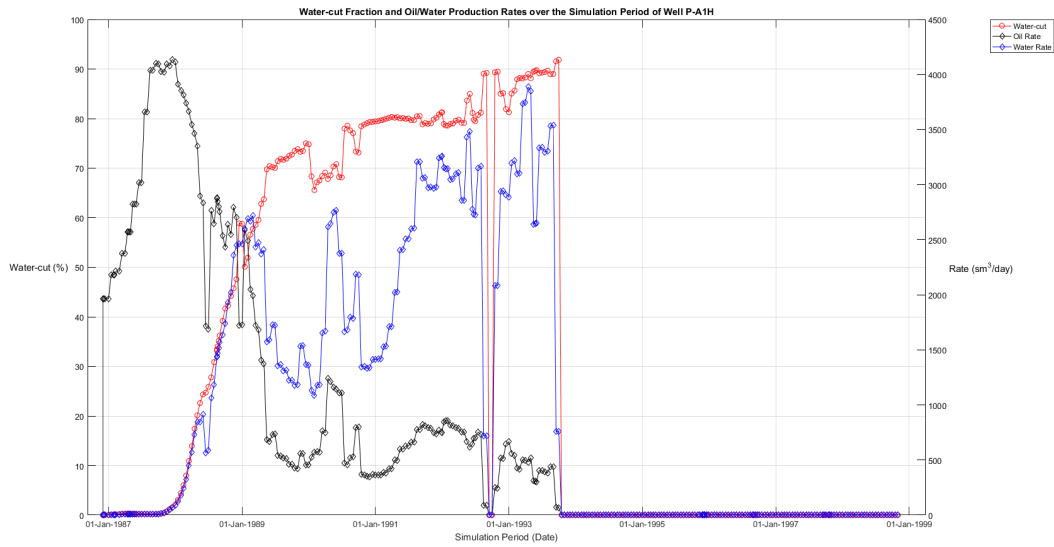


Figure 2.10: Well P-A1H production data ([click here for well position](#))

% of field cumulative oil produced: 39.16 %

% of field cumulative water produced: 41.63 %

Production Well P-A2AH

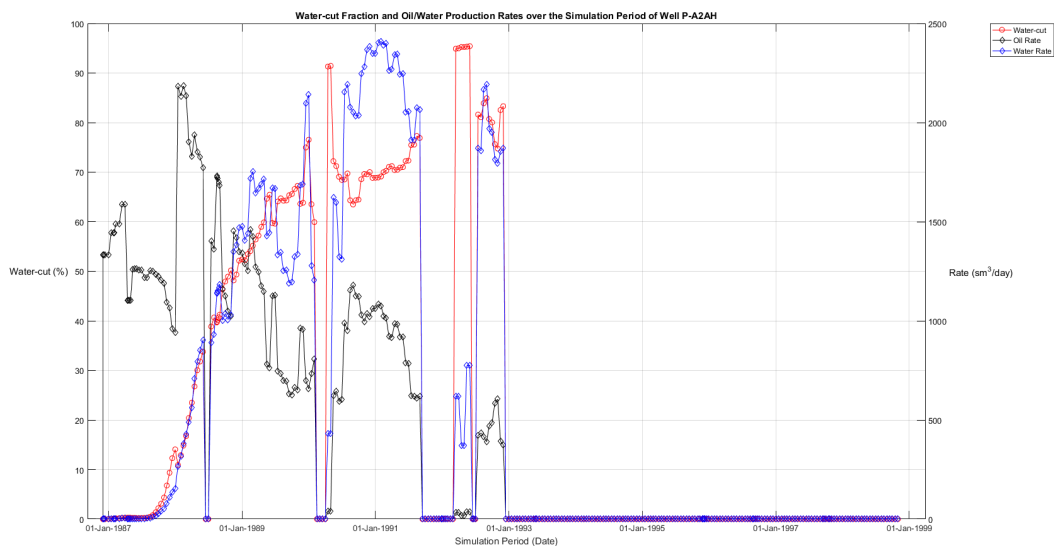


Figure 2.11: Well P-A2AH production data ([click here for well position](#))

% of field cumulative oil produced: 20.24 %

% of field cumulative water produced: 19.44 %

Production Well P-A17

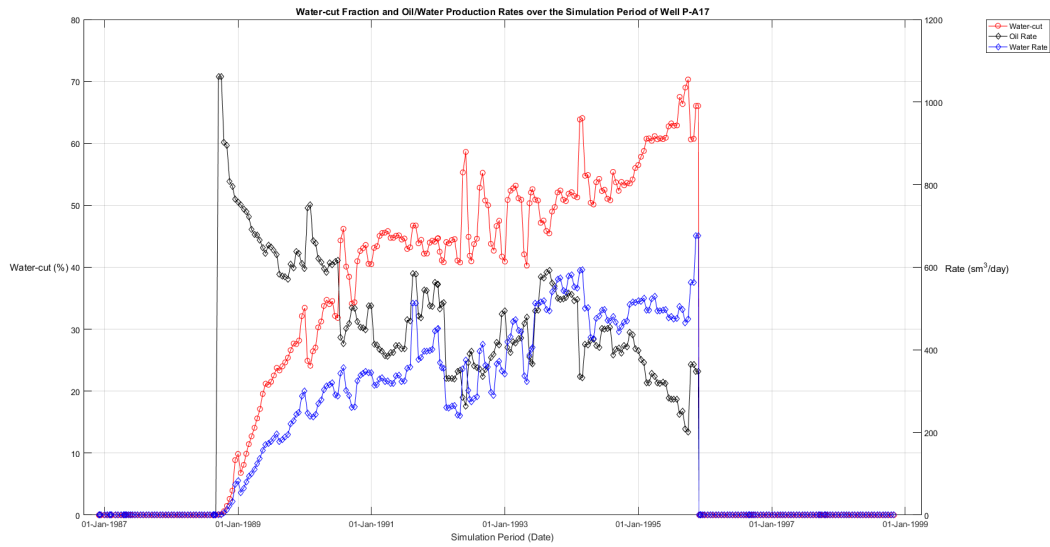


Figure 2.12: Well P-A17 production data ([click here for well position](#))

% of field cumulative oil produced: 14.51 %

% of field cumulative water produced: 9.524 %

Production Well P-A35

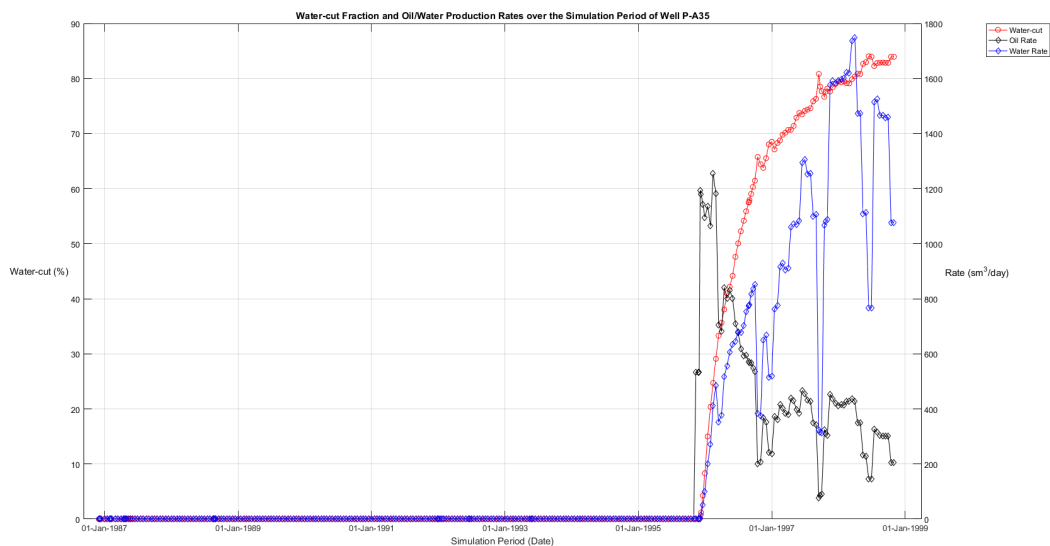


Figure 2.13: Well P-A35 production data ([click here for well position](#))

% of field cumulative oil produced: 6.333 %

% of field cumulative water produced: 11.01 %

Production Well P-A39A

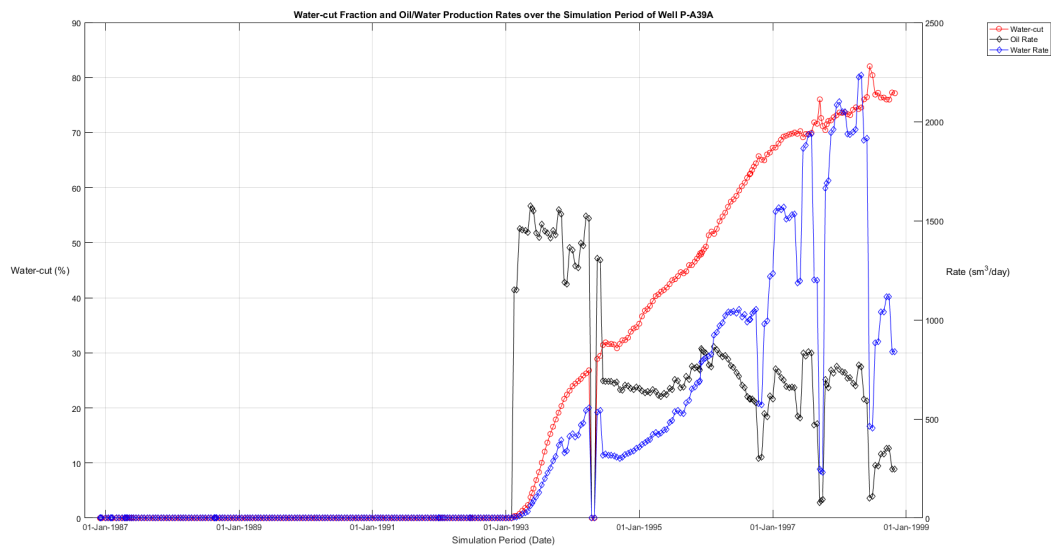


Figure 2.14: Well P-A39A production data ([click here for well position](#))

% of field cumulative oil produced: 19.76 %

% of field cumulative water produced: 18.4 %

Injection Well I-A5H

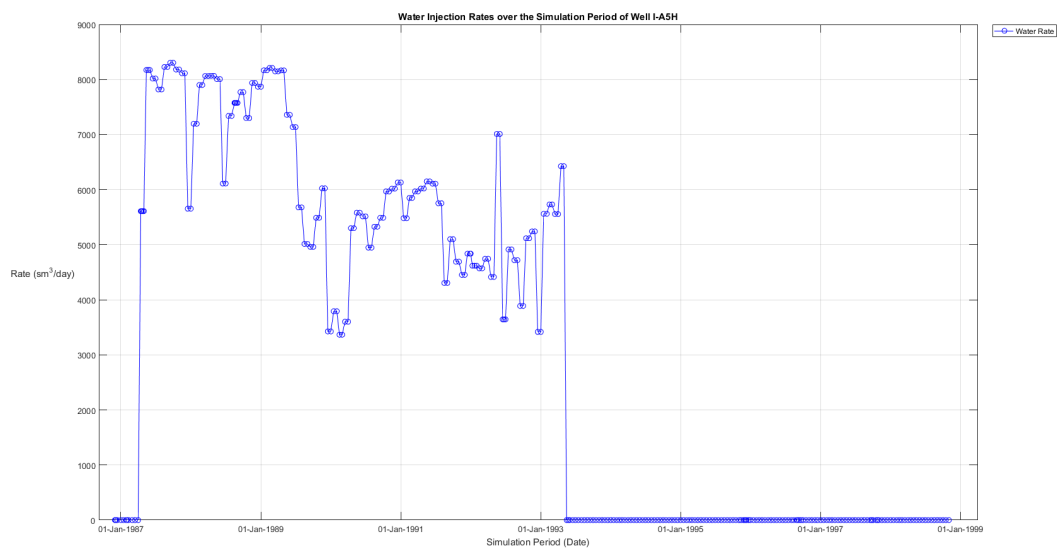


Figure 2.15: Well I-A5H injection data ([click here for well position](#))

% of field cumulative water injected: 58.64 %

Injection Well I-A38

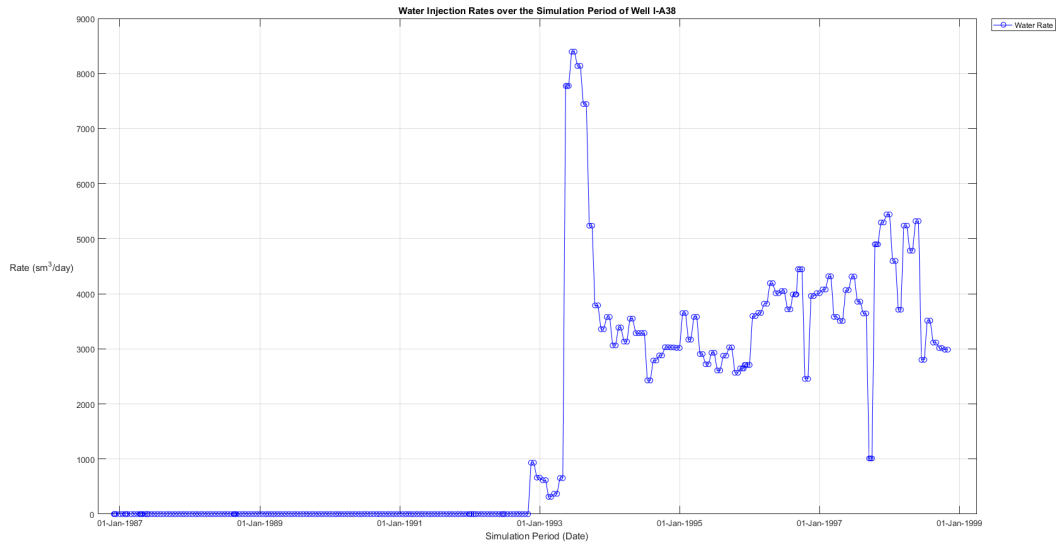


Figure 2.16: Well I-A38 injection data ([click here for well position](#))

% of field cumulative water injected: 37.36 %

Injection Well I-H2

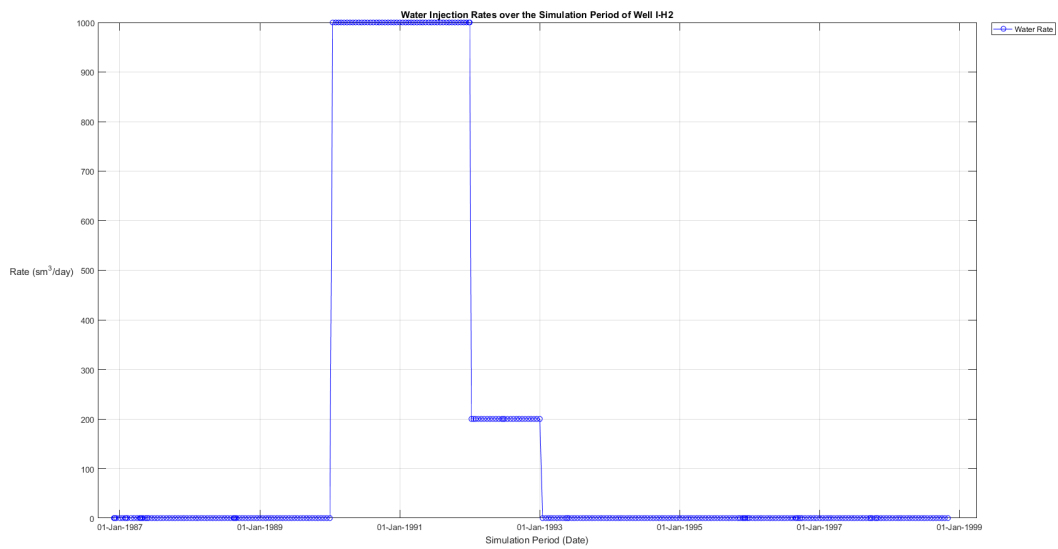


Figure 2.17: Well I-H2 injection data ([click here for well position](#))

% of field cumulative water injected: 3.997 %

2.6 Well Observed Production Data

During the time period that the simulation model runs (1st December 1986 until 1st November 1998) real well production data were recorded. These observed data are going to be used during the history matching operations on [chapter 4](#).

The figures below show the observed production data for all producing wells. Oil/water production rates (Black/Blue curves, Right y-axis) and water-cut (Red curve, Left y-axis) over time:

Production Well P-A1H

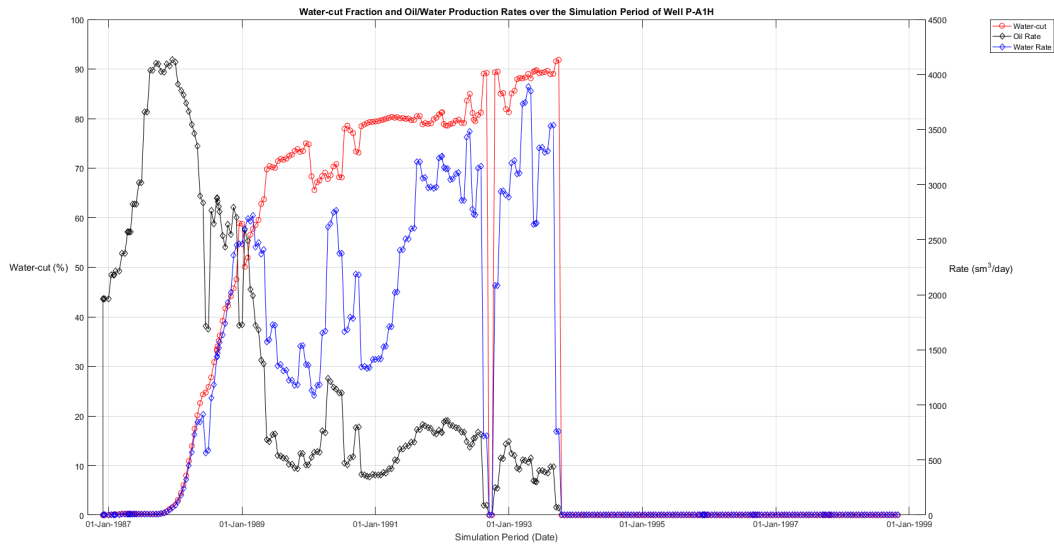


Figure 2.18: Well P-A1H observed production data ([click here for well position](#))

Production Well P-A2AH

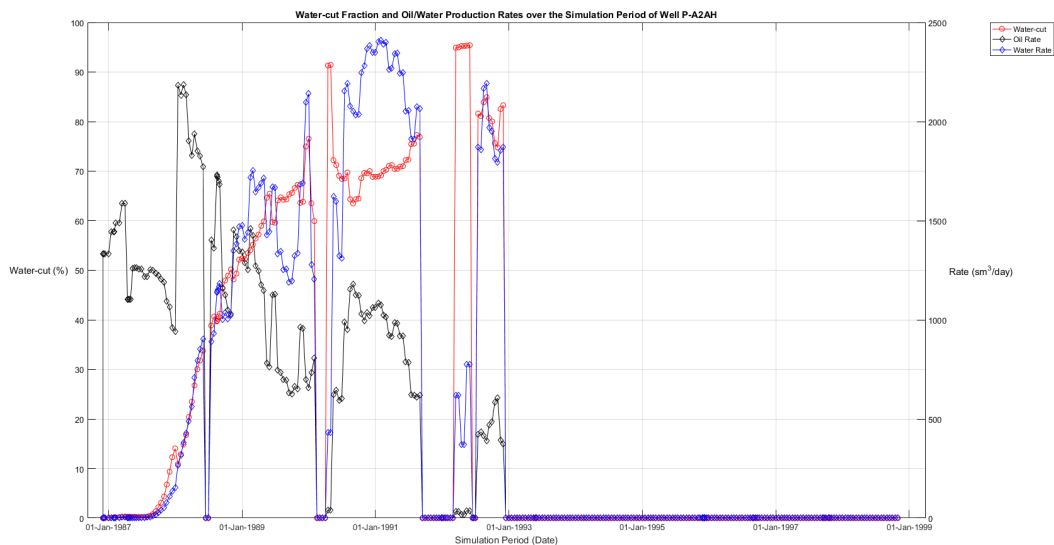


Figure 2.19: Well P-A2AH observed production data ([click here for well position](#))

Production Well P-A17

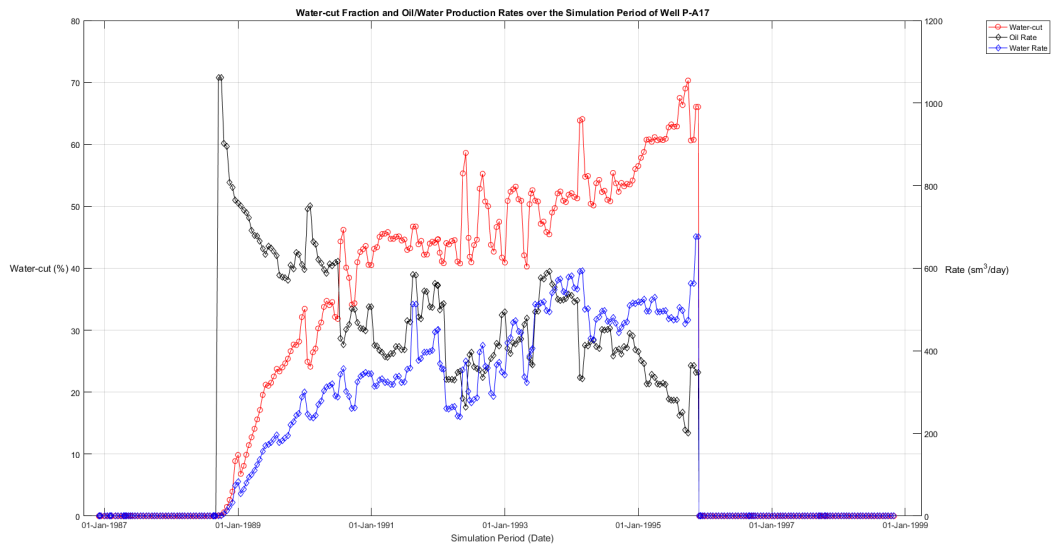


Figure 2.20: Well P-A17 observed production data ([click here for well position](#))

Production Well P-A35

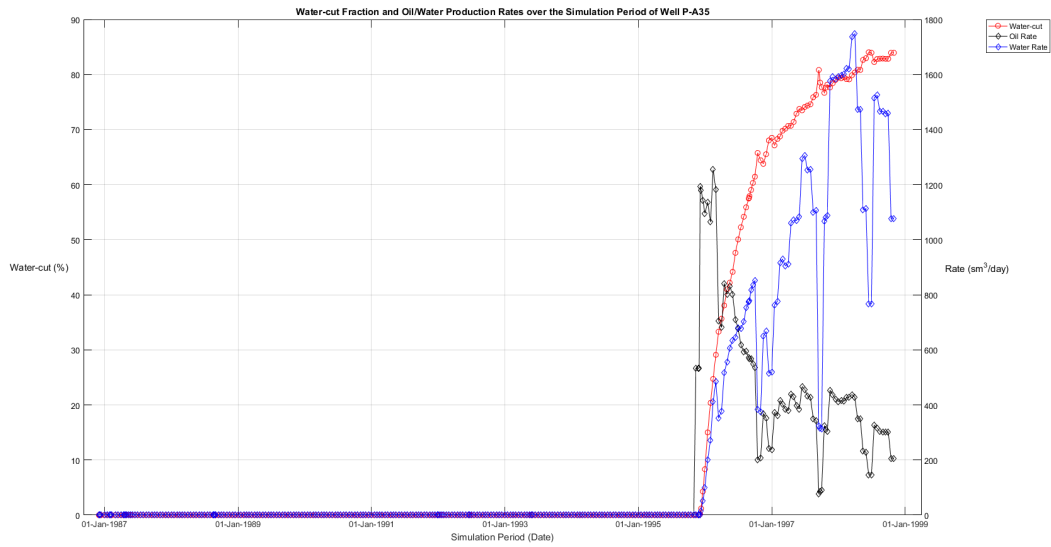


Figure 2.21: Well P-A35 observed production data ([click here for well position](#))

Production Well P-A39A

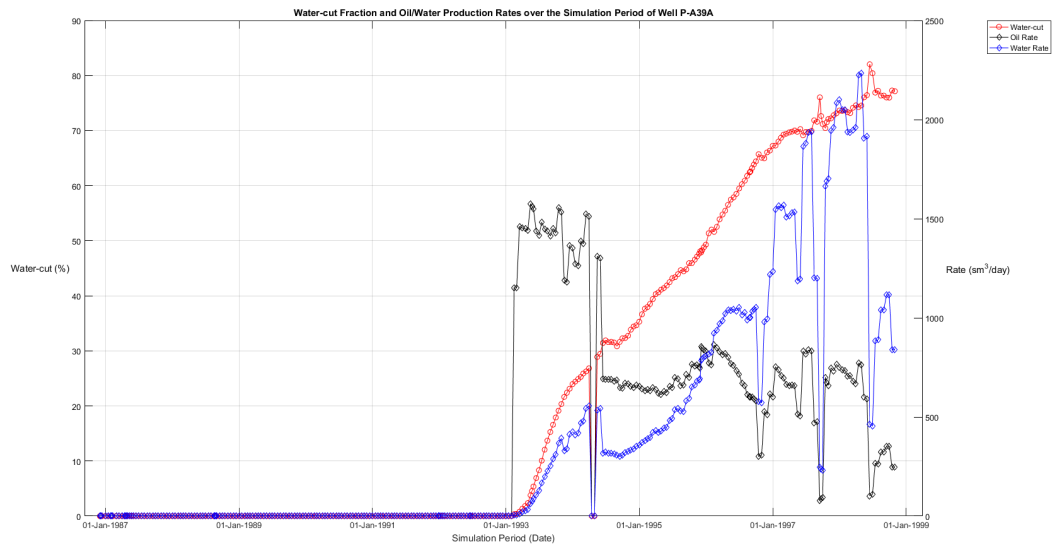


Figure 2.22: Well P-A39A observed production data ([click here for well position](#))

Chapter 3

Well Placement Optimization aided by PlanOpt

The initial model presented on [chapter 2](#) will be subjected to optimization procedures with *PlanOpt* Reservoir Simulation software in order to achieve increased oil production during the simulation period. All the assumptions and actions taken prior to optimization will also be discussed together with the final results of the optimization process.

3.1 Model Setup Prior to Optimization Process

PlanOpt software has a basic limitation. The distribution of wells that creates can only be vertical wells. On the sections below it will be discussed how the initial model was prepared in order to be introduced to *PlanOpt* software.

3.1.1 Pre-existing Production Wells

PlanOpt is going to be utilized in order to find new well positions compared to the original ones in order to achieve increased oil production. The number of original producing wells is five which means that from the distribution of wells that *PlanOpt* will create, after the optimization process five -or if it is possible less than five- wells will be chosen that will meet with specific control variables, constraints and limits. For this reason all pre-existing production wells should be disabled before introducing the initial model as input in *PlanOpt* software. The initial model's *DATA* file was modified and all producing wells were deleted.

3.1.2 Injection/Production Wells Management

The producing/injecting pattern of the initial model can not be followed by *PlanOpt*. The software in order to operate needs a field control variable (Oil production rate, Water production rate etc) value which will be kept constant until a limit or constraint is met and then is forced to alter. However, by observing the field production rates on [figure 2.7](#) concerning the initial model that is not the case. The injection profile as shown on [figure 2.9](#) also follows the field production pattern. By observing these figures it can be derived that although both field production and injection rates change continuously with time, there is a pattern that field injection rate is always higher than the field production rate.

Since *PlanOpt* constrains the field production rate to be constant, the same should apply for the injection wells in order to have pressure stability during the simulation period. Since the setup of the optimization should not diverge from the initial model the following action were taken.

Production Wells Averaging

Since the field production rate should be a constant control variable in order to be as close to the initial model as possible the summed average production rate of all wells will be used as shown on the figure below.

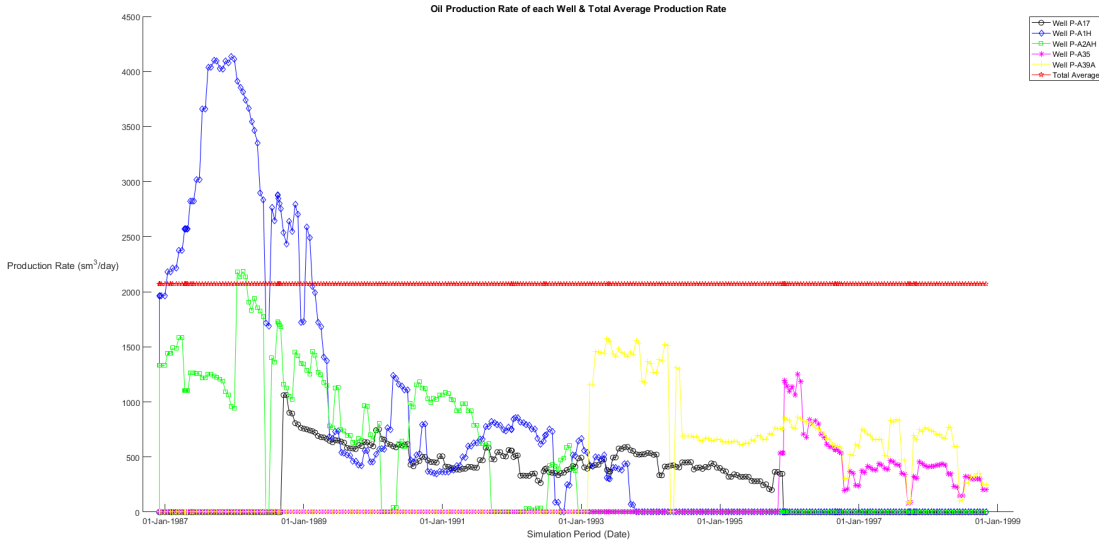


Figure 3.1: Oil production rates of all wells and summed average oil production rate of all wells (Red curve)

The summed average production rate of all wells is $2072.3 \text{ sm}^3/\text{day}$ of oil.

Injection Wells Averaging

The averaging of the injection wells is more complex than the previous case with the production wells. The specific production wells that during their operation resulted to the production rates as shown on the figures above will not be present during the optimization process and thus only the average value of their summed production was needed as a reference value for the optimization control variable.

The injection wells of the initial model will continue to exist during the optimization setup and operations and so their behavior (*I-A5H* is a vertical injection well, *I-A38* is a vertical/horizontal injection well) and operation pattern should be similar to the one they had on the initial model.

For this reason, all the injecting wells will be present at the optimization phase. Well *I-H2* which is not a real well and simulates a water influx from an adjacent region will continue to operate with exactly the same way like the initial model. Wells *I-A5H* and *I-A38* will operate with the same pattern (same injection start date and shut-in date) but with their injection rate averaged for as long they operate as shown on the figure below.

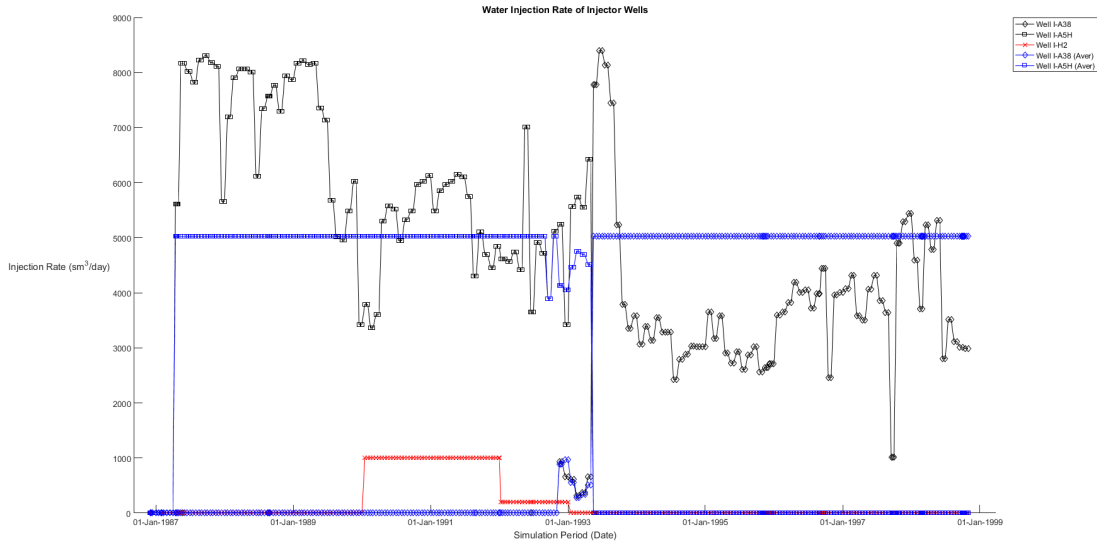


Figure 3.2: Water injection rates of injecting wells on initial model (Black curves) and average water injection rates of injecting wells (Blue curves)

As stated above well *I-H2* (Red curve) does not contribute to the average water injection value since it is not a real injection well. There is a small period of time that both wells are injecting, during this period the average water injection rate of each well was scaled so that the sum of the average water injection rates is constant at $5026.1 \text{ sm}^3/\text{day}$ of water.

After the average injection value was calculated for both injecting wells the initial model's *DATA* file was modified to include the above mentioned changes on the injection well scheduling.

3.2 Optimization Setup Processes

After the initial model was modified properly it is introduced in *PlanOpt* environment to setup and then begin the optimization process. This section describes all steps and procedures that were taken to optimize well placement that resulted in increased oil production.

3.2.1 Exclusion Zones

The first action to take when the modified initial model is introduced in *PlanOpt* is to set exclusion zones around the already existing wells (in this case around the pre-existing injection wells since no producing wells are present on the modified initial simulation model).

When wells are placed near each other -especially when their cells are neighboring with other wells' cells- interference may be caused while producing.

Exclusion zones prevent *PlanOpt* to place production wells on cells that are part of the zones. The range of the zones depends on the distance provided as input which is a circle with its center at the center of the cell with a pre-existing well and its radius is the distance provided by the user.

The exclusion zone chosen for this project is 90 m so as to create a zone which consists of all cells that are adjacent to the existing injection wells as shown on figure below.

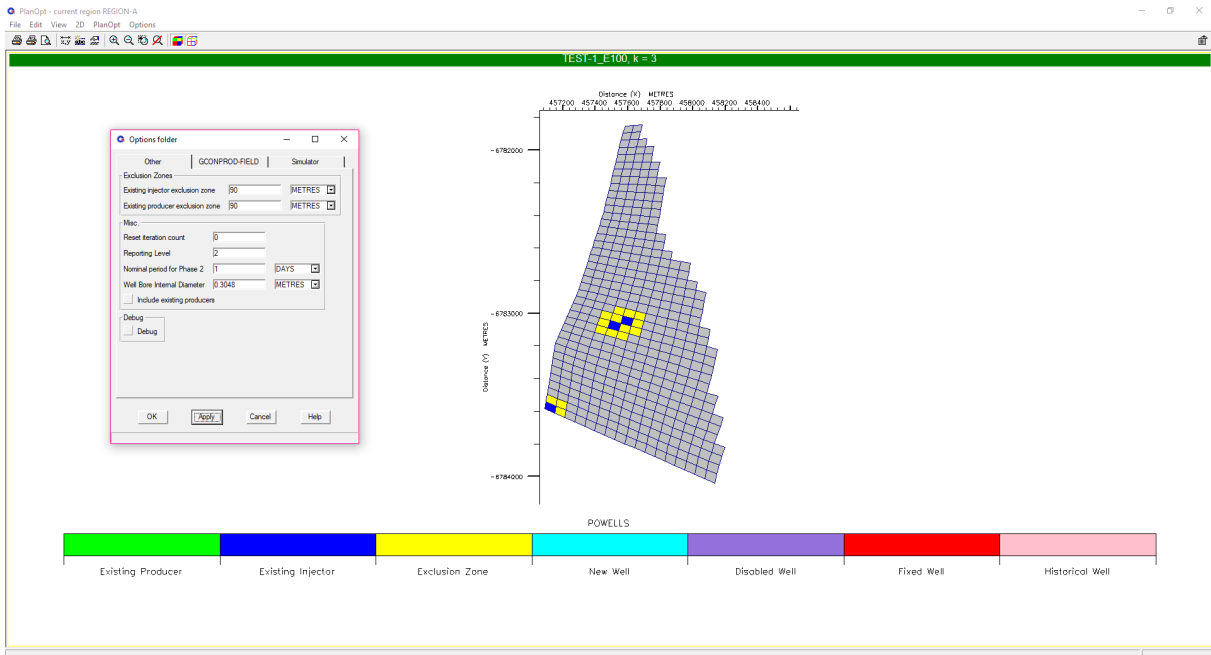


Figure 3.3: PlanOpt, setting the exclusion zones

3.2.2 Phase-1

Phase-1 is responsible for generating the initial distribution of wells based on specific criteria (minimum and maximum mobile saturations and well geometry).

The model that will be produced after optimization and the initial one should be similar so that they can be compared. All the wells present on the initial model have their connections between the 3rd and 12th layer of the reservoir, so the initial distribution of wells the will be created by PlanOpt will be constraint so that every new well will have its connections between these layers as shown on the figure below.

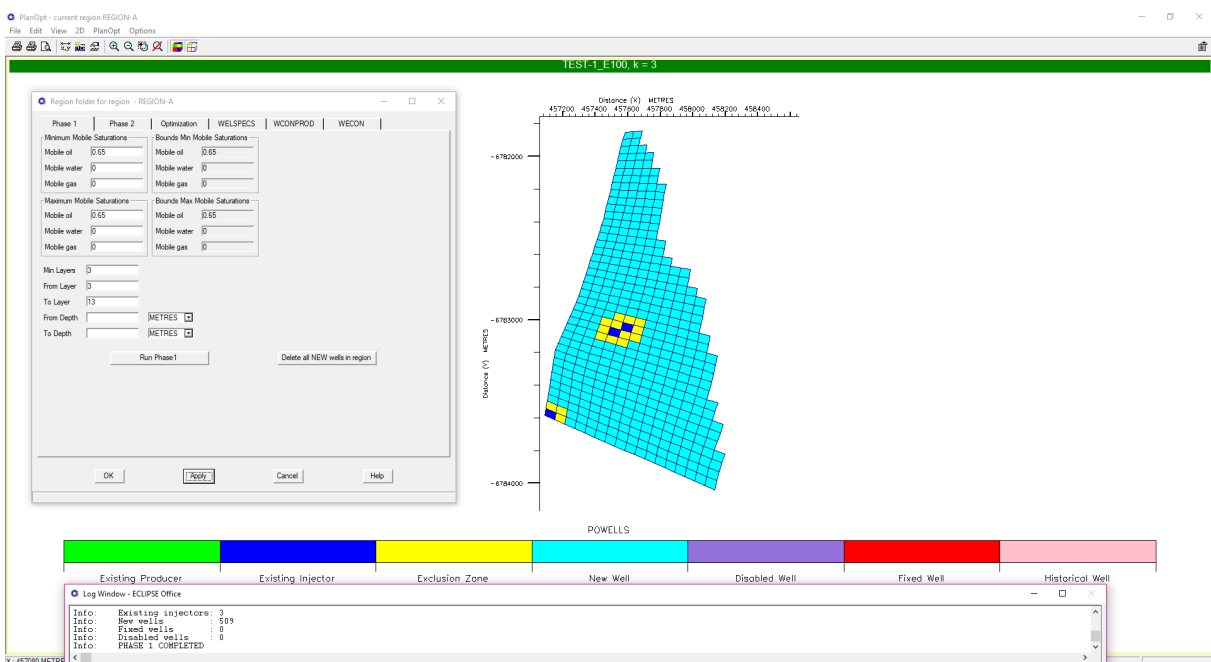


Figure 3.4: PlanOpt, after running phase-1

The *Log Window* prints that 509 new wells were added on the model. This well distribution will be subjected to further refinement until optimization starts and the desired number of wells is met.

3.2.3 Phase-2

Phase-2 is an optional step before optimization. Before proceeding to either *phase-2* or optimization the group rate control value should be assigned. Group rate control is the desired field oil production rate (which was calculated on [section 3.1.2](#) for the specific run) as shown on the figure below.

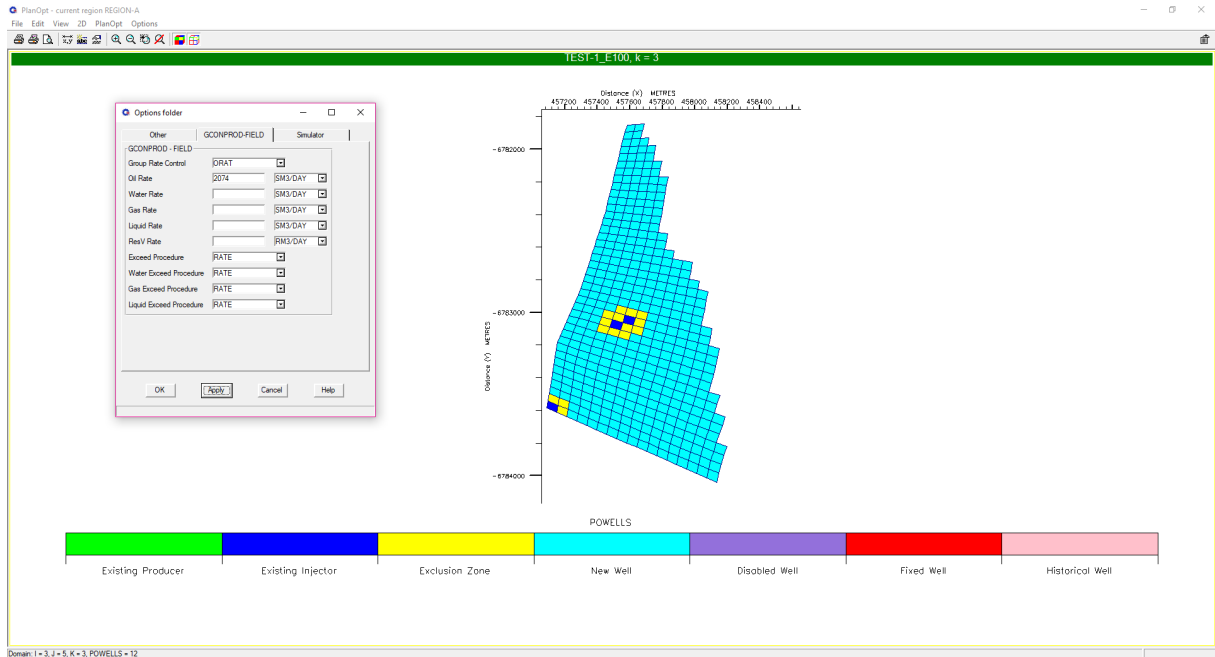


Figure 3.5: *PlanOpt*, setting group rate control (field oil production rate)

After the group rate control value is inserted the setup of *phase-2* can start as shown on the figure below.

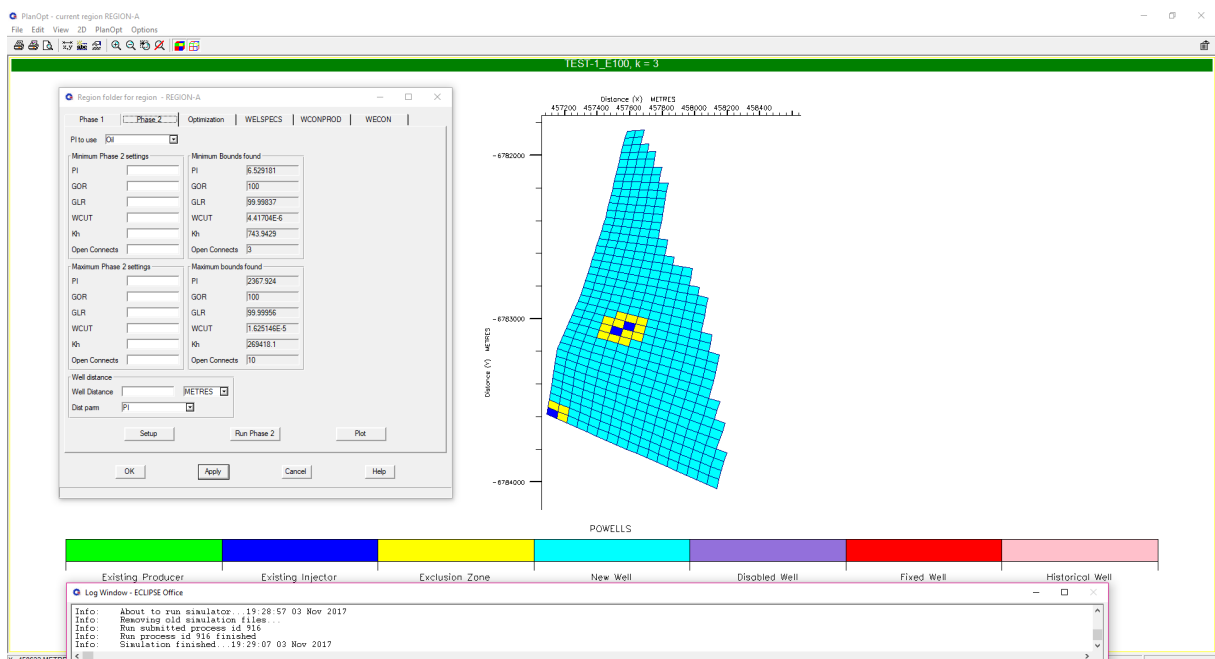


Figure 3.6: *PlanOpt*, setup of phase-2

When *phase-2* setup runs, the modified model inserted in *PlanOpt* runs for a nominal period of time (1 days on the current project) and calculates several well parameters (*PI*, *GOR*, *GLR*, *Water-cut*, *Kh* and the number of open connections) and finds their maximum and minimum bounds. By modifying the minimum or/and maximum parameters' range results in discarding the wells whose corresponding parameter values are not in the user specified range.

Another way to utilize the above parameters in *phase-2* is *Well distance* option. The wells of the initial distribution are ranked based on the *distance parameter* that is chosen, then based on the *well distance* inserted all the wells inside the specified radius are compared and the one with the highest rank will be active while the rest are going to be discarded.

This option was used on the current project since the way that it chooses which wells will stay active results in the least possible well interference as shown on the figure below.

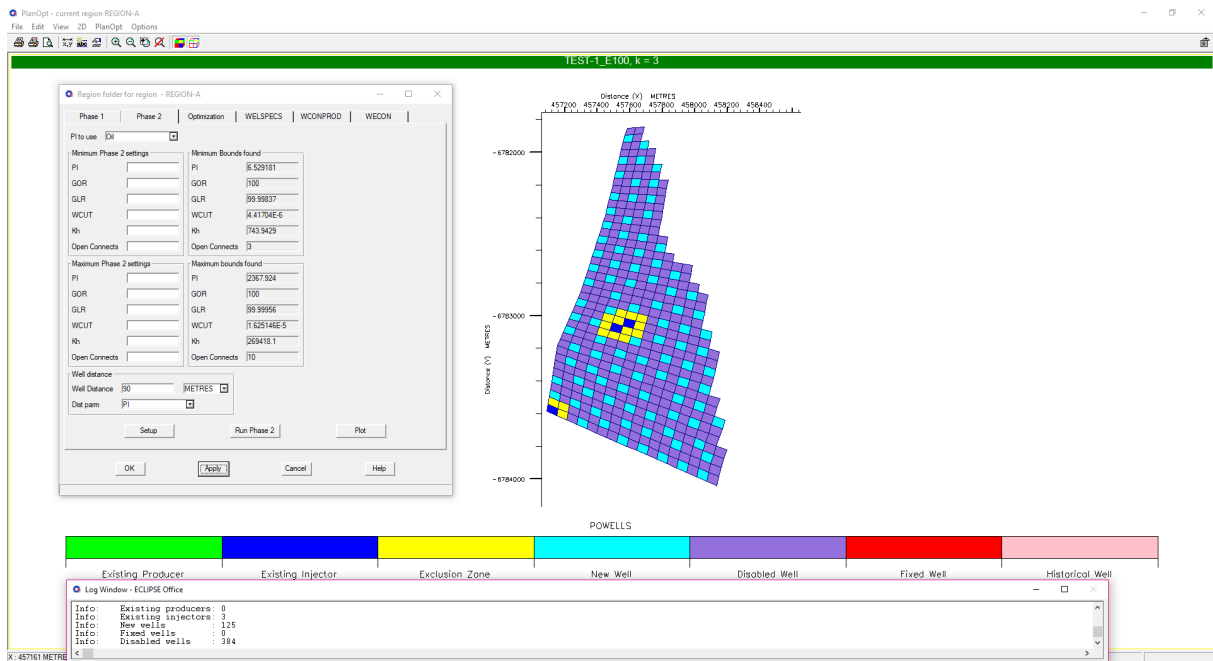


Figure 3.7: PlanOpt, after running phase-2

After *phase-2* is finished 384 wells were reported on *Log Window* that were disabled. Judging by the position of the remaining wells it can be noted that there are no wells adjacent to each other.

Running *phase-2* takes approximately 1 minute. If all the wells that were disabled during *phase-2* were to be included on the optimization operation, then the running time of optimization would greatly increase since more iteration would be needed in order to reach the desired number of wells.

3.2.4 Limits-Constraints

Since *phase-2* is finished, the next step is to set the limits and constraints of wells based on which the optimization will run. The basic limit on the current project is the bottom-hole pressure and the constraints that will be used are focused on managing the water-cut level of each well.

Bottom-hole Pressure Limit

In order to calculate what will be the bottom-hole pressure limit of each well, the worst case scenario is going to be examined. That is, a well drilled until the deepest active cell (at 1947 m depth below sea

bottom) producing almost solely water (extreme water-cut value). It is assumed that the fluid needs to be elevated from the well to the sea bottom and from there it will join a transport pipeline. The equation below calculates the minimum hydrostatic bottom-hole pressure needed to elevate the fluid column at the sea bottom level:

$$P_{bhp} = \rho_{fl} \left(\frac{kg}{m^3} \right) g \left(\frac{m}{s^2} \right) h(m) \times 10^{-5} = 191 \text{ bar} \quad (3.1)$$

where

P_{bhp} : is the calculated bottom-hole pressure limit

ρ_{fl} : is the density of the fluid, $1000 \frac{kg}{m^3}$ at the worst case scenario

g : is the gravity acceleration, $9.81 \frac{m}{s^2}$

h : is the height of the well/fluid column, 1947 m at the worst case scenario

As shown on the figure below a value of 200 bar is introduced in *PlanOpt*. The extra pressure of 9 bar are set as a safety margin:

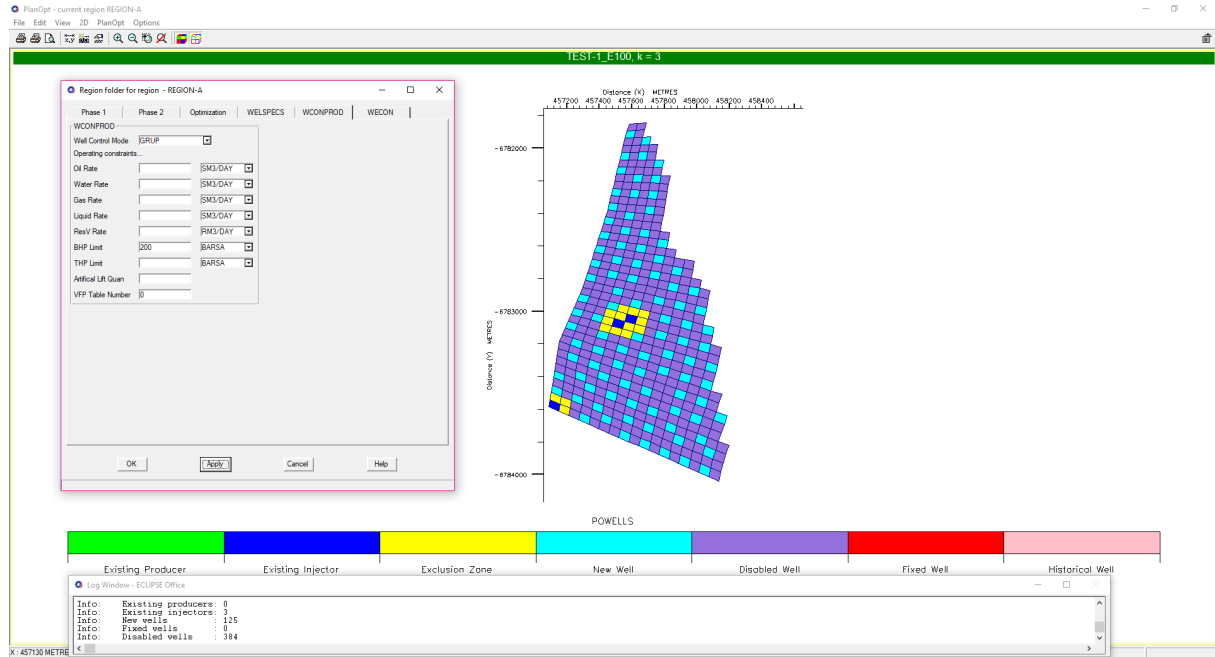


Figure 3.8: *PlanOpt*, bottom-hole pressure limit

Water-cut level constraints

During the development of the current diploma thesis project, several optimization runs of *PlanOpt* were conducted without constraining the wells using water-cut management. All runs resulted in cumulative oil production which was lower or almost equal than the one produced while running the initial simulation model as presented on figure 2.6. Even when optimization runs were conducted with the group rate control variable (mentioned on section 3.1.2) being assigned higher values than $2074 \text{ sm}^3/\text{day}$, the results were also disappointing.

Since water-cut was not constrained, during optimization *PlanOpt* was choosing wells regardless the fact that their water-cut was taking extreme values after some simulation steps and finally resulted in producing small quantity of oil. Finally water-cut constraints were used as shown on the figure below:

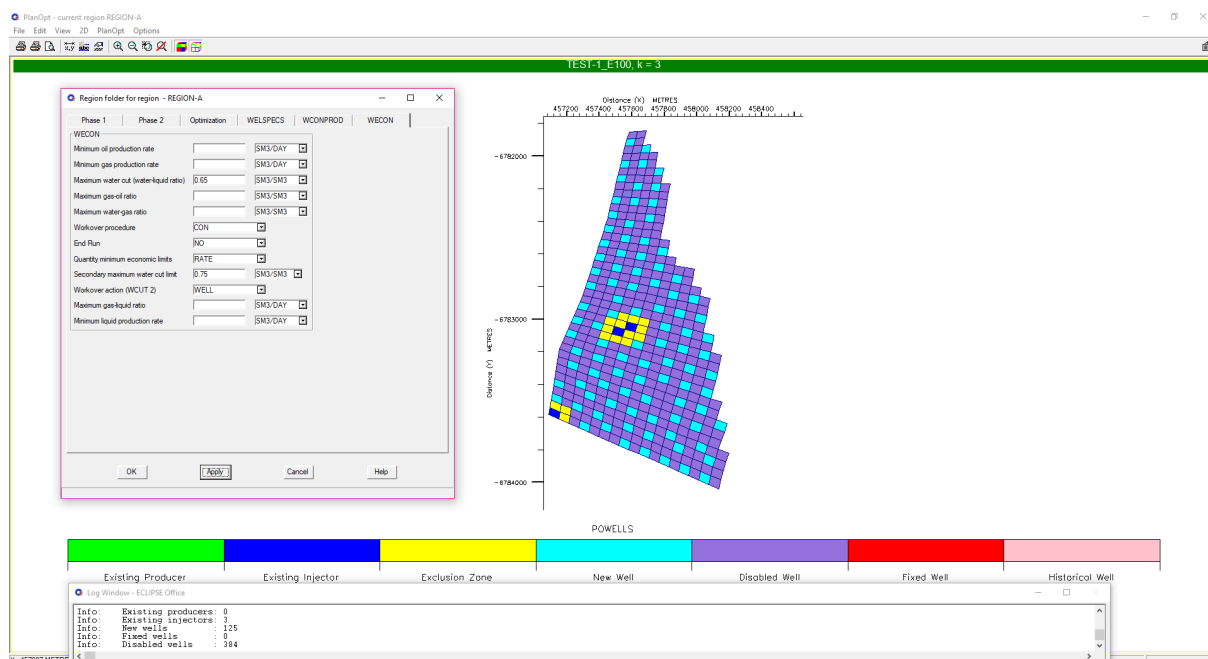


Figure 3.9: PlanOpt, water-cut constraints

When applying water-cut constraints *PlanOpt* utilizes *ECLIPSE* capability of conducting work-overs on wells. When setting active *Maximum water-cut* by introducing a value, if the water-cut of the well ever reaches this value then *Workover procedure* is triggered. There are several work-over procedures:

- *+CON*, if a well reaches maximum water-cut then the connection with the higher water-cut and all connections below it are shut
- *CON*, if a well reaches maximum water-cut then the connection with the higher water-cut is shut
- *WELL*, if a well reaches maximum water-cut then the well is shut

If *Secondary maximum watercut* is set active when all connection of a well are shut due to actions of the previous constraint then all connection open again until they meet the secondary constraint. When the secondary constraint is met *Workover action (WCUT 2)* is triggered and the chosen work-over is carried out.

After running several optimization projects with completely the same setup and different combinations of water-cut work-overs, the best option was found and presented on the figure above. *CON* work-over carries out the best results since only the connection that has reached the water-cut constraint is shut. The specific reservoir contains a region in the 7th and 8th layers with inactive cells which means that the layers above and below this region have no communication in the vertical direction. As a result when using *+CON* type of work-over which shuts all the connections below the connection that has reached the maximum water-cut constraint it is possible that connections whose water-cut values were not even close to the maximum water-cut constraint will be shut resulting in lower oil production rates.

The upper limit for the water-cut constraint was set to be 75 % for all optimization attempts since most of the wells of the initial model were shut or set to work-over procedures after this value was violated. Furthermore after setting the water-cut constraint higher than 75 % the cumulative oil production results were poor.

The lower limit for the water-cut constraint was set to be 60 % since below that value optimization process was always terminated due to high quantity of simulation and optimization errors due to the fact

that the maximum water-cut constraint was set to an extremely low value and the optimization process could not find wells to meet with the specific constraints.

3.2.5 Target Number of Wells - Well Reduction

The final step of the setup before optimization begins is to set the target number of wells that the optimization will try to reach, the percentage of well reduction that will be carried out at each iteration and the minimum number of wells that will be discarded during each iteration are shown on the figure below:

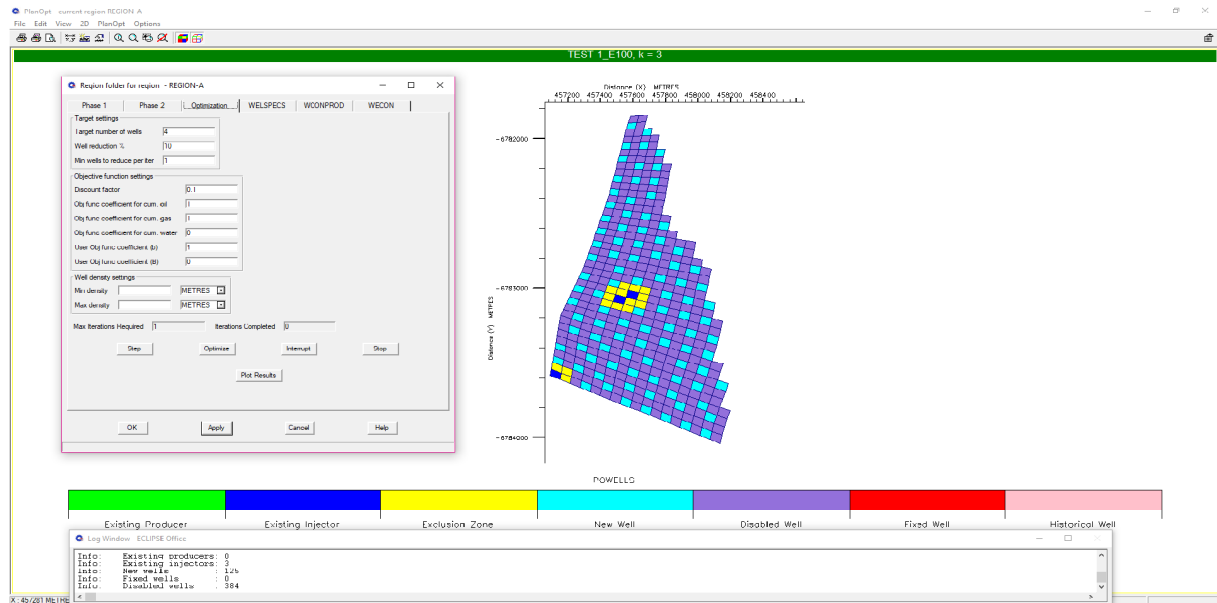


Figure 3.10: PlanOpt, Target Number of wells, well reduction and minimum number of well to discard at each iteration

3.2.6 Optimization

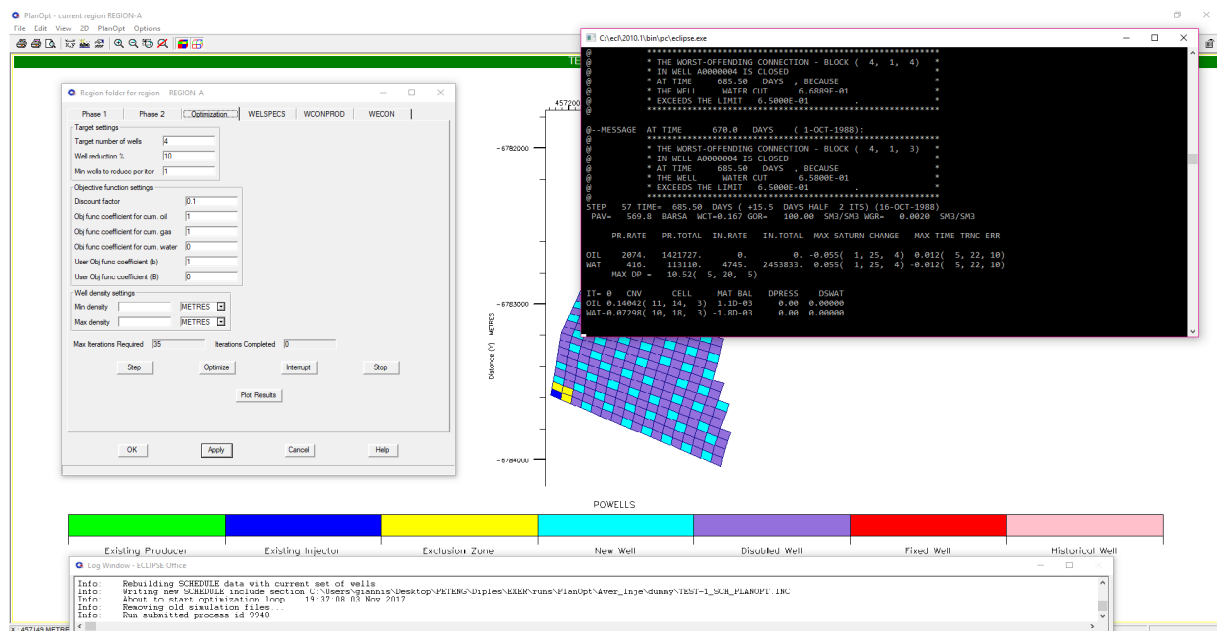


Figure 3.11: PlanOpt, optimization initiates

Based on the remaining number of wells from the initial well distribution, the target number of wells and the percentage of well reduction set by the user the total number of iterations is calculated when optimization starts. The optimization start time is printed on the *Log Window* as shown on [figure 3.11](#).

After optimization terminates successfully the end time is printed on the *Log Window* and the target number of wells chosen during the optimization process is displayed on *PlanOpt* as shown on [figure 3.12](#).

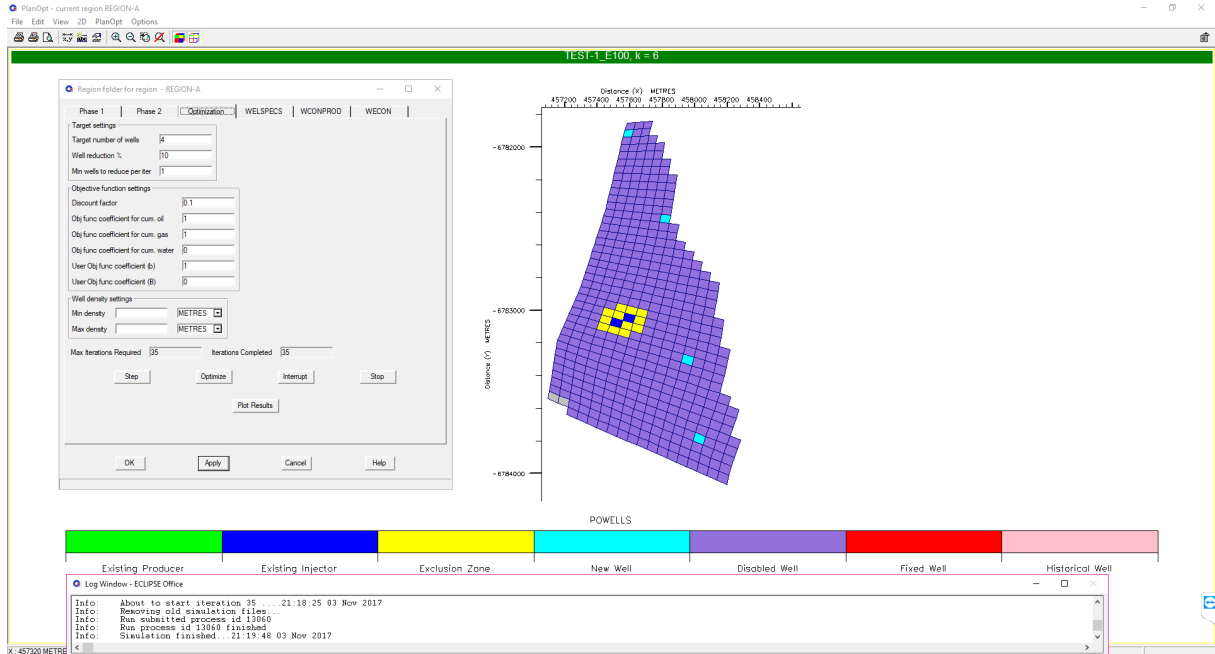


Figure 3.12: *PlanOpt*, optimization terminates

The optimization process needs about 2 hours to be completed for the current setup mentioned above.

After optimization is finished a new *DATA* simulation file is created by *PlanOpt* which contains all the information about the new model that was developed by the software.

For each optimization run two new *DATA* files were created one for a target number of wells of five and one of four in order to compare the models and examine if there is a possibility of achieving the same cumulative production with one drilled well less.

3.3 Oil Production Maximization

When the water-cut constraint was added on the optimization process the final optimized model resulted in higher cumulative oil production. However, further optimization should be conducted in order to find the maximum cumulative oil production that can be achieved while utilizing the water-cut constraint.

As mentioned on [section 3.2.4](#) maximum water-cut constraint is one variable able to vary the resulted cumulative oil production. The second variable that affects the resulted cumulative oil production after optimization is the group control variable (only when maximum water-cut constraint is active).

Water-cut values were chosen to range from the value of 60 % (lower water-cut constraint limit) to the value of 72 % (upper water-cut constraint limit) as shown on the table below.

Group rate control variable (oil rate) values were chosen to vary from the value of 2074 sm^3/day (lower limit of the group control rate) to the value of 3600 sm^3/day as shown on the table below.

No.	Water-cut (%)
1	63.0
2	64.0
3	64.4
4	64.5
5	64.6
6	65.0
7	65.5
8	66.0
9	67.0
10	70.0
11	72.0

Table 3.1: Water-cut values

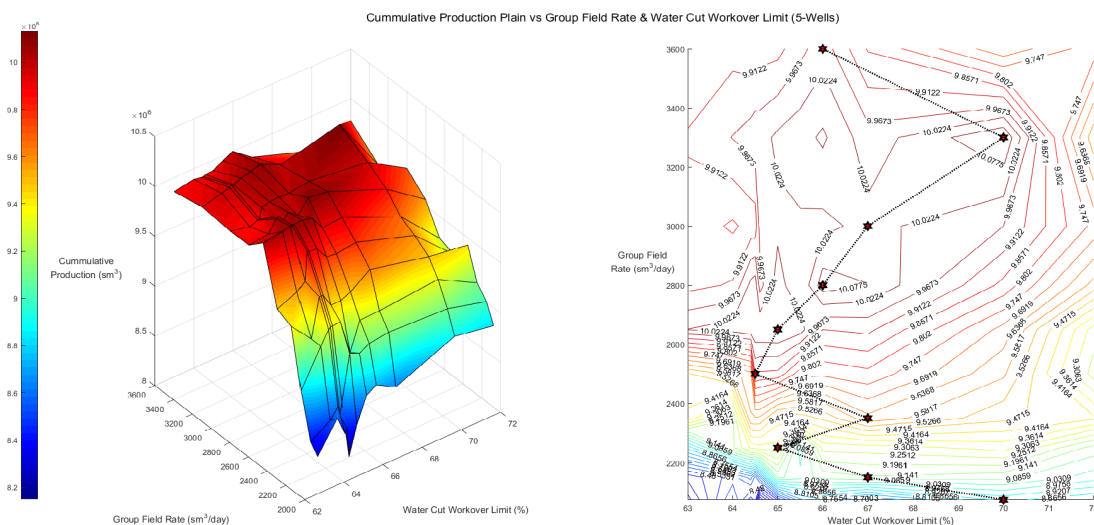
No.	Oil rate (sm^3/day)
1	2074
2	2150
3	2250
4	2350
5	2500
6	2650
7	2800
8	3000
9	3300
10	3600

Table 3.2: Group field oil rate

The number of water-cut values times the number of group rate control values is the number of optimization runs needed in order to create a dependency of cumulative oil produced after each simulation with both the water-cut constraint and the group control rate.

After the optimization runs were finished a 3D plot of a plain was created where each water-cut and group control rate values (x-axis, y-axis) correspond to a specific cumulative oil produced value (z-axis). Finally a contour plot was created based on the cumulative oil produced data and the corresponding water-cut and group control rate values. The contour plots are 2D plots which depict 3D plots of plains or meshes. All continuous lines having the same color denote that every point that belongs on the line have the same value.

Apart from the cumulative oil production plain-contour plots for 5 and 4 wells, there will be plain-contour plots of the percentage of increase of cumulative oil production on the cumulative production of the initial model and finally of the percentage of the original mobile oil in place that have been produced. The figures of the plains-contour plots mentioned above are presented below:



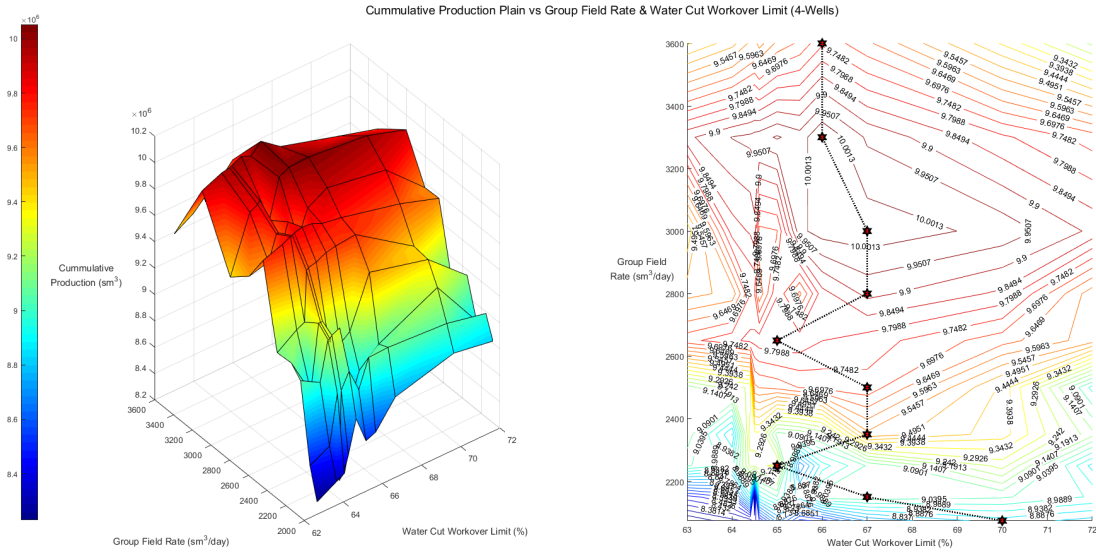


Figure 3.14: Oil cumulative production plain and contour plot for 4 wells

By observing the plains on the figures above it is clear that there is a strong dependency of the cumulative oil production on the group field rate. As group field rate increases production also increases until a "hill" of maxima is reached. After that point as group field rate keeps increasing, production decreases. As far as the water-cut is concerned there is a pattern dictating the cumulative oil production as water-cut work-over limit increases which is minor compared to the one of group field rate. As water-cut work-over limit increases there is also a small increase in cumulative oil production until a maximum value is reached after which production decreases as water-cut work-over limit keeps increasing.

It should be noted here that simulation runs concerning the water-cut work-over limit of 60% were omitted from figures since most of them produced huge amount of errors during the optimization procedure as explained on section 3.2.4.

In order visualize the magnitude of dependency of cumulative oil production on group rate control and water-cut work-over limit curves below were produced:

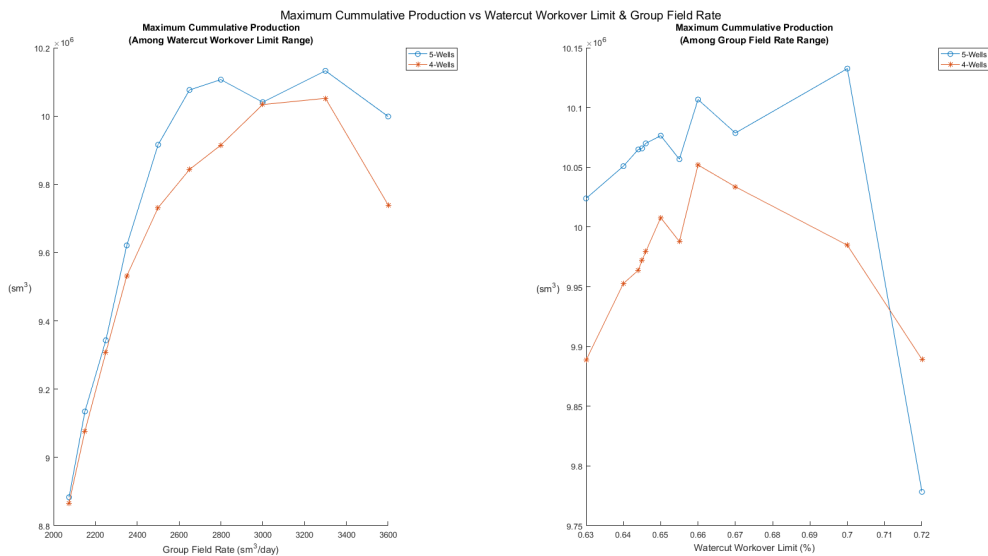


Figure 3.15: Maximum cumulative oil production curves

The left curve shows the maximum values of cumulative oil production among all water-cut work-over limit simulation runs with respect to group field rate while the right curve shows the maximum values of cumulative oil production among all group field rate simulation runs with respect to water-cut work-over limit. In both plots as the corresponding x-axis variable increases cumulative oil production also increases until a maximum value is reached after which production starts to decrease. However, at the left plot the range of values of the cumulative oil production is of 10^6 magnitude and at the right plot the range is of 10^5 magnitude meaning that the group field rate variable dependency compared with the water-cut work-over limit variable dependency is higher by one order of magnitude. Since group field rate is the main reason of cumulative oil production increase, the maximum cumulative oil production of each group field rate value among all water-cut work-over limit values (left plot of the figure above) were printed as black/red stars on the contour line plots of figure 3.13 and figure 3.14.

The figures below present information about the percentage of increase of cumulative oil production with respect to the initial model and the percentage of original mobile oil in place that have been produced:

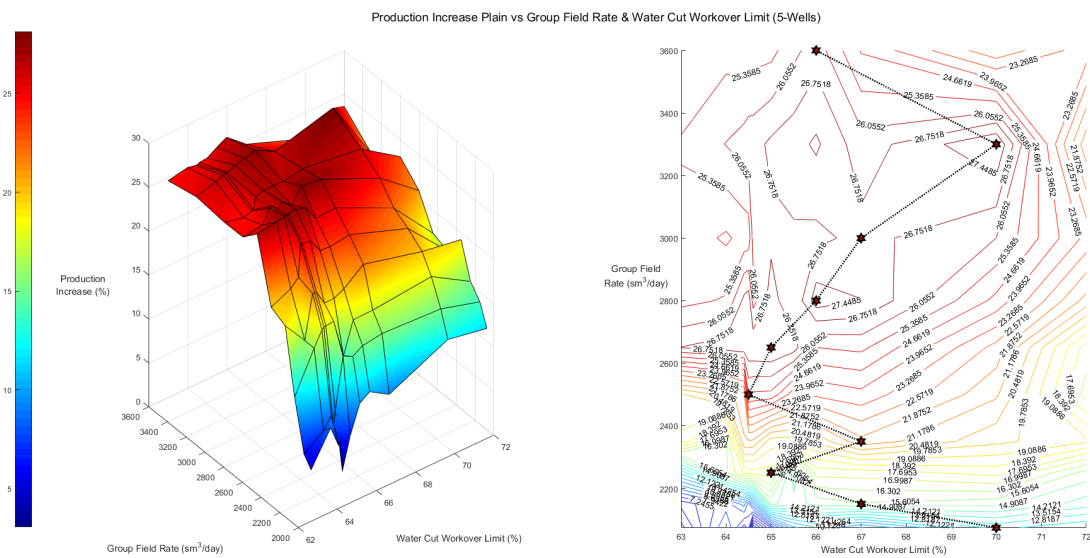


Figure 3.16: % of increase of cumulative production plain and contour plot for 5 wells

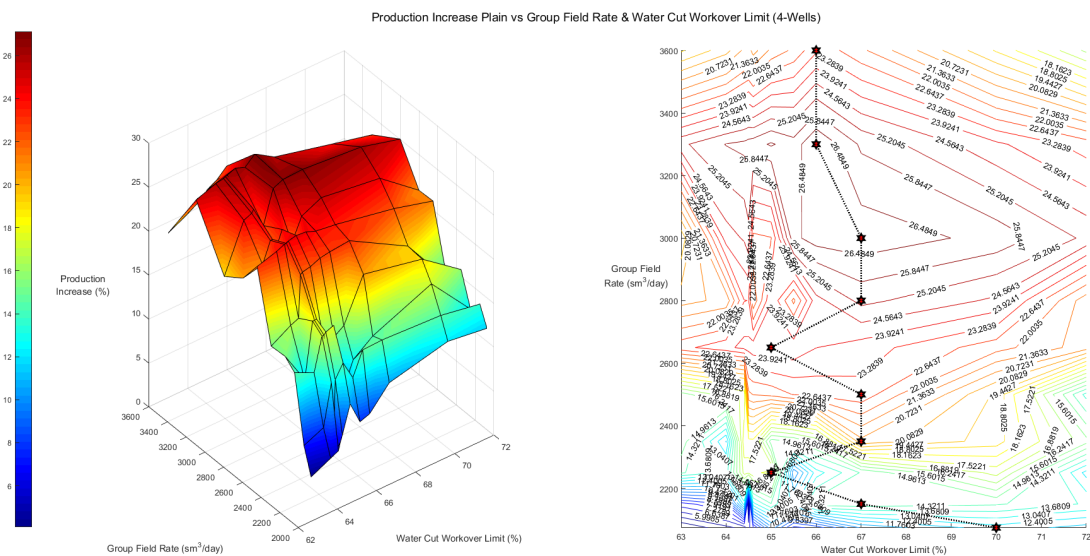


Figure 3.17: % of increase of cumulative production plain and contour plot for 4 wells

3.3. OIL PRODUCTION MAXIMIZATION

By observing the figures above it can be derived that the optimization process, regardless of the values chosen from tables 3.1 and 3.2, results in cumulative oil production which is always higher than the one of the initial model.

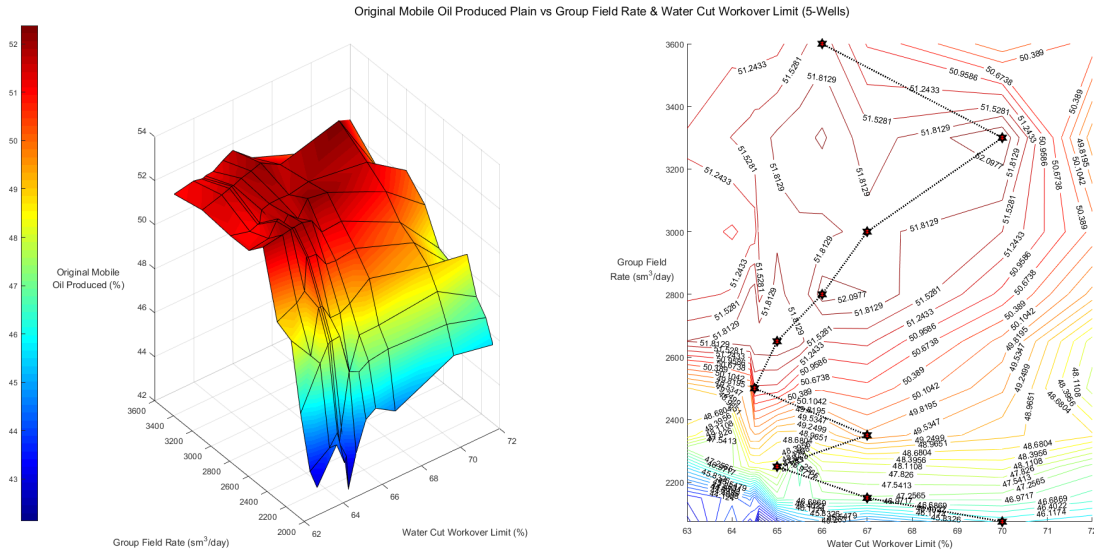


Figure 3.18: % of original mobile oil in place produced plain and contour plot for 5 wells

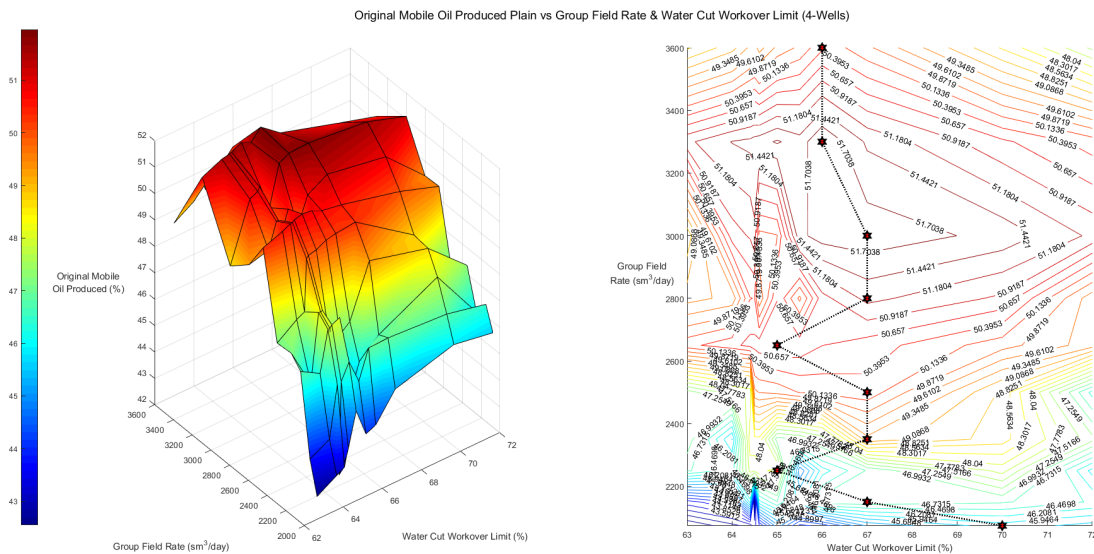


Figure 3.19: % of original mobile oil in place produced plain and contour plot for 4 wells

Since the cumulative production of all models created by the optimization process was always higher than the one resulted from the initial model (figures 3.16 and 3.17) the percentage of oil produced out of the original mobile oil in place will also be accordingly higher as shown on the figures above.

Finally the maximum percentage of increase of cumulative oil production with respect to the initial model and the percentage of original mobile oil in place that have been produced among the water-cut work-over limits values with respect to group field rate values will be presented on the figure below, since group field rate values had major effect (one order of magnitude greater than the corresponding effect of water-cut work-over limit values) on the results of the simulation runs.

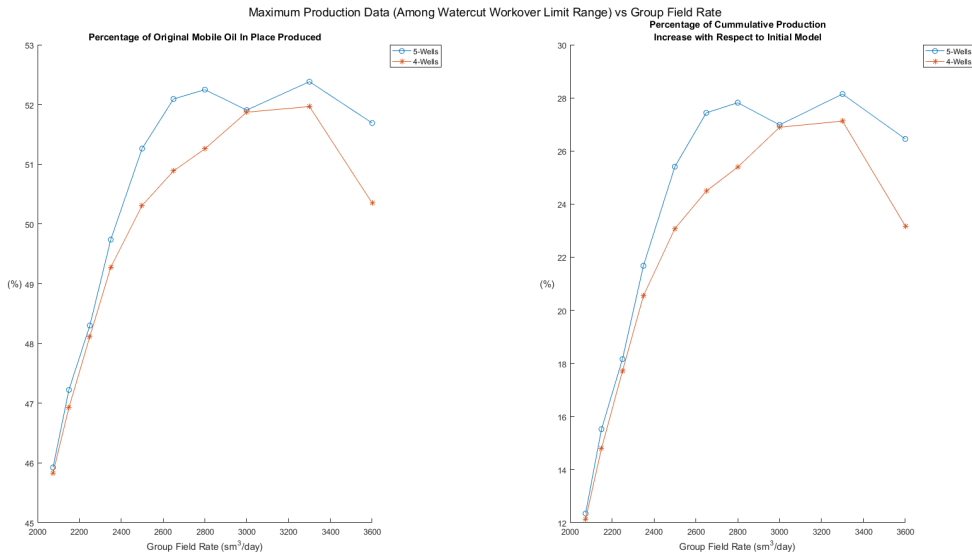


Figure 3.20: Maximum % of increase of cumulative oil production with respect to the initial model and original mobile oil in place that have been produced

By observing the figures presented above, there are regions on the 3D plain that although the water-cut work-over limit step is tiny the cumulative oil production value changes abruptly.

The figure below shows all the lines that create the 3D plain in a 2D plot in order to describe the mentioned behavior above:

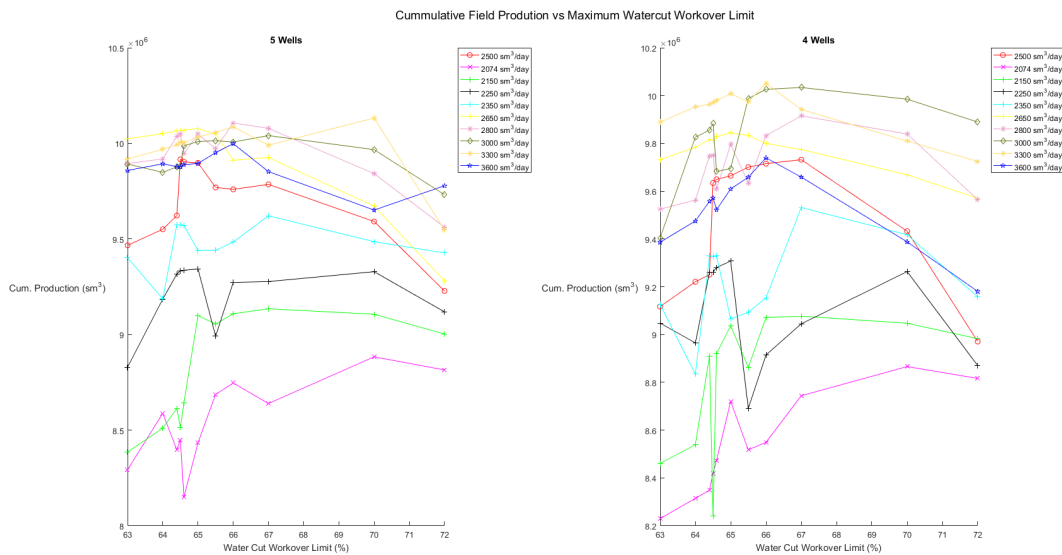


Figure 3.21: Cumulative oil production vs Water-cut work-over limit

For example by observing the red curve of the left plot between the 3rd and the 4th value of cumulative oil production an abrupt increase is visible although the water-cut work-over limit changes from 64.4 % to 64.5 %. The same behavior appears also on other curves of the plots above. The majority of the curves appear to develop this behavior in water-cut work-over limit ranges where the values chosen are very close to each other like the example mentioned above.

The behavior described above is impossible to have some sort of physical meaning since a change of 0.1 %

on the water-cut work-over limit can not cause an almost 7% increase on the cumulative oil production.

In order to understand the reason of the above behavior *FlowViz 3D* reservoir simulation viewer was used for the simulation models concerning the 3rd and the 4th point of the red curve on the left plot.

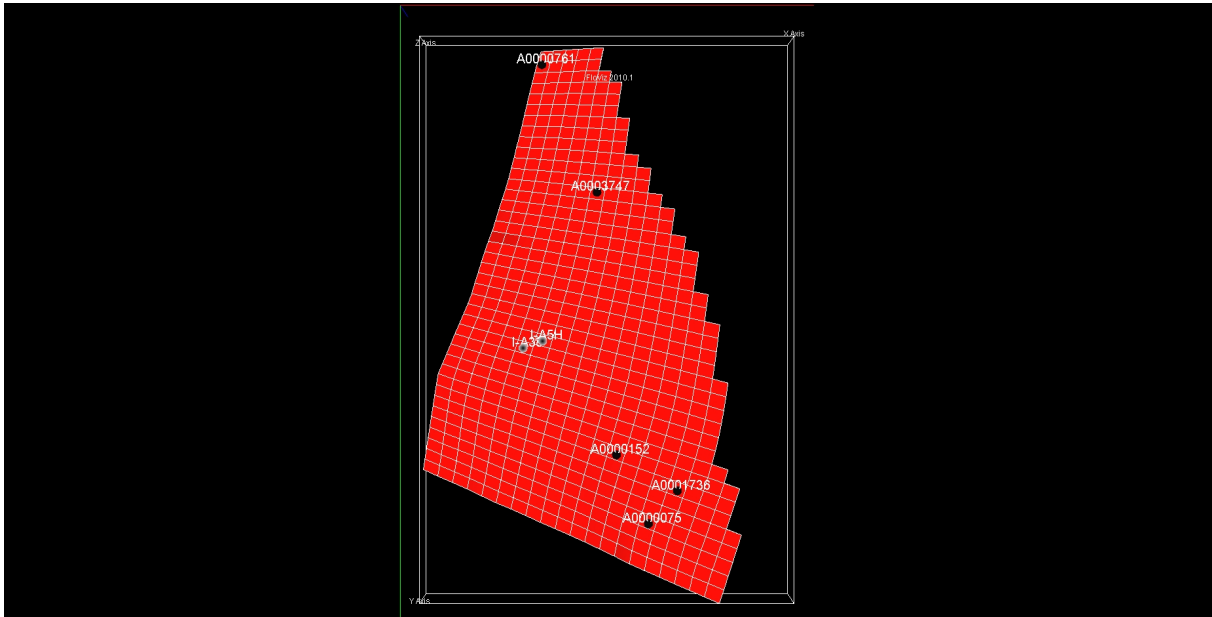


Figure 3.22: Water-cut work-over limit of 64.4 % well position

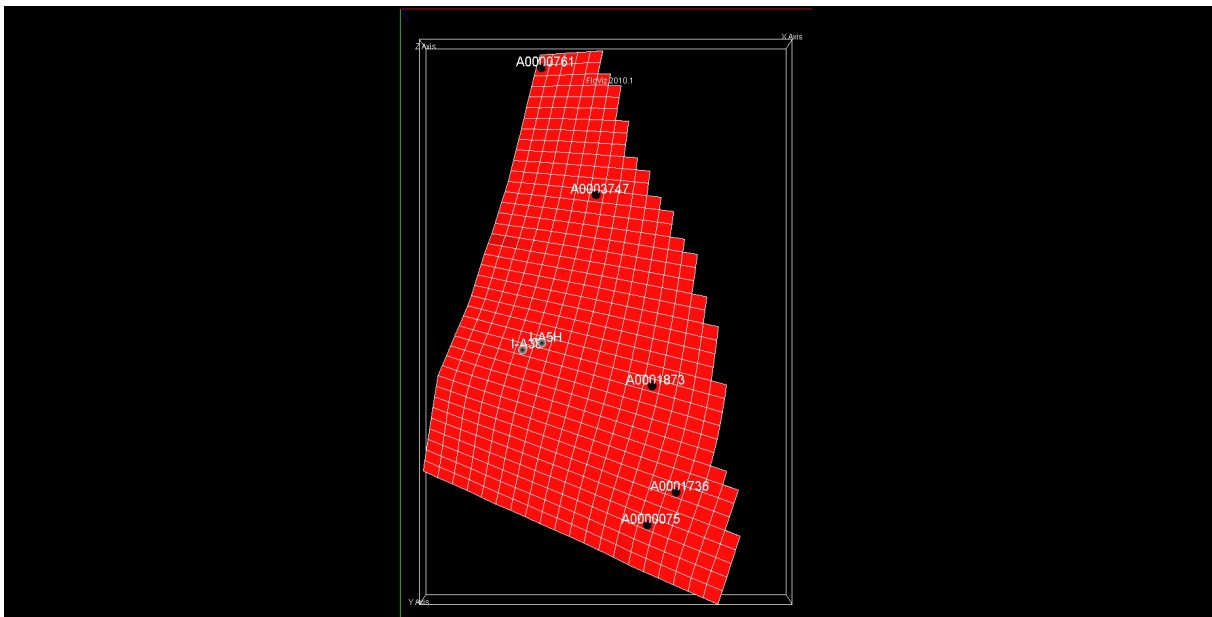


Figure 3.23: Water-cut work-over limit of 64.5 % well position

By observing the figures above it can be concluded that while four out of five wells remain exactly at the same position in the two simulation models, the fifth well has different position in the simulation models concerning the 64.4% and 64.5% water-cut work-over limit. Apparently the 0.1% of change in the water-cut work-over limits between the two simulation models affected the optimization process. The optimization process in order to comply with the new water-cut work-over constraint had to chose each time a new well position regarding the fifth well. The new well that was chosen resulted finally in higher cumulative oil production since the region that was placed was further away from other producing wells. On the other hand by looking on [figure 3.21](#) there are similar simulation results that the small change

of water-cut work-over limit produced a well position pattern that finally resulted in an abrupt drop of cumulative oil production. *PlanOpt* can not predict what future effect might have the position of wells near each other and so further constraints might be needed in order to force the wells being positioned far from each other to minimize well interference and in the same time chose well positions that will maximize the oil production.

3.4 Optimal Simulation Model Analysis

In all figures presented above concerning the optimization runs and the resulted models it can be observed that all runs having target number of wells set to 4 have always lower cumulative oil production than runs having target number of wells set to 5. At this point in order to chose which model will be chosen as having produced the best simulation outputs only the cumulative oil production is taken into account. There are several other parameters which should be taken into account when making the final selection of which model to chose like the cumulative water production, the water injection rates and of course economic factors which will lead in choosing the final number of wells that will be drilled. On the current diploma thesis project since the aim is to maximize the cumulative oil production, the model resulting so will be chosen to be further discussed.

The simulation model which produced the higher cumulative oil production will be further discussed. The figure below shows the cumulative oil production with respect to the water-cut work-over limit for the group field rate value of $3300 \text{ sm}^3/\text{day}$.

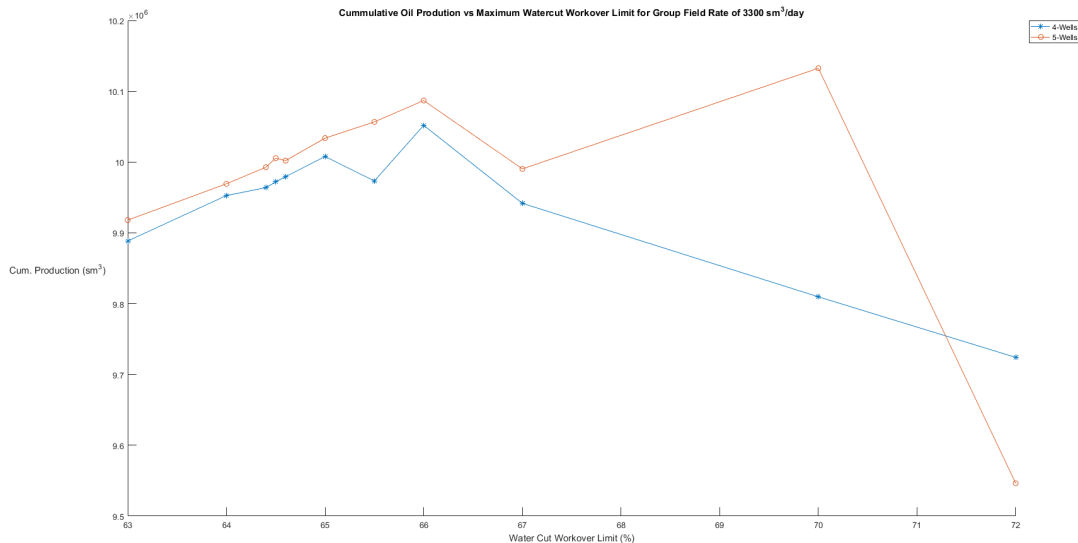


Figure 3.24: Cumulative oil production vs Water-cut work-over limit for $3300 \text{ sm}^3/\text{day}$

By observing figure 3.21 it could be concluded that the curves corresponding to the group field rate of $3300 \text{ sm}^3/\text{day}$ included the maximum value of cumulative oil production. The maximum value corresponds to 70 % water-cut on the curve concerning the 5 wells pattern. The simulation model which resulted to the maximum value of cumulative oil production will be presented below.

The discard sequence of wells during the optimization process concerning the optimal simulation model is presented on appendix B. By observing which wells are discard after each iteration of the optimization process, there should be a pattern that all wells around the injection wells are discarded from the beginning apparently because early water breakthrough occurs resulting to high water-cut and low oil production rates.

On the following section field data and well production data of the optimal simulation model are going to be presented.

3.4.1 Field Data

All figures below present both the curves of the initial simulation model (Black curves) and the optimal simulation model (Red curves) for ease of comparison.

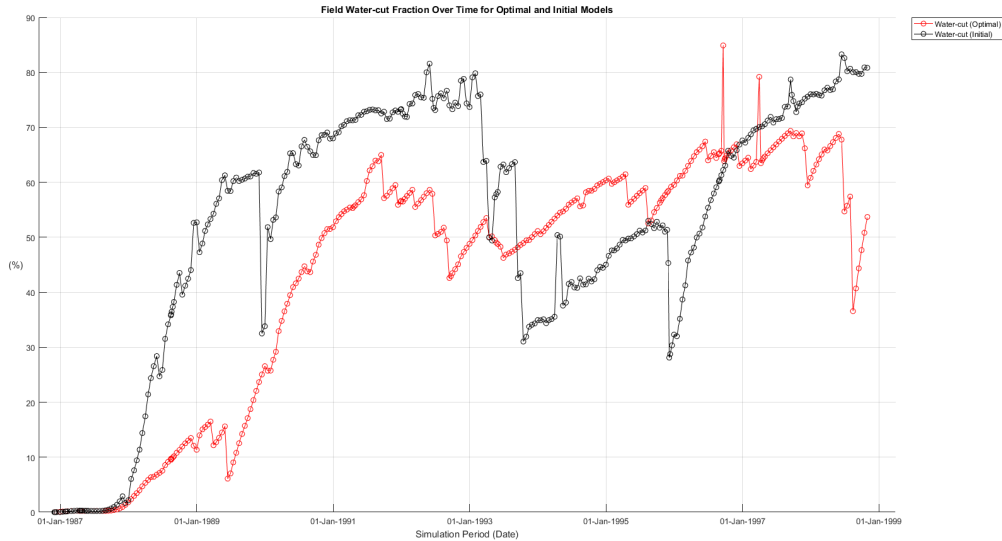


Figure 3.25: Field water-cut fraction over simulation time, Optimal model (Red curve) - Initial model (Black curve)

The water-cut fraction of the optimal model is lower than the corresponding water-cut of the initial model for most of the simulation time resulting to lower percentage of water compared to that of the oil.

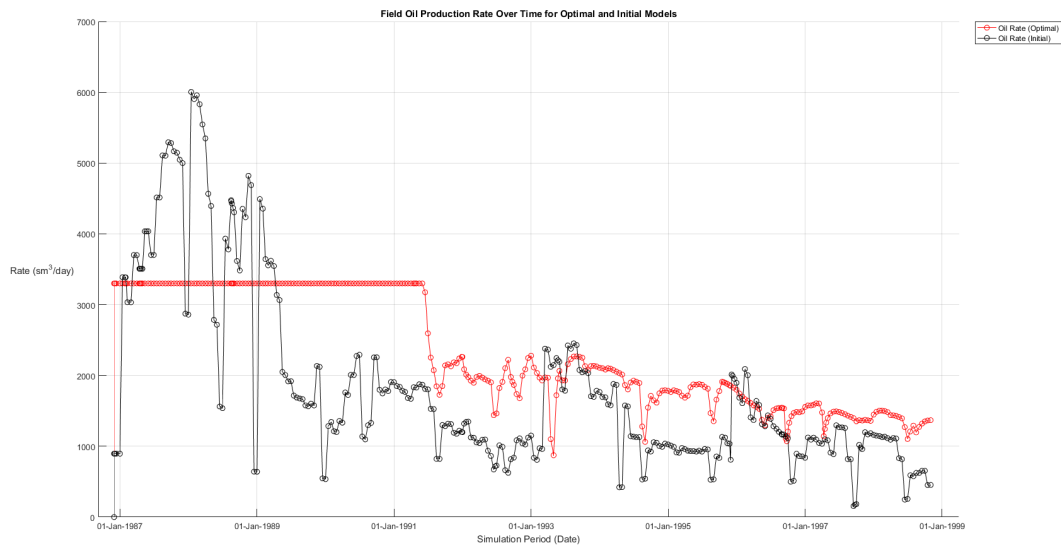


Figure 3.26: Field oil production rate over simulation time, Optimal model (Red curve) - Initial model (Black curve)

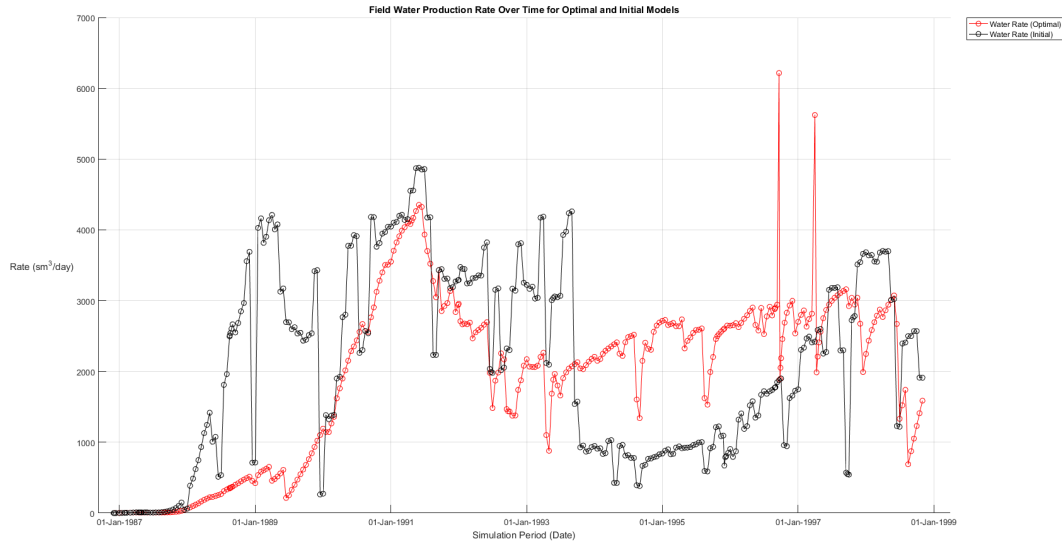


Figure 3.27: Field water production rate over simulation time, Optimal model (Red curve) - Initial model (Black curve)

By observing the figures above it can be concluded that the simulation model created by *PlanOpt* during the optimization process begins producing based on the group rate control variable since as shown on figure 3.26 field oil production rate is stable at $3300 \text{ sm}^3/\text{day}$. After several simulation steps some limits and constraints of the model (well bottom-hole pressure, water-cut work-over limit) are violated resulting to lower field oil production rate. However, during the greatest part of the simulation period field oil production rate of the optimal model is higher than the one of the initial model.

As far as field water production rate is concerned it can be observed in both the curves for the initial and optimal simulation model that there are several simulation periods with abrupt increases and decreases of the curves. This behavior is due to the fact that a well might be shut or a new well might open or even if a specific connection of a well is shut due to high water-cut, resulting to abrupt decrease of water production rate.

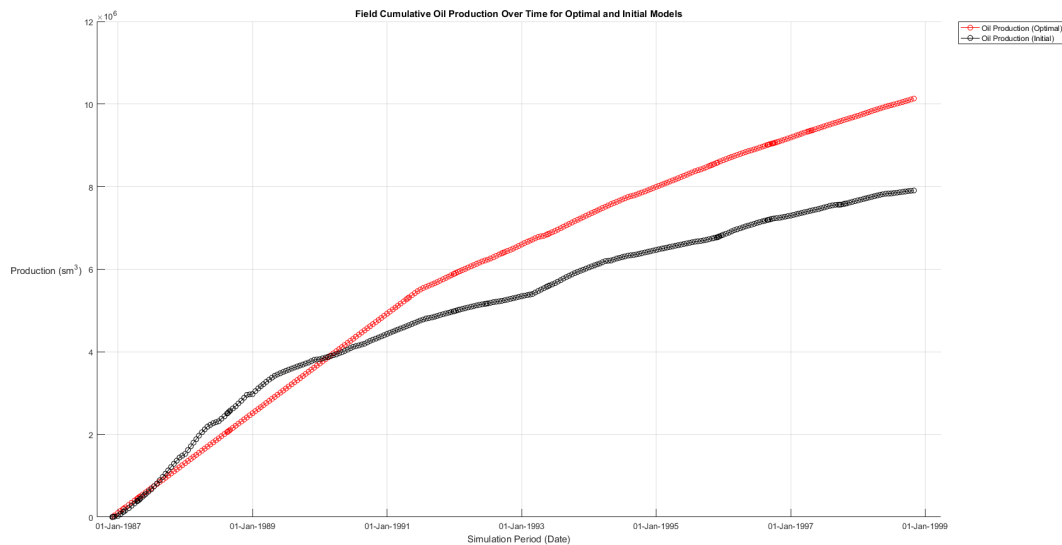


Figure 3.28: Field cumulative oil production over simulation time, Optimal model (Red curve) - Initial model (Black curve)

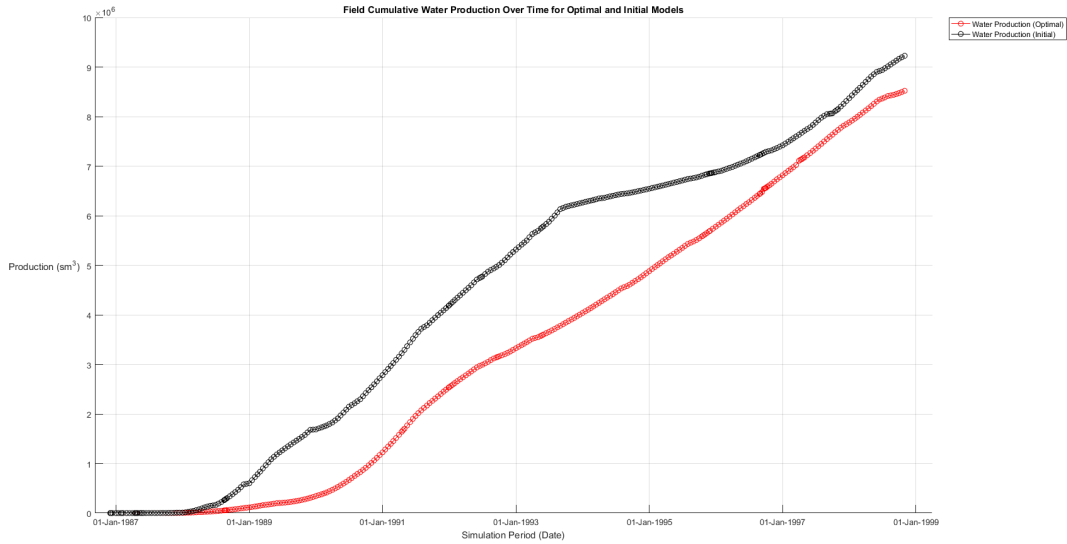


Figure 3.29: Field cumulative water production over simulation time, Optimal model (Red curve) - Initial model (Black curve)

By observing the figures above it can be concluded that the optimal model not only produces more quantity of oil at the end of the simulation period but also that produces less quantity of water which means that possible water treatment costs might be reduced if the scheduling of the optimal model was to be followed. The oil production increase at the end of the simulation period is 28.15 % and the water production decrease at the end of the simulation period is 7.66 %.

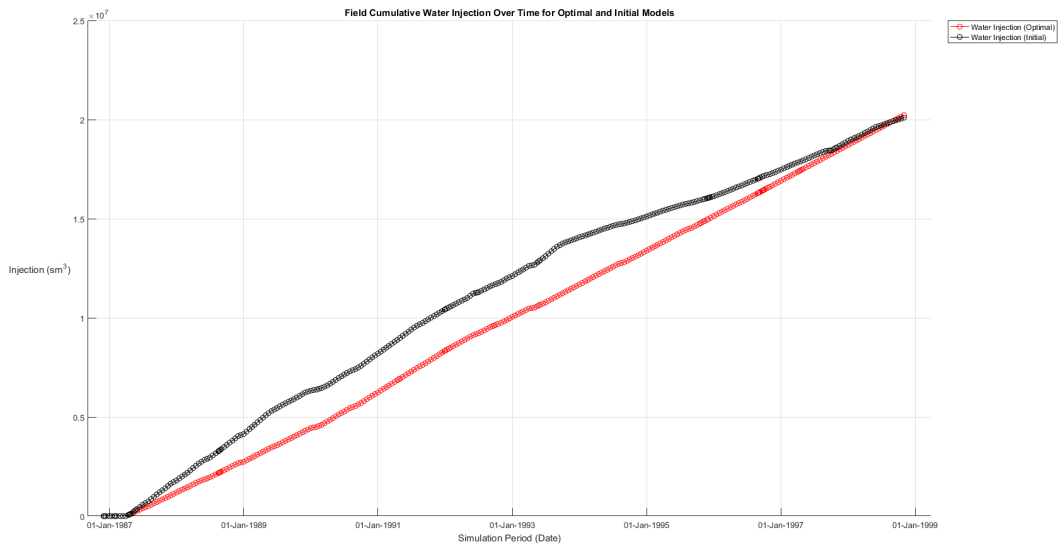


Figure 3.30: Field cumulative water injection over simulation time, Optimal model (Red curve) - Initial model (Black curve)

As noted on section 3.1.2 the average calculated water injection rate was used on the modified initial simulation model that was going to be introduced in *PlanOpt* software meaning that although the injection rates of the optimal model will be the average calculated values the cumulative water injected at the end of the simulation period should be equal between the initial and the simulation models created by the *PlanOpt* software. By observing the figure above it is obvious that the cumulative water injected

at the end of the simulation period for both the initial and the optimal model are equal with a tiny error of 0.66 %. The error has been produced because while calculating the average injection rates for each well the rounded value at the fifth important digit was used resulting to the tiny error propagation throughout the simulation period.

3.4.2 Well Production Data

On this section well production data are going to be presented for all producing wells. As far as production wells are concerned oil and water production rates (Black/Blue curves, Right y-axis) and water-cut (Red curve, Left y-axis) will be presented.

As far as injection wells are concerned the results are identical with the information presented on [figure 3.1.2](#) since the injection pattern of all simulation models created by *PlanOpt* for each injection well is the average injection rate of each well that existed on the initial model without taking into account injection well *I – H2* since it is an injection well simulating a water influx from an adjacent region.

Together with the above mentioned data that is going to be presented below, information will be printed for all wells about the percentage of:

- oil cumulative production of each production well on the field cumulative oil production
- water cumulative production of each production well on the field cumulative water production

Production Well P-A0000026

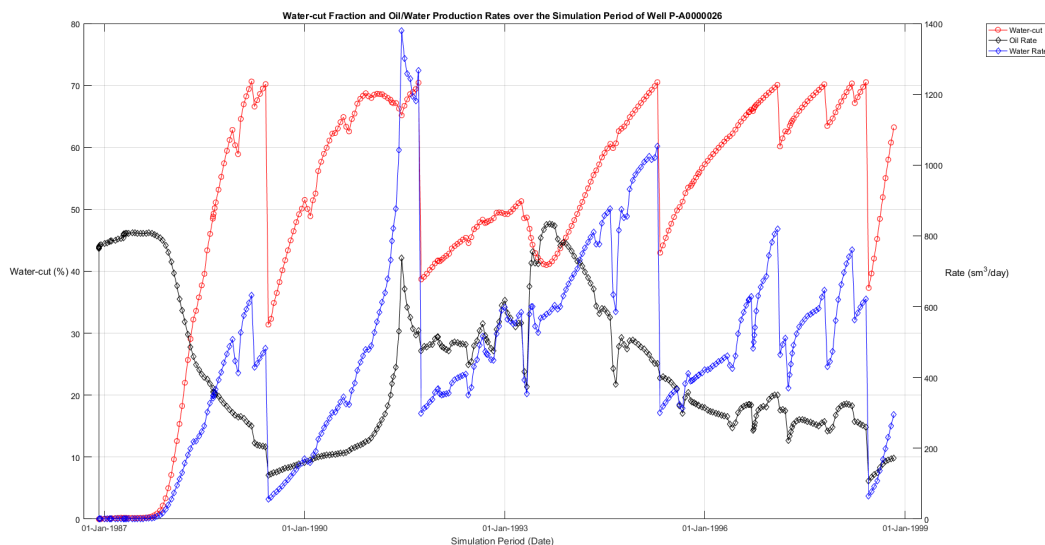


Figure 3.31: Well P-A0000026 production data ([click here for well position](#))

% of field cumulative oil produced: 18.19 %

% of field cumulative water produced: 23.46 %

Production Well P-A000075

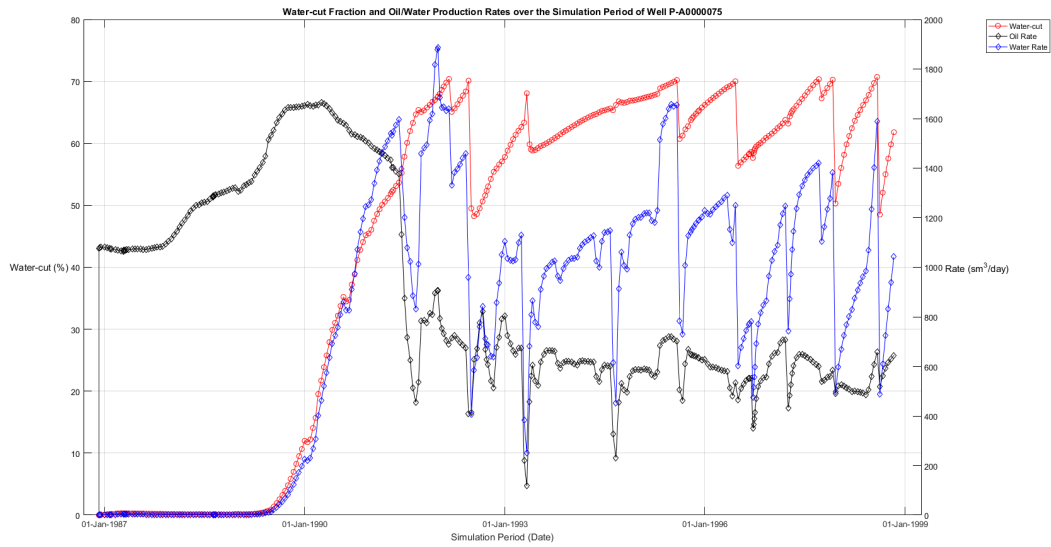


Figure 3.32: Well P-A000075 production data ([click here for well position](#))

% of field cumulative oil produced: 38.24 %

% of field cumulative water produced: 40.43 %

Production Well P-A0000703

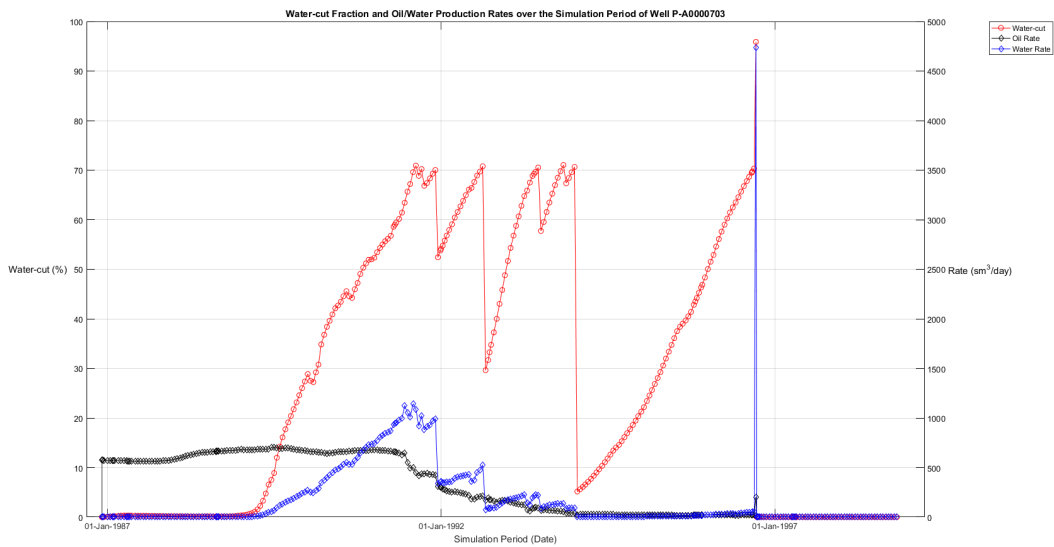


Figure 3.33: Well P-A0000703 production data ([click here for well position](#))

% of field cumulative oil produced: 12.62 %

% of field cumulative water produced: 9.13 %

Production Well P-A000761

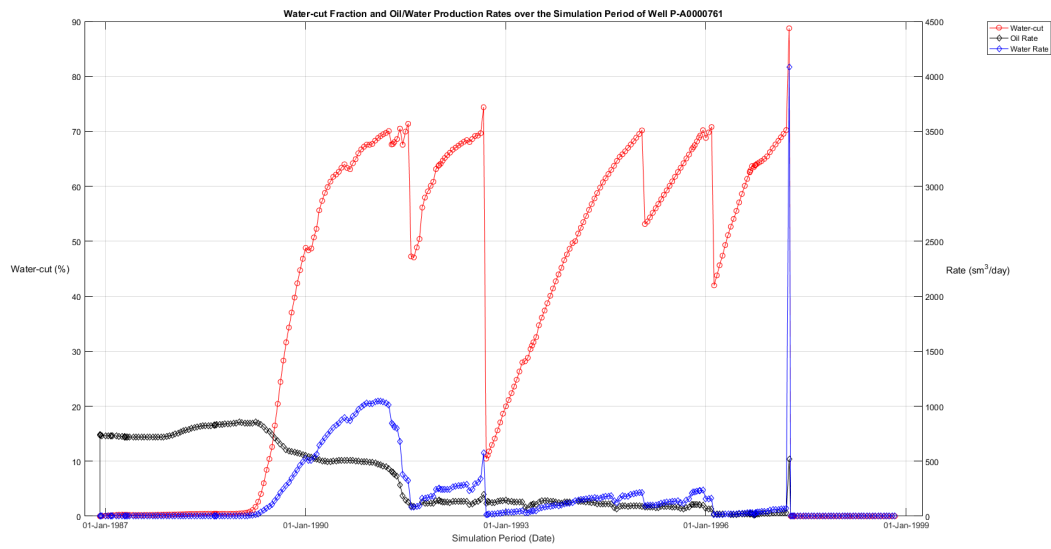


Figure 3.34: Well P-A000761 production data ([click here for well position](#))

% of field cumulative oil produced: 12.87 %

% of field cumulative water produced: 9.97 %

Production Well P-A0003787

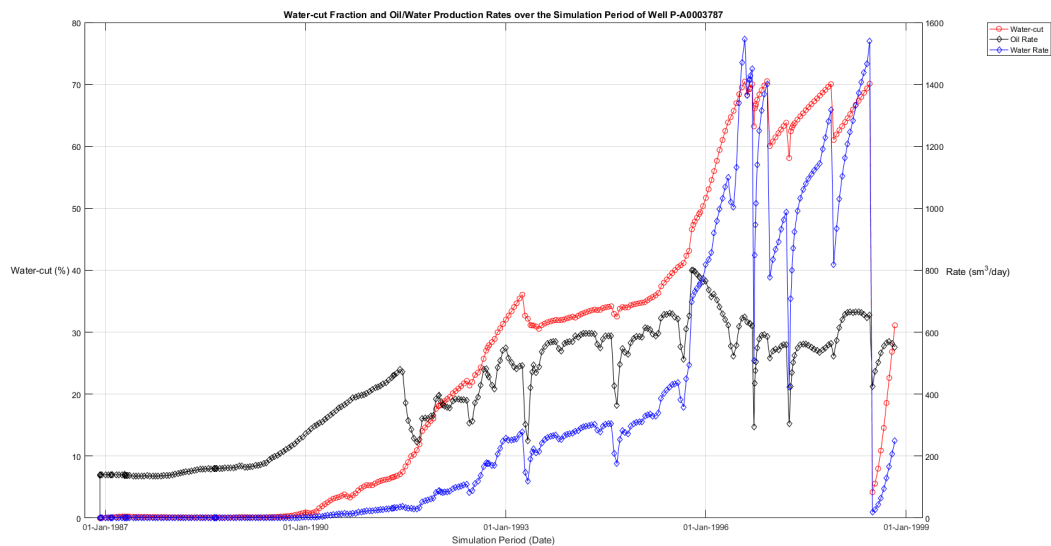


Figure 3.35: Well P-A0003787 production data ([click here for well position](#))

% of field cumulative oil produced: 18.08 %

% of field cumulative water produced: 17.02 %

The curves presented on the figures above concerning the production wells of the optimal model appear to have a common behavior. Each time water-cut (Red curve, left y-axis) reaches the value of 70 % an abrupt decrease on water-cut occurs. This behavior results from the implementation of the water-cut work-over constraint which is set active each time water-cut tends to take values higher than 70 % and shuts the well connection which produces with the higher water-cut value. This constraint forces the well to produce at lower water-cut values and finally results in achieving higher cumulative oil production.

Chapter 4

Production Data History Matching aided by SimOpt

SimOpt is part of *ECLIPSE* reservoir simulation software assisting history matching of production data. It is common that the results of a simulation model concerning the production data of a field have to be matched with the on-field measurements of production data (observed production data). When the simulation model and the observed production data diverge several parameters of the simulation model can be set to vary within a reasonable range in order to achieve matching of the curves concerning the simulation model and the observed production data. *SimOpt* optimizes the history matching process mentioned above using a regression procedure. The production data of the initial simulation model and the observed production data of the current diploma thesis will be matched by utilizing the features of *SimOpt* software as will be presented below.

4.1 Observed Production Data

The first step when operating *SimOpt* is to load the available observed production data (history production data) corresponding to the simulation model. The observed production data that are going to be matched on the current project are:

- Observed oil production rate of each production well denoted as *WOPRH*
- Observed water production rate of each production well denoted as *WWPRH*
- Observed water-cut fraction of each production well denoted as *WWCTH*

For each producing well of the field the three above data sets of observed production are introduced in *SimOpt* software. Each data set consists of pairs of the date that the observation was made and the observed value. Furthermore, each data set has to be accompanied with a value concerning the error of the measurements.

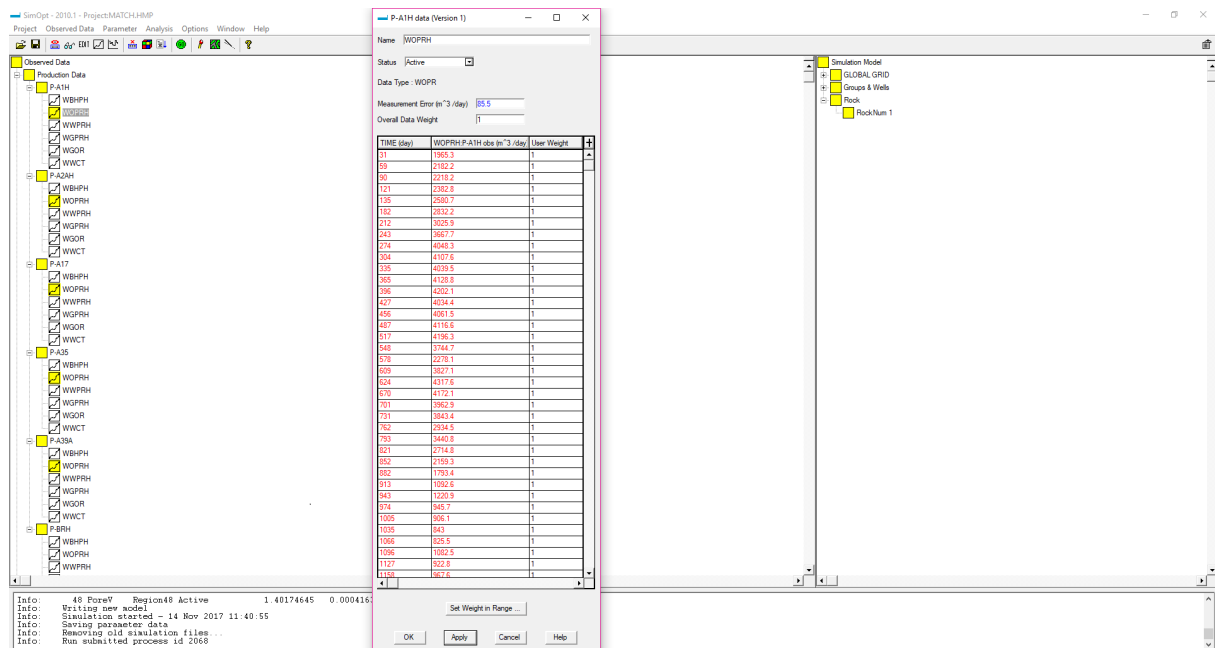
As stated on [9] the measurement of flow-rates at the time that the specific observed data were collected, was conducted with the error ranging around 5 % of the measured value. Since each data consists of numerous measured values the 5 % of the average value of each data set was used as input in *SimOpt*.

The table below shows the measurement errors introduced in *SimOpt* for each data set and for each production well:

Wells	WOPRH (sm^3/day)	WWPRH (sm^3/day)	WWCTH (%)
P-A1H	85.5	63.0	2.04
P-A2AH	40.4	39.5	1.65
P-A17	24.5	17.0	1.97
P-A35	20.0	47.8	3.34
P-A39A	41.2	38.7	2.14

Table 4.1: Measurement errors of observed production data sets

The figure below presents the input of the measurement errors of the observed production data sets in *SimOpt* software.

Figure 4.1: Measurement error input in *SimOpt* software

On the left column of *SimOpt* software the observed data tree is presented. The white color squares represent data sets which are not going to be used (in-active data sets) and the yellow color squares represent data sets which will be used (active data sets) in the history matching process that will follow.

4.2 Parameters

There are several reservoir parameters that can be set to vary in order to achieve matching between the simulation model data and the observed data like transmissibility, permeability, porosity well connection transmissibility etc. On the current project the parameters that are going to be used are:

- X -transmissibility
- Y -transmissibility
- Z -transmissibility
- Porosity

The above parameters are applied regionally meaning that the user must set which regions of the reservoir will have its parameters varied during the matching procedure. Since the reservoir consists of 12 active layers each one will be set as a separate region for each different reservoir parameter from the list above.

Finally as will be shown on the figure below there are going to be 12 parameters concerning the X -transmissibility of the reservoir, 12 parameters concerning the Y -transmissibility of the reservoir and so on having a final number of 48 regional parameters at the end.

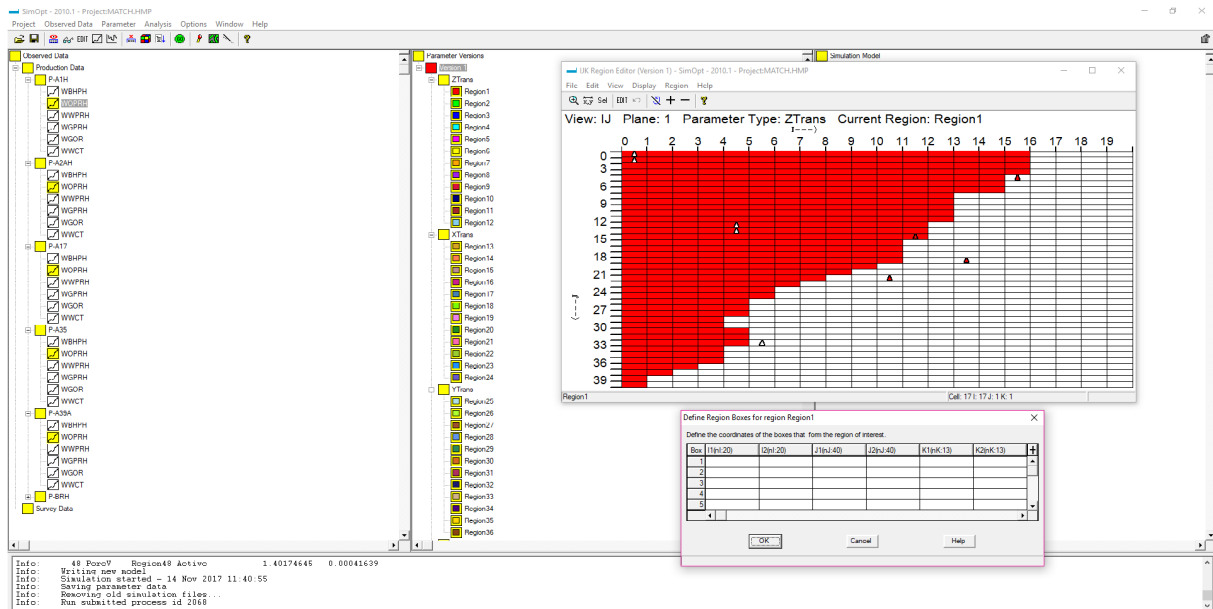


Figure 4.2: Setting up the regional parameters for the history matching process

The figure below shows the range of multipliers of the regional parameters:

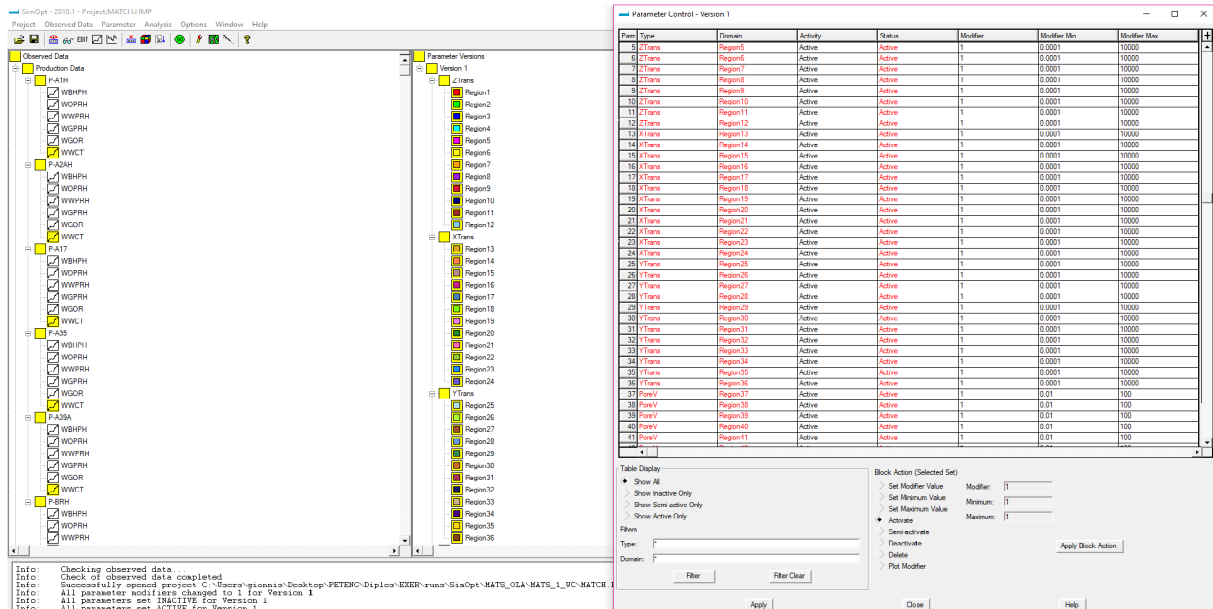


Figure 4.3: Setting up the range of multipliers of the regional parameters

After the regional parameters are created their available range of modification should be specified. Transmissibility and porosity parameters in *SimOpt* software are changed using modifiers. Modifiers are numbers which will be multiplied with their corresponding parameter original value in order to change it. A multiplier with value above unity will increase the value of the parameter and a multiplier

with a value below unity will decrease the value of the parameter. All the regional parameters chosen above will be set to vary during the regression procedure in order to achieve matching between simulation and observed data.

4.3 Optimization

After the observed data have been imported in the *SimOpt* software together with their corresponding measurement errors and all the chosen regional parameters have been assigned to their corresponding regions of interest the optimization process can start. Below are presented the simulation option that *SimOpt* is capable of.

4.3.1 Evaluation Run

Before regression procedure begins it is important to examine the mismatch of the curves of the observed and the simulation model data. A normal simulation run (evaluation run) of the initial model is conducted and the *RMS* value between observed and simulation model data is calculated showing the magnitude of the mismatch. Furthermore, graphs containing the curves of the simulation model data and the observed data are available in order to visualize the magnitude of the mismatch and also at which data points the mismatch is more intense.

The figure below shows the results after the evaluation run has been terminated:

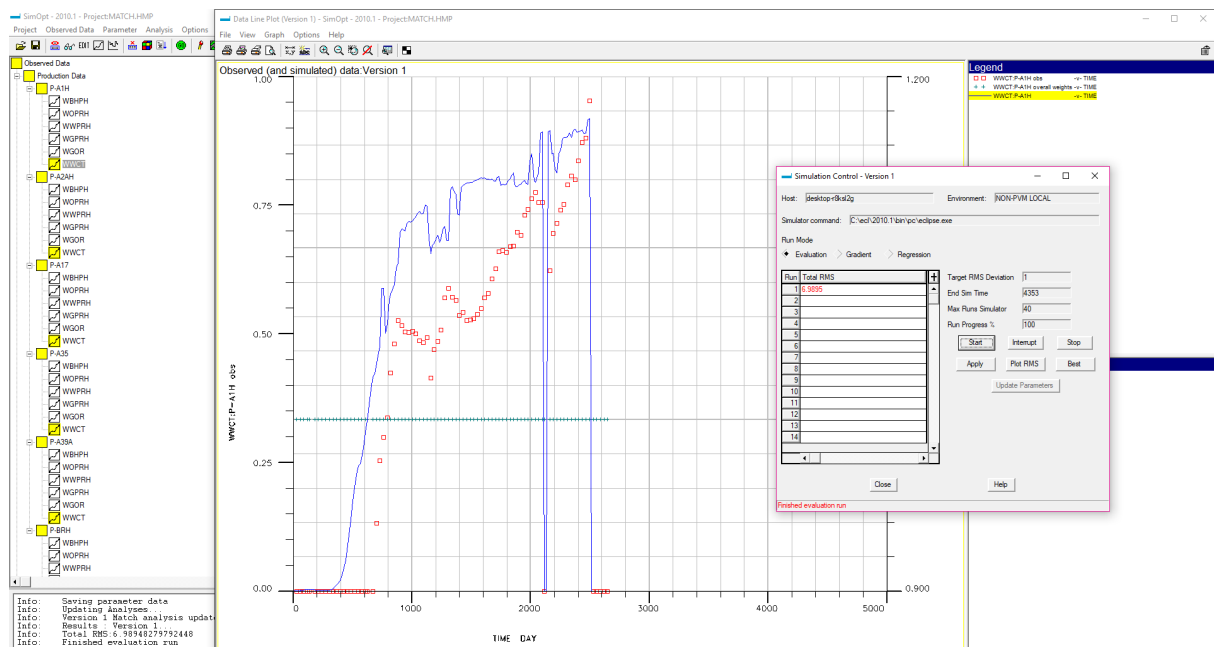


Figure 4.4: Results after the evaluation run has terminated

The resulted *RMS* value between the observed and the simulation model data is printed after the evaluation run is finished. After the evaluation run is finished the graphs presenting the observed data sets which are set as active will also present the curves of the corresponding simulation model data which were calculated during the evaluation run. The duration of the evaluation run as stated above is similar to a normal simulation run, thus for the current project it needs approximately 60 seconds to finish.

4.3.2 Gradient Run

The gradient run is the most important feature of the *SimOpt* software since it calculates the gradients of the formed objective function with respect to each regional parameter as discussed on sections 1.4.1 and 1.4.2. These information will help making the final decision about which parameters should be set to vary for matching the simulation model data with the observed data as stated on section 1.4.3.

The figure below show the information created after the gradient run was terminated:

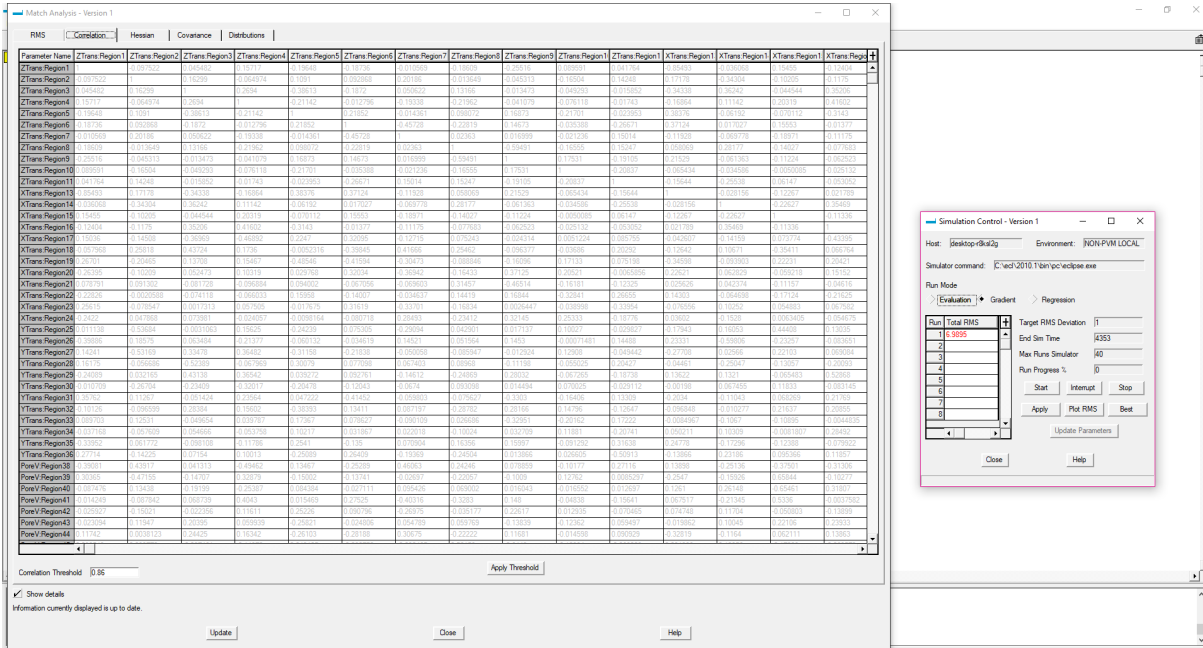


Figure 4.5: Correlation matrix

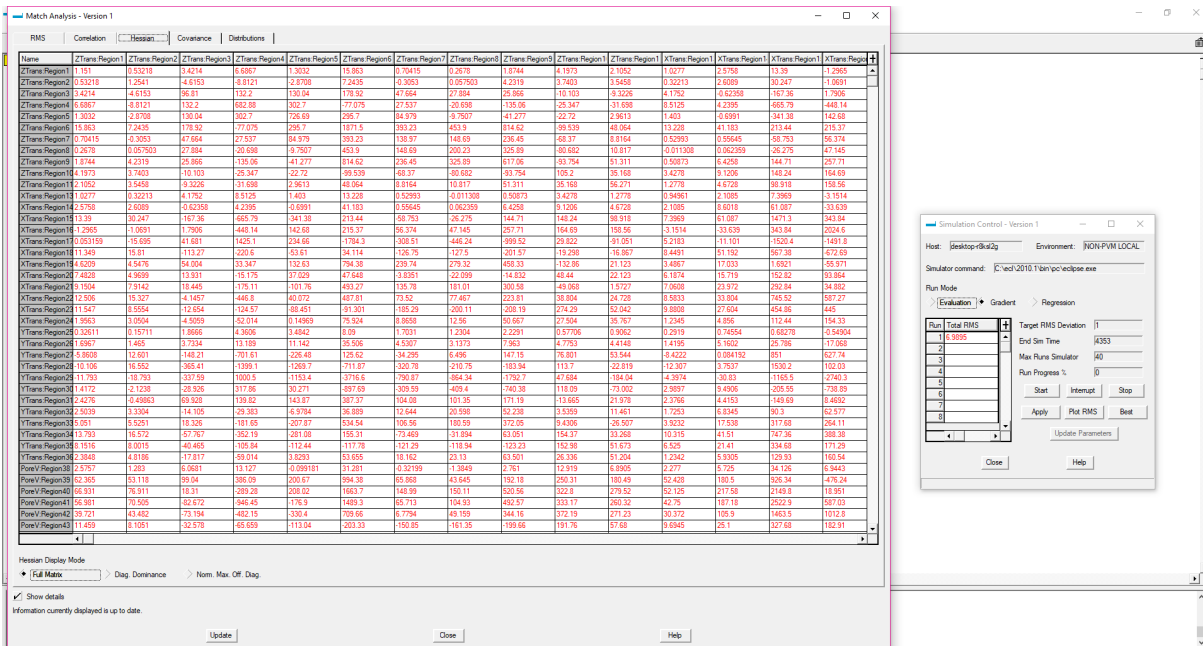


Figure 4.6: Hessian matrix

By consulting the entries of the correlation matrix the pairs of parameters having their correlation value near 1 (strongly correlated) or -1 (strongly anti-correlated) are found. A correlation threshold value

exists (Ct) denoting the range inside which a pair of parameters is considered strongly correlated $[Ct, 1]$ or strongly anti-correlated $[-1, -Ct]$.

Strongly anti-correlated parameters should be merged before the regression operations start meaning that instead of having two regions (one for each parameter), the regions should be merged to a new region which will consist of the two previous regions and will be represented by one new regional parameter.

Strongly correlated parameters should not co-exist during the regression operations meaning that one of the parameter's pair should be discarded. The choice is based on the information provided by the Hessian matrix. The parameter having the highest diagonal dominance or normalized maximum off-diagonal value is the one that should be discarded since it performs in a way that slows down the regression performance.

For the current project a gradient run needs approximately 7 minutes to finish.

4.3.3 Regression Run

After the regional parameters have been chosen by consulting the information provided by the gradient run the regression process can start. During the regression run the parameters will have their values modified based on the directions that the calculated gradients will show. After each iteration of the regression run the calculated RMS between the simulation model and the observed data is printed.

The figure below shows *SimOpt* after regression has started.

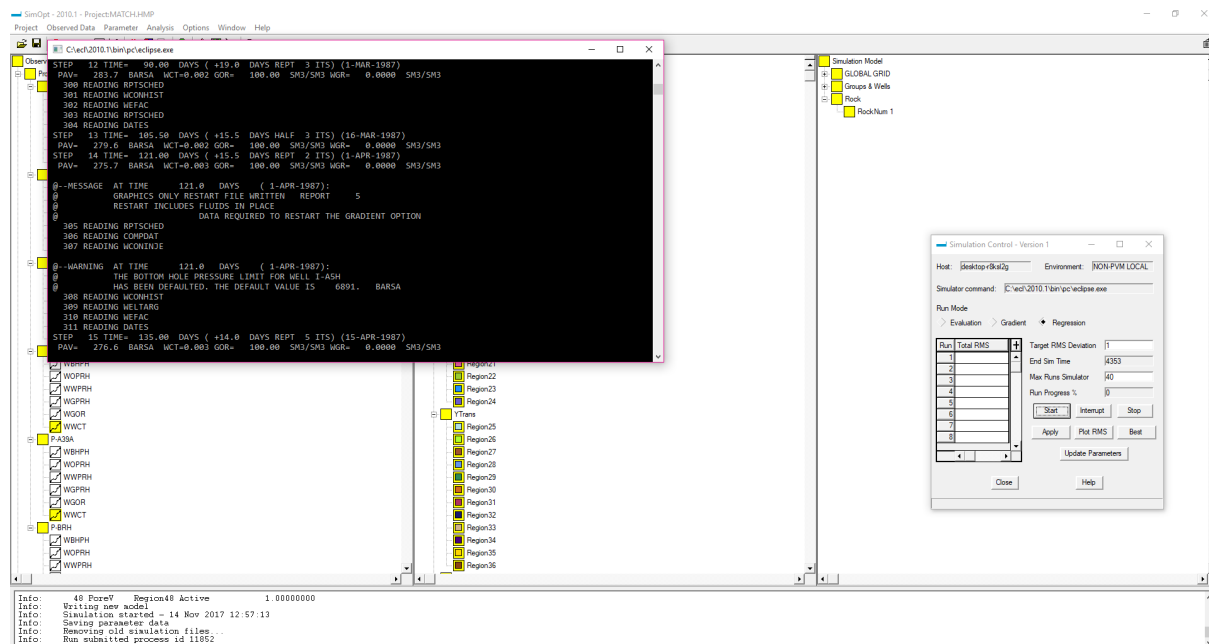


Figure 4.7: Regression run initiation

The user can set the number of iteration after which the regression run will be terminated, otherwise if the regression process happens to converge before the set number of iterations is reached then regression is again terminated since RMS can not be minimized any more. The RMS at the end of each iteration can be plotted on a figure during the regression run so as to visualize the quality of matching after each iteration. By observing the RMS curve during the regression run one can judge if there is need for proceeding in more iterations or terminating since the future improvement of the match between the simulation model and observed data will be minor.

The figure below shows *SimOpt* when the regression run has been terminated and the RMS curve that has been created and updated after each iteration.

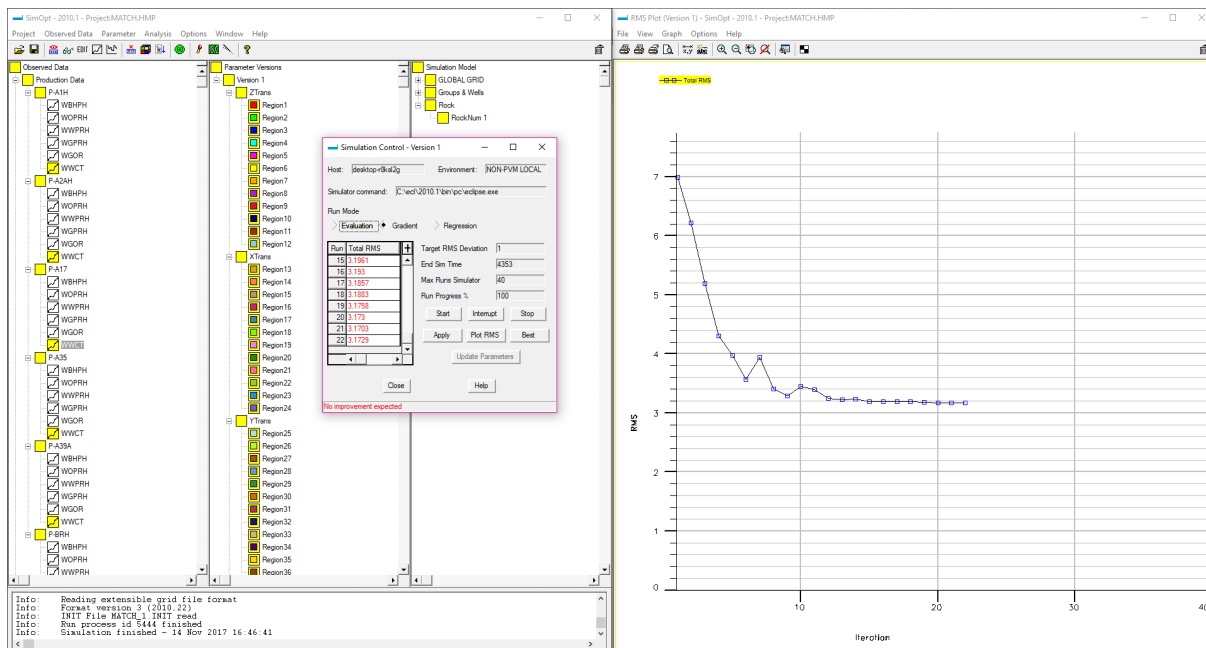


Figure 4.8: Regression run termination

Note that when regression starts and finishes the time is recorded on the log window at the bottom of *SimOpt* software and so the overall time of regression run can be calculated. For the current project a regression run needs approximately 11 minutes for each iteration to finish. For the current set of runs presented above, depending on the number of iteration needed by the regression operations to converge which varied from 20 to 31 iterations, the corresponding regression run time varied approximately from 3 hours and 40 minutes to 5 hours and 41 minutes.

4.4 History Matching Optimization

In order to achieve the best matching between the simulation model and observed data several optimization were tried. After coming to a conclusion about the parameters that produced the best matching results that are X , Y , Z -transmissibilities and porosity the observed data used had to be analyzed in order to find the combination of data sets that would provide the best matching.

For each production well the observed data were oil rate ($WOPRH$), water rate ($WWPRH$) and water-cut fraction ($WWCTH$) that is the fraction of water rate over the total liquid rate which is the sum of oil and water rates. Water-cut is a value which can be derived if the oil and water rates are known or if the water-cut fraction is known together with either the oil or the water rate then water or oil rates can be derived respectively.

It is going to be examined if better match can be achieved between simulation runs whose only difference will be the combinations of different data set types. On each simulation run the regional parameters are going to be the same together with all the observed data sets measurement errors. However, each time a different combination of observed data set type is going to be set as active that is the specific observed data sets are going to be matched with the simulation model data.

On each simulation run an evaluation run is conducted before regression is initiated and the initial RMS value between the current active observed data sets and the simulation model data sets is calculated. After the regression process has terminated the final RMS value is calculated. Finally, each observed data set type ($WOPRH$ or/and $WWPRH$ or/and $WWCTH$) that was set as inactive when the model was imported in *SimOpt* software is set as active and a final evaluation run is conducted with all observed

data set types active and with all the regional parameters having taken their final modified values. The resulted *RMS* values of the final evaluation run from all different simulation runs concerning all the possible combinations of observed data set types will judge which simulation achieved the best matching.

The figure below shows the *RMS* curves of all simulation runs with each one corresponding to one combination.

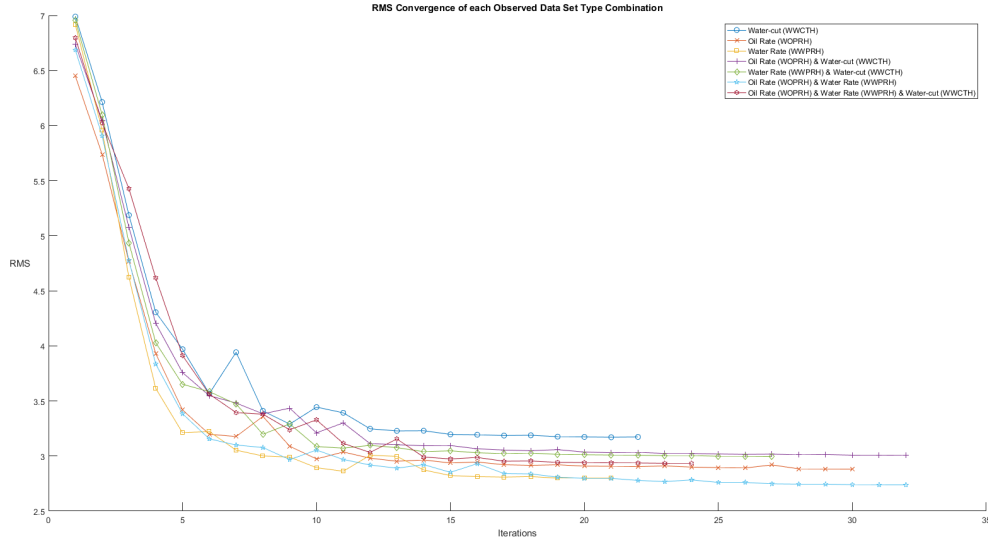


Figure 4.9: *RMS* convergence of each observed data set type combination

Although some simulation of specific combinations of observed data set types seem to achieve better matching since their final *RMS* value is better - Water Rate (Yellow with squares curve) and Oil Rate & Water Rate (Cyan with Stars curve) - it should be taken into account that not all the observed data set types were active during the regression process and only after the final evaluation run where all the observed data set types will be active, the simulation results will be comparable.

The table below presents the initial *RMS*, the final *RMS* and the final *RMS* after evaluation with all the observed data set types active:

Observed Data Set Type Combinations	Initial <i>RMS</i>	Final <i>RMS</i>	Final <i>RMS</i> after Evaluation
<i>Water-cut</i>	6.9895	3.1703	3.0301
<i>Oil Rate</i>	6.4500	2.8813	3.0650
<i>Water Rate</i>	6.9172	2.7986	3.1238
<i>Oil Rate & Water-cut</i>	6.7381	3.0062	2.9303
<i>Water Rate & Water-cut</i>	6.9552	2.9954	2.9799
<i>Oil Rate & Water Rate</i>	6.6877	2.7375	2.9369
<i>Oil Rate & Water Rate & Water-cut</i>	6.7964	2.9346	2.9346

Table 4.2: Initial *RMS*, final *RMS* and final *RMS* after evaluation

By observing the final *RMS* values after the evaluation run where all the observed data set types are set active, it can be concluded that the simulation run resulting to the minimum *RMS* value is the one with the Oil Rate & Water-cut combination of observed data set types. Although this particular combination appeared to have poor results after the regression run (see Purple with Plus signs curve on figure 4.9), after the final evaluation run its *RMS* value was the best compared to *RMS* values that

the other simulation runs produced. The next step is to produce figures of the observed and simulated data sets in order to visualize and inspect the quality of the matching. The following figures will present curves of:

- The observed data sets (Red with Circles curve)
- The initial simulation model data sets (Black with Circles curve)
- The final simulation models data sets after the evaluation run:
 1. Water-cut as active data set during regression (Blue curve)
 2. Oil rate as active data set during regression (Orange curve)
 3. Water rate as active data set during regression (Yellow curve)
 4. Oil rate & water-cut as active data set during regression, model produced the minimum *RMS* value after evaluation (Purple with Squares curve)
 5. Water rate & water-cut as active data set during regression (Green curve)
 6. Oil rate & water rate as active data set during regression (Cyan curve)
 7. Oil rate & water rate & water-cut as active data set during regression (Light Brown curve)

The quality of the matching depends on how near are the curves of the observed data sets and the final simulation models data sets in comparison with the curves of the initial simulation models data sets. The visualization of the history matching process with the curves on the figures below aids in judging each different simulation run model in a qualitative aspect which is the only mean to avoid the situation of over-fitting of the simulation model curves with the observed data ones. Given a situation where over-fitting is severe the quantitative manner of judging the matching process, which is the *RMS* value between observed and simulation model data sets, would classify the achieved matching as successful since when over-fitting of curves occurs their produced *RMS* value is minor. However, a simulation model which has its data sets over-fitted over the observed data sets is highly prone to produce erroneous results over the simulation periods between the data sets' points and subsequently during the time period of future operation plans where the simulation model results will be needed in order to guess the profiles of several production data (oil rate, water rate etc.).

Well P-A1H

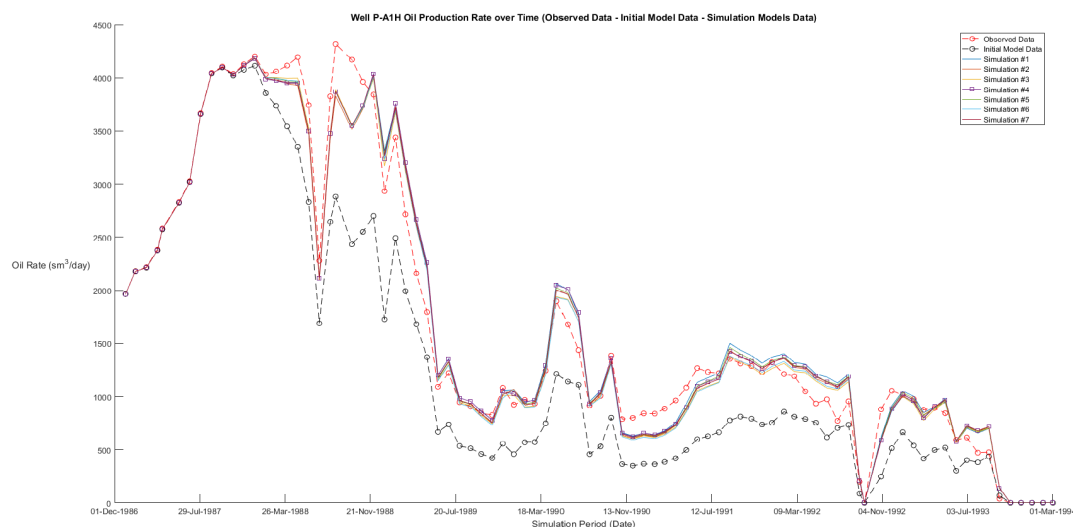


Figure 4.10: Oil production rate over time of Well P-A1H

4.4. HISTORY MATCHING OPTIMIZATION

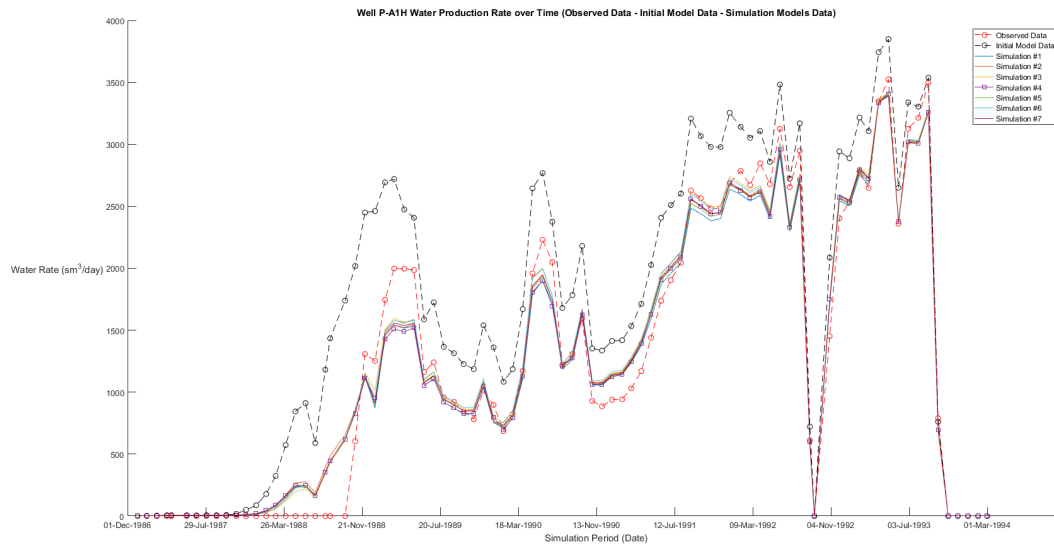


Figure 4.11: Water production rate over time of Well P-A1H

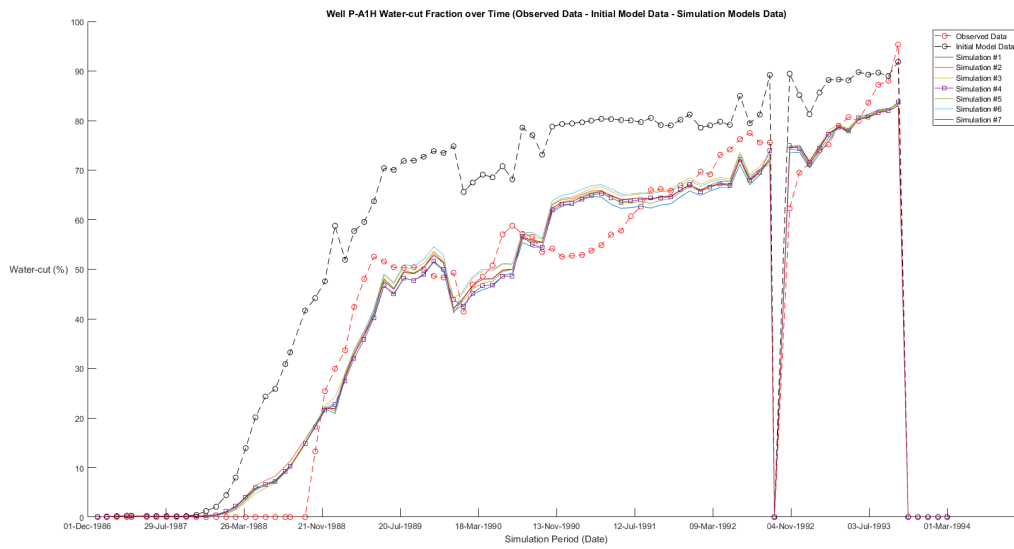


Figure 4.12: Water-cut fraction over time of Well P-A1H

Well P-A2AH

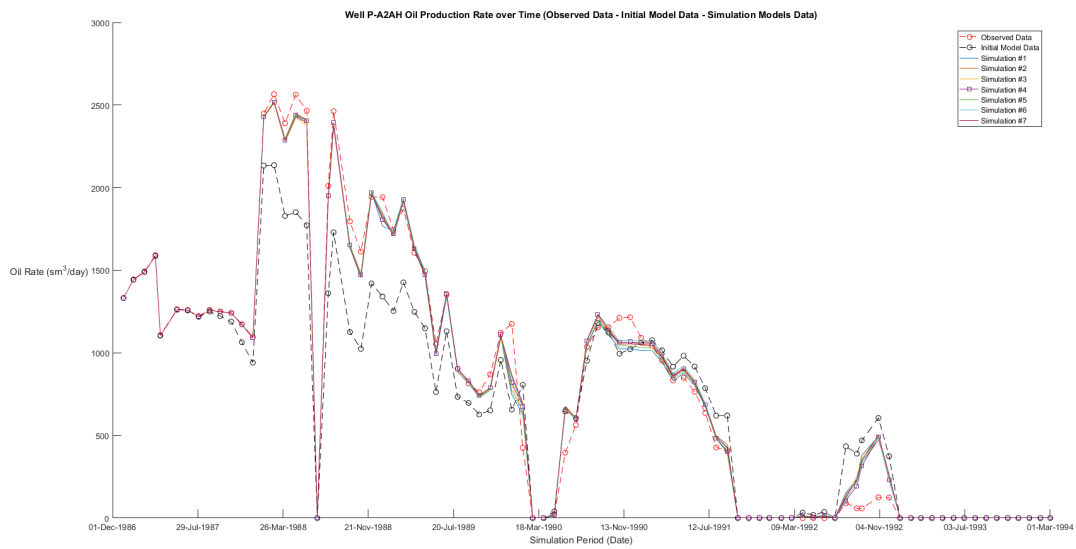


Figure 4.13: Oil production rate over time of Well P-A2AH

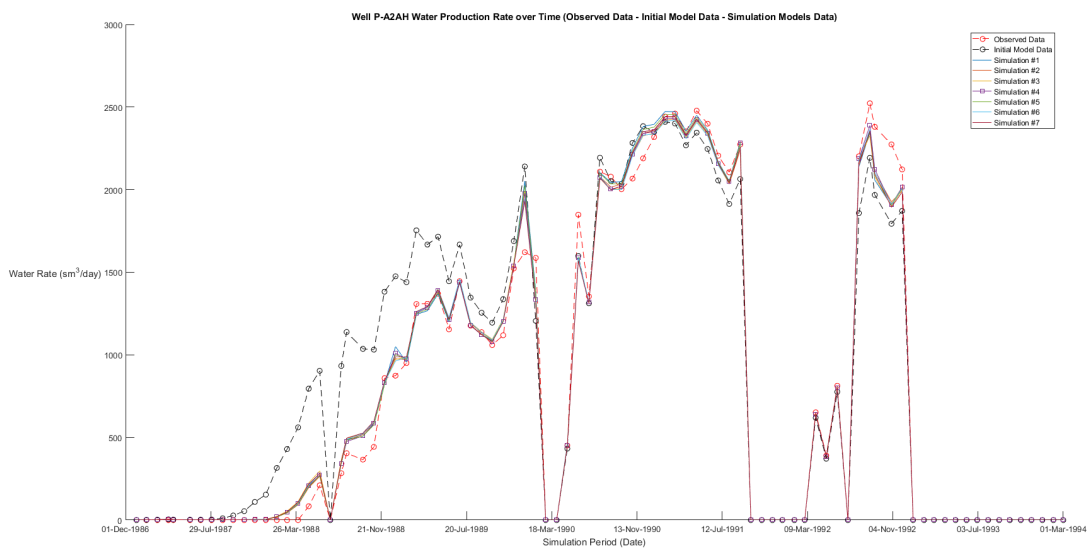


Figure 4.14: Water production rate over time of Well P-A2AH

4.4. HISTORY MATCHING OPTIMIZATION

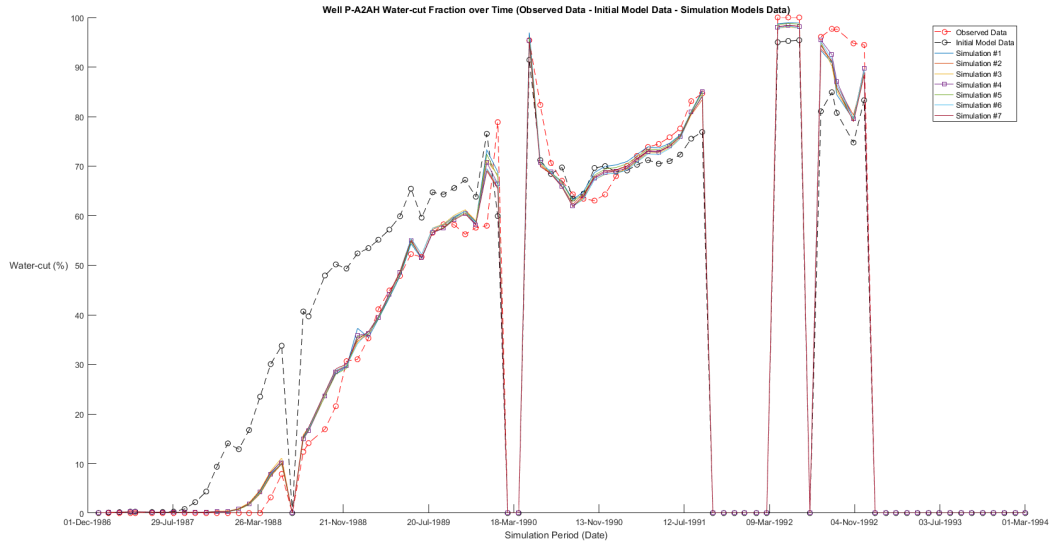


Figure 4.15: Water-cut fraction over time of Well P-A2AH

Well P-A17

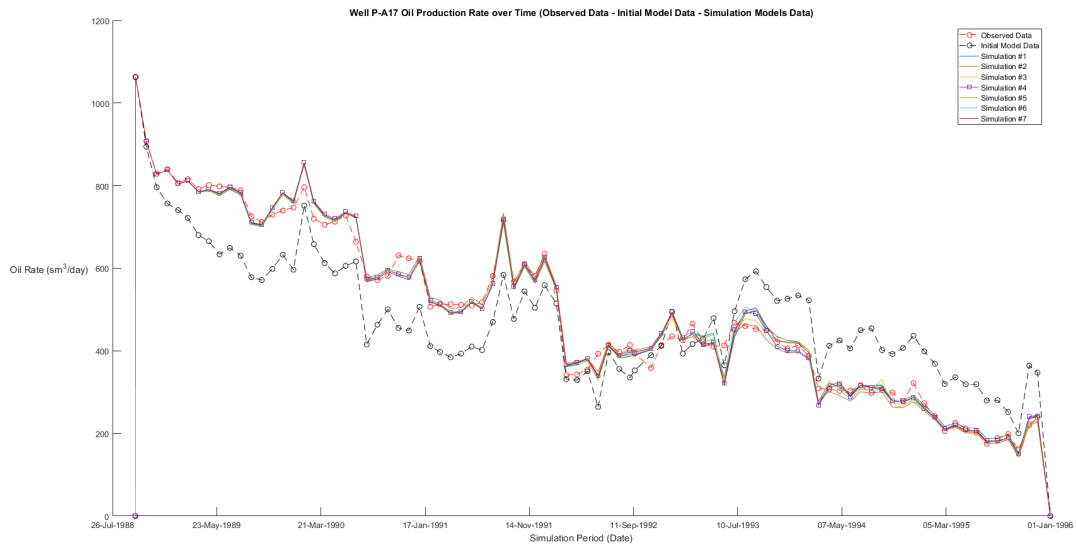


Figure 4.16: Oil production rate over time of Well P-A17

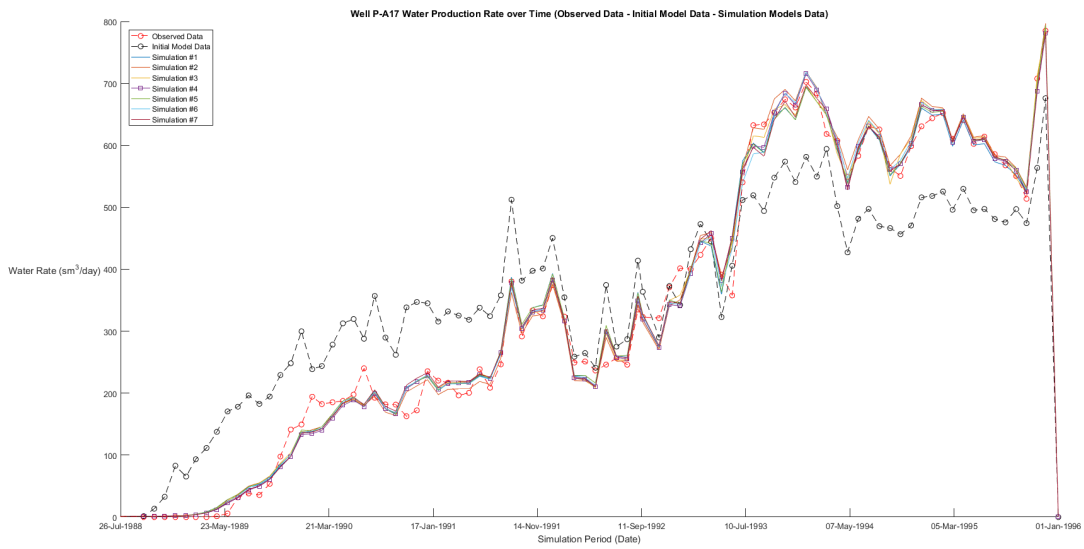


Figure 4.17: Water production rate over time of Well P-A17

4.4. HISTORY MATCHING OPTIMIZATION

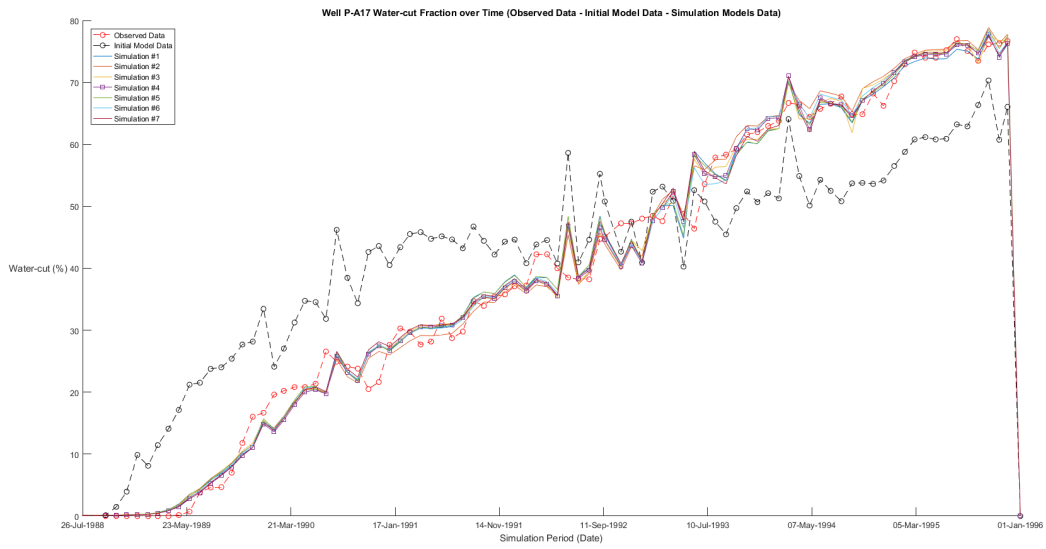


Figure 4.18: Water-cut fraction over time of Well P-A17

Well P-A35

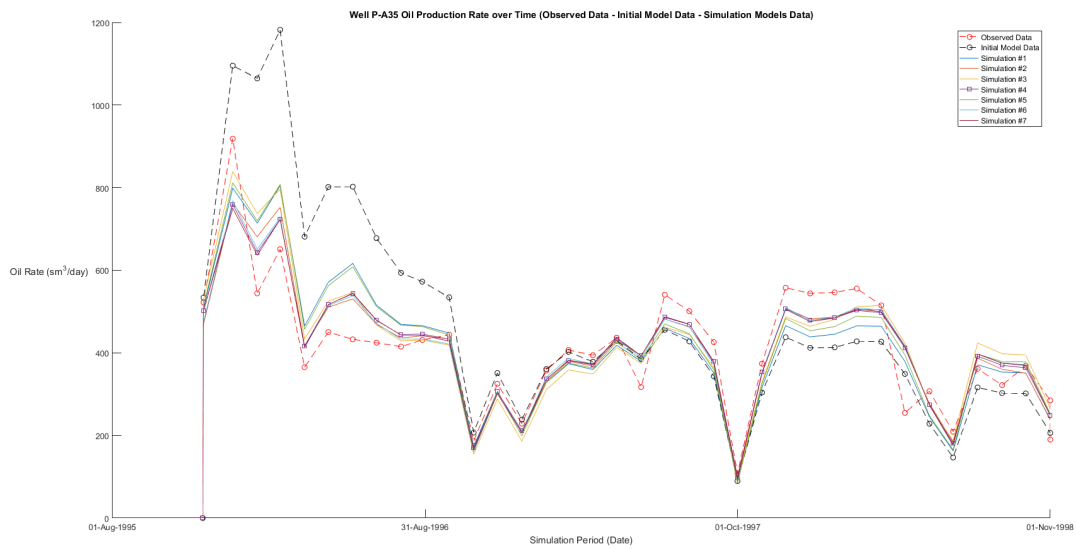


Figure 4.19: Oil production rate over time of Well P-A35

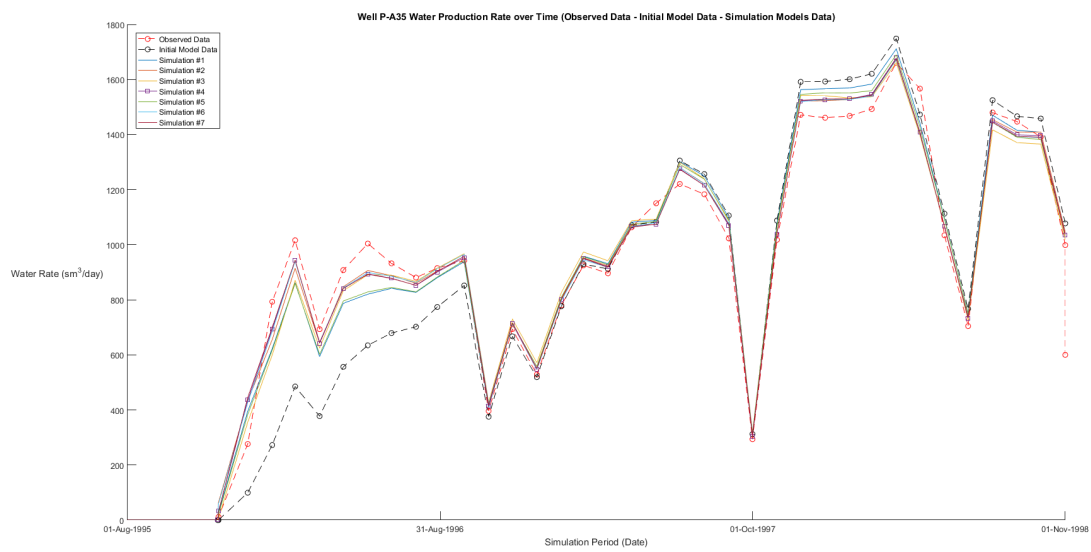


Figure 4.20: Water production rate over time of Well P-A35

4.4. HISTORY MATCHING OPTIMIZATION

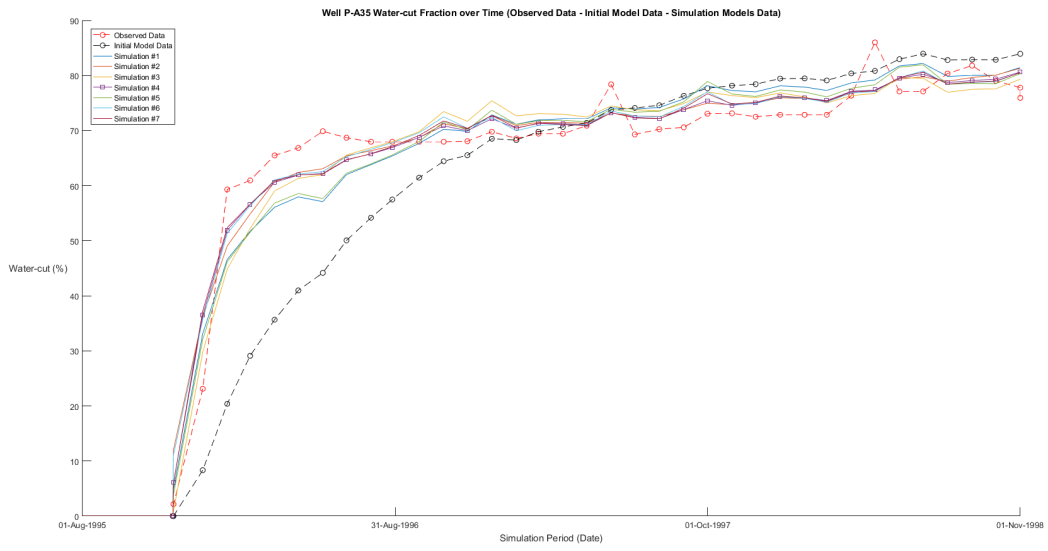


Figure 4.21: Water-cut fraction over time of Well P-A35

Well P-A39A

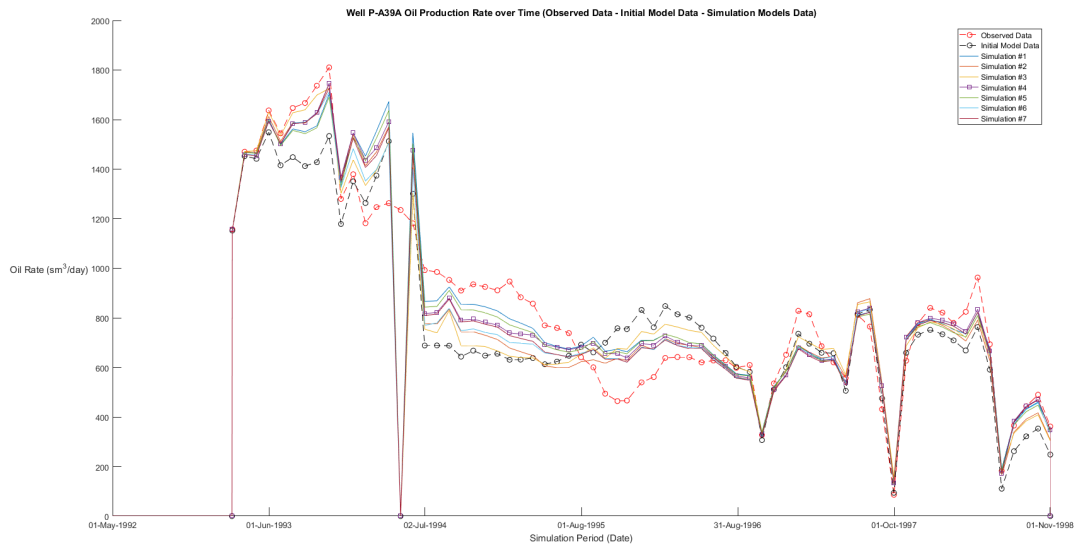


Figure 4.22: Oil production rate over time of Well P-A39A

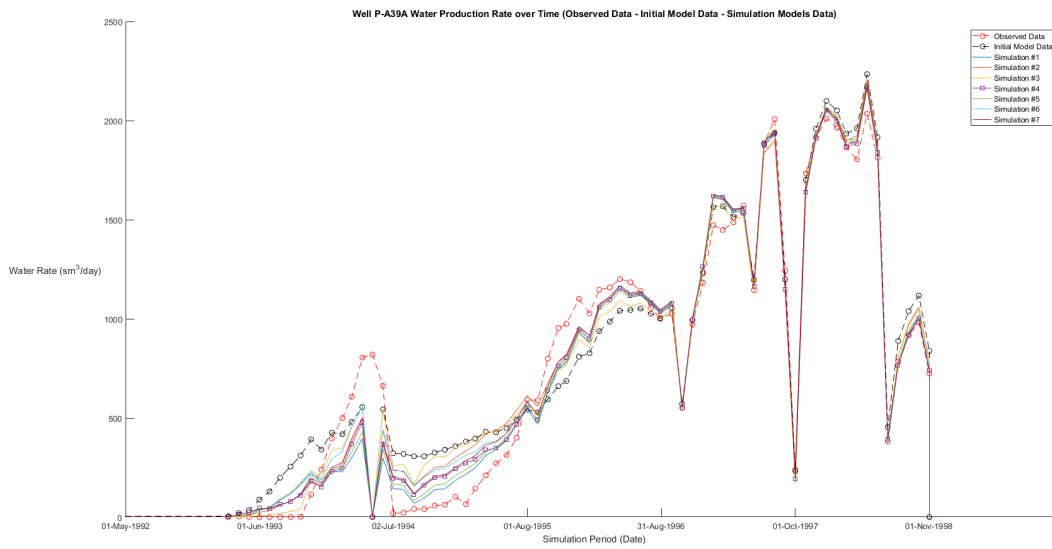


Figure 4.23: Water production rate over time of Well P-A39A

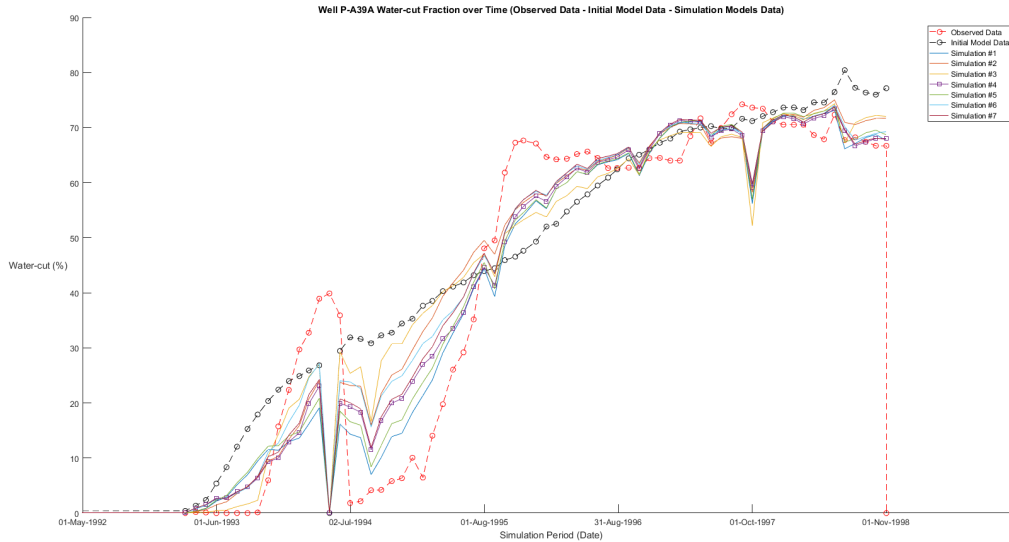


Figure 4.24: Water-cut fraction over time of Well P-A39A

All the figures presented above appear to have a common behavior. There is obvious mismatch between the observed and initial simulation model data sets among all three different data set types.

The simulation model runs which aimed to reduce the mismatch between the observed and initial simulation model data sets appear to produce better results since the curves representing the data sets of each different simulation run are closer to the observed data sets. This can also be ascertained by the results of table 4.2 where in all different simulation runs the *RMS* value resulted after the evaluation of the model with all the observed data sets is lower than the initial *RMS* value that the model produced by at least 42.84 %.

By further observing table 4.2 and the figures above the different simulation runs that were conducted, in order to inspect the possible difference in the *RMS* value produced (after evaluating the model with all data sets as soon as regression has finished) when having different combinations of data set types active during regression, appear to have minor difference between each other not exceeding the value of 6.19 %. This behavior is also visible in all curves presented above since all of them are having almost the same shape with only tiny differences between them regardless of the data set type.

The behavior described above is ascribed to the fact that the data set types, that are oil rate and water rate are interdependent since both are influenced by the water-cut fraction. Each time a different combination of the observed data set is used as active during the regression run there might be only a small changes in the resulted *RMS* values of each different model since the results of the simulation model concerning the oil and water rate together with their corresponding water-cut fraction are interdependent.

Since the different simulation runs with different observed data sets set as active during regression failed to provide important improvement to the history matching process the next step would be adding more parameters. In other words the regional discretization of each reservoir parameter, that are *X*, *Y*, *Z*-transmissibilities and porosity which at the specific project was set to be as one layer on the *Z* direction for each reservoir parameter, could be more complex having at the end more regional parameters to vary towards the matching of the curves. Furthermore, possible geological information could be exploited which would mean even more regional parameters e.g. fault transmissibilities.

Chapter 5

Conclusion

5.1 Well Placement Optimization

Well placement optimization aided by *PlanOpt* succeeded since the new simulation models which were created by the software produce larger quantity of oil than the initial simulation model at the end of the simulation period. Furthermore, the achieved oil production of each new simulation model is produced using a number of production wells that is equal or lower than the number of existing wells on the initial simulation model. The optimization procedure was affected each time by the values of the control variables (group field oil rate), the operational limits (bottom-hole pressure) and the operational constraints (water-cut work-over limit). Apart from the bottom-hole pressure limit which was kept unchanged for all the new simulation models that were created (see [section 3.2.4](#)), group field oil rate and water-cut work-over limit were set to vary within a specified range creating a confined plain of solutions, with each solution corresponding to a unique new simulation model.

Group field oil rate had major influence on the maximization of oil production compared to water-cut work-over limit. Although the increase in oil production resulted from optimizing with respect to water-cut work-over limit was minor compared to the effect of the group field oil rate, water-cut work-over limit activation was the major parameter which forced all the new simulation models created by *PlanOpt* software to have an increased oil production. Before incorporating water-cut work-over limit in the optimization processes all the resulted simulation models, regardless of the group field rate value that was being used, produced much less quantities of oil than the initial simulation model. By activating the option of water-cut work-over limit on the optimization processes each model was able to include operations of shutting and opening well connections throughout the simulation period in order to reduce the produced water-cut fraction leading to increased oil production. The combined effect of optimizing group field oil rate while water-cut work-over limit was active forced the new simulation models that were created to produce higher quantity of oil at the end of the simulation period. Finally, by having also the value of the water-cut work-over limit optimized the new simulation models which were created, resulted to an additional, but lesser in magnitude, increase in the quantity of oil production at the end of the simulation period.

Both group field oil rate and water-cut work-over limit were set to vary within a range. Discrete values had to be chosen from within these ranges each time a new optimization run had to be initiated. Since the resulted oil production of each new simulation model that was created was a function of both group field oil rate and water-cut work-over limit, if n , m where the numbers of discrete values from within each range respectively, then, in order to create a plain showing the dependency of the oil production at the end of the simulation period with respect to both water-cut work-over limit and group field oil rate $n \times m$ optimization runs would be needed to be conducted. The higher the values of n and m , the higher

the resolution of the resulted plain of solutions. As the resolution of the plain is increasing it is more possible to reach even closer to the value of a local maximum. However, the higher is the resolution of the expected plain the higher is the number of the optimization runs that should be conducted in order to acquire the results to create the solution plain and finally the higher is the computation time that is going to be needed. For the current diploma thesis project n and m were chosen so as to create a plain where the dependency on water-cut work-over limit and group field oil rate would be discernible.

Further development of the current project of well placement optimization would be creating a more refined plain increasing in that way its resolution. This would probably result in finding a new optimal model since the refined plain would reveal a location nearer to the maximum value or a new maximum value. Another important aspect that should also be taken into account in a future development of this project is the economic viability of this project. Although oil production is increased and the number of wells can also be decreased, in order to monitor the flow rates of water and oil at each connection of the well and also being able to shut and open a specific connection requires more specialized equipment meaning that an economic analysis of the whole project should be conducted. Finally, the optimization of well placement that was implemented using *PlanOpt* software could be conducted by using *CMOST* optimization tool of *CMG* software in order to compare the results of both software optimization tools which utilize different optimization algorithms.

5.2 History Matching Optimization

There are several remarks concerning the history matching optimization. While having the same regression parameters in all the optimization attempts each time different observed data set types were kept active during the regression process and finally when optimization was finished an evaluation was conducted by having all the observed data set types active. This procedure was carried out until all possible combinations of data set types being active were applied in order to inspect possible differences between each optimization run.

Judging by a quantitative perspective each different simulation run produced different results since the *RMS* value after the final evaluation was different among every model. For each simulation run a different objective function is formed since the data set types that are active during regression change resulting to different output results at the end of the regression process and finally different results after the final evaluation. The best model was the one which produced the minimum *RMS* value. However, the *RMS* values for all different optimization runs were not exceeding each other by a maximum of 6.19%. Judging by a qualitative perspective though, it is important to not only take into account that all the history matching curves corresponding to each different optimization run are having minor differences between each other which happens due to the fact that their resulted *RMS* values have also minor differences as stated above, but also that all curves appear to have the same behavior and shape.

The fact that water-cut is a function of oil and water rate is crucial in interpreting the history matching results since the data set that the optimization process was incorporating were oil production rate, water production rate and water-cut fraction. Although at each different simulation run different data set types were active during regression, the final step was always to evaluate the results having all the data set types active. Since water-cut and oil and water rate are depended the simulation model that was resulted each time after the final evaluation had a common behavior because of the above mentioned dependency of the above mentioned data sets.

Further development of the current project of history matching optimization would be creating a more complex set of parameters which would be based on geological and geophysical information resulting to more efficient history matching. Finally, the optimization of history matching that was achieved by using *SimOpt* software could be conducted by using *CMOST* optimization tool of *CMG* software in order to

compare the results of both software optimization tools which utilize different optimization algorithms.

Appendix A

Well Position on Initial Simulation Model

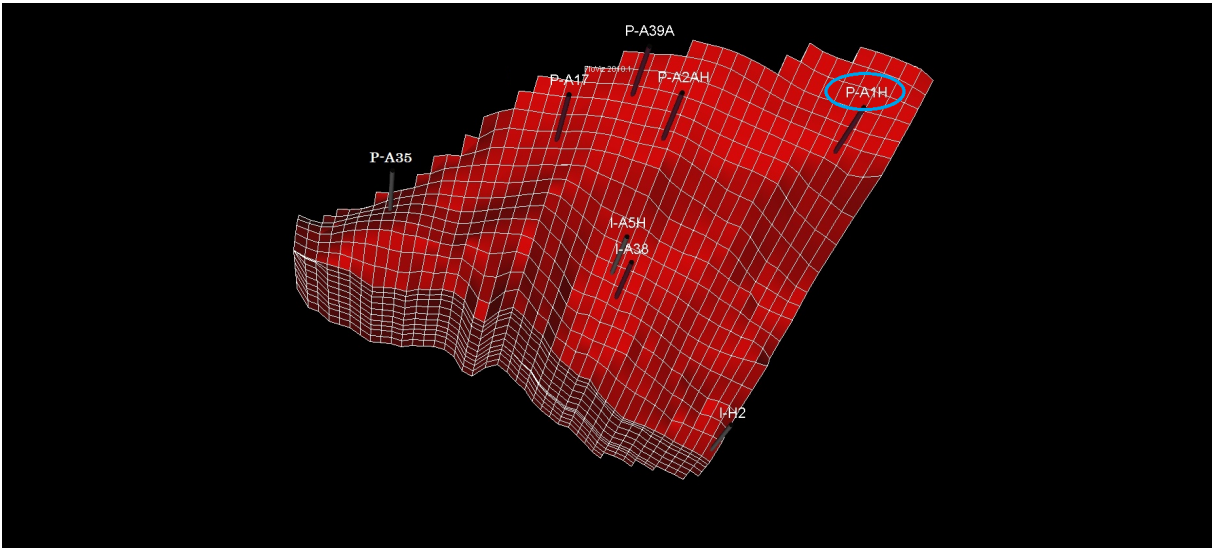


Figure A.1: Well P-A1H position ([click here to return](#))

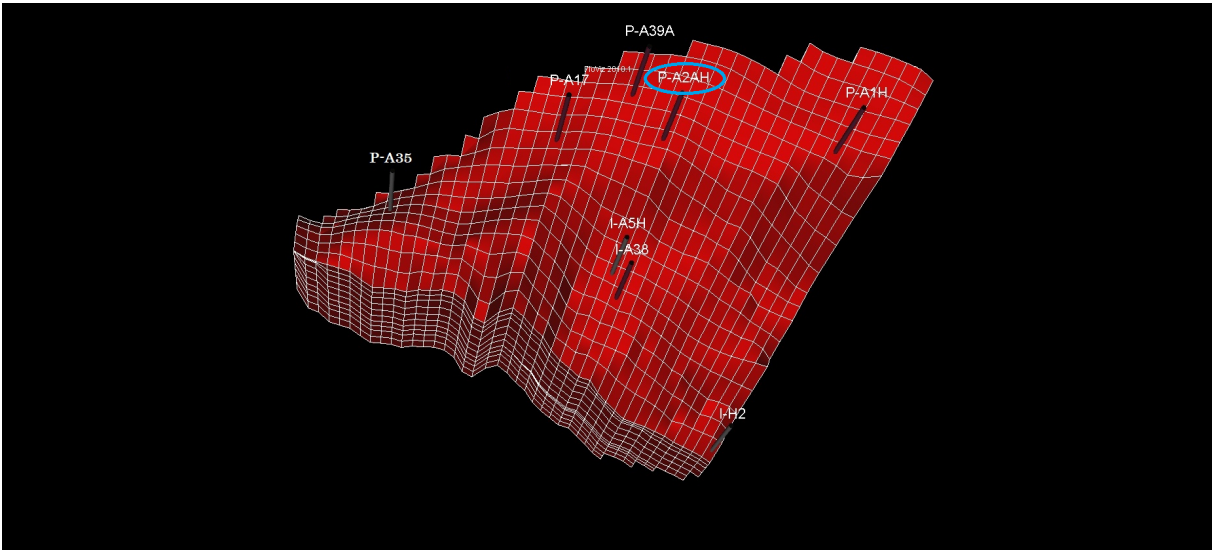


Figure A.2: Well P-A2AH position ([click here to return](#))

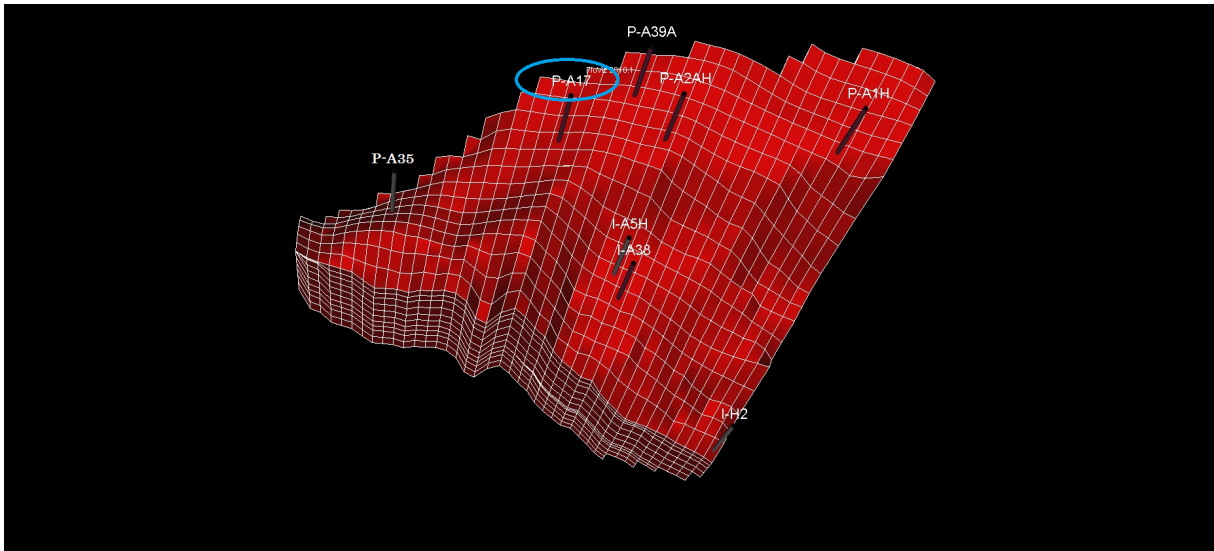


Figure A.3: Well P-A17 position ([click here to return](#))

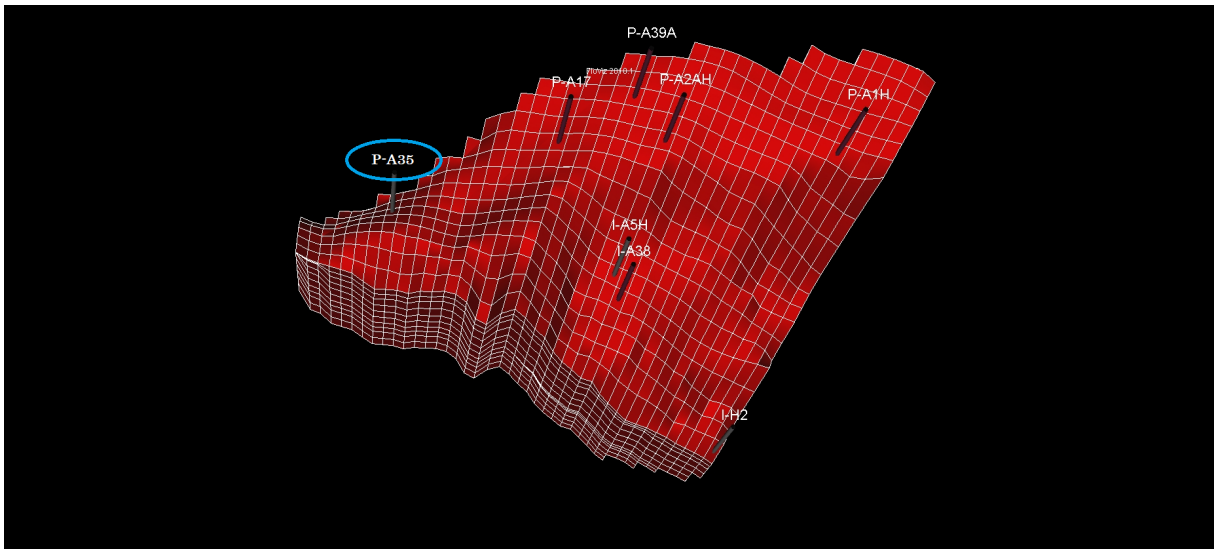


Figure A.4: Well P-A35 position ([click here to return](#))

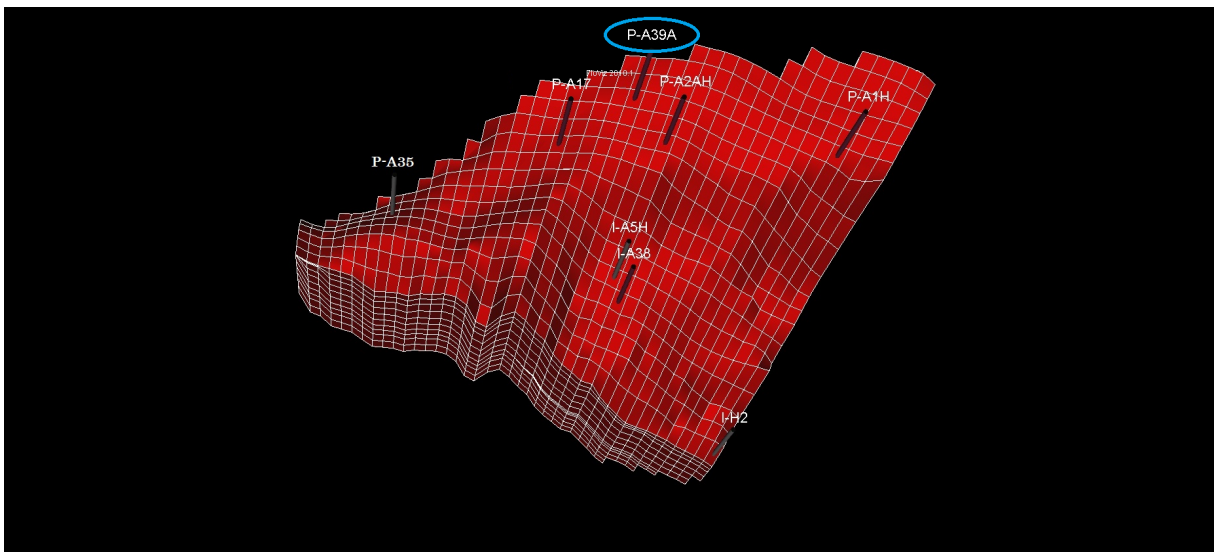


Figure A.5: Well P-A39A position ([click here to return](#))

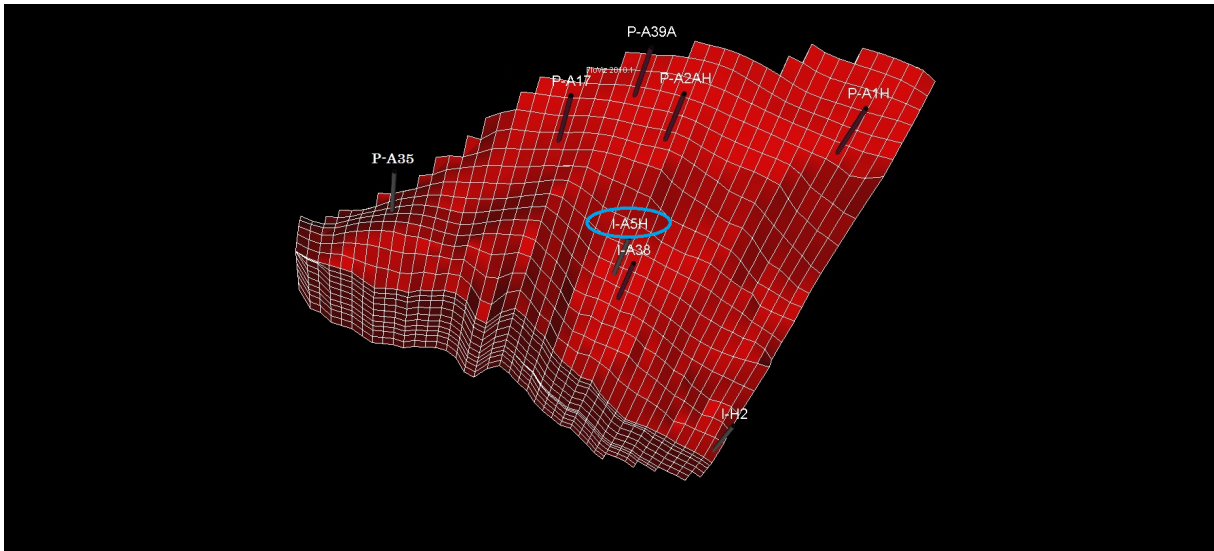


Figure A.6: Well I-A5H position ([click here to return](#))

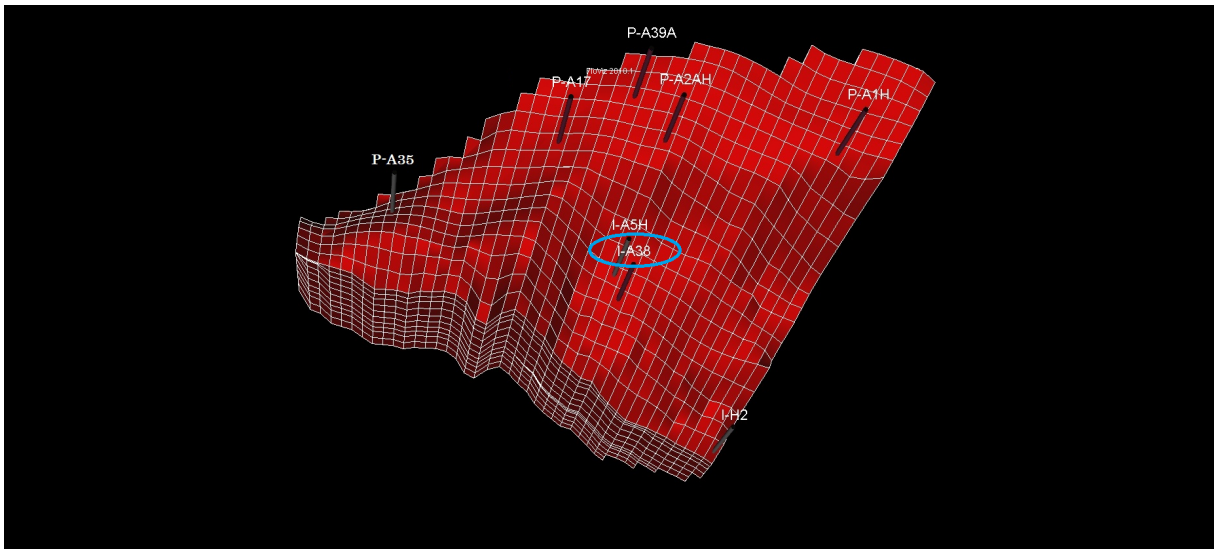


Figure A.7: Well I-A38 position ([click here to return](#))

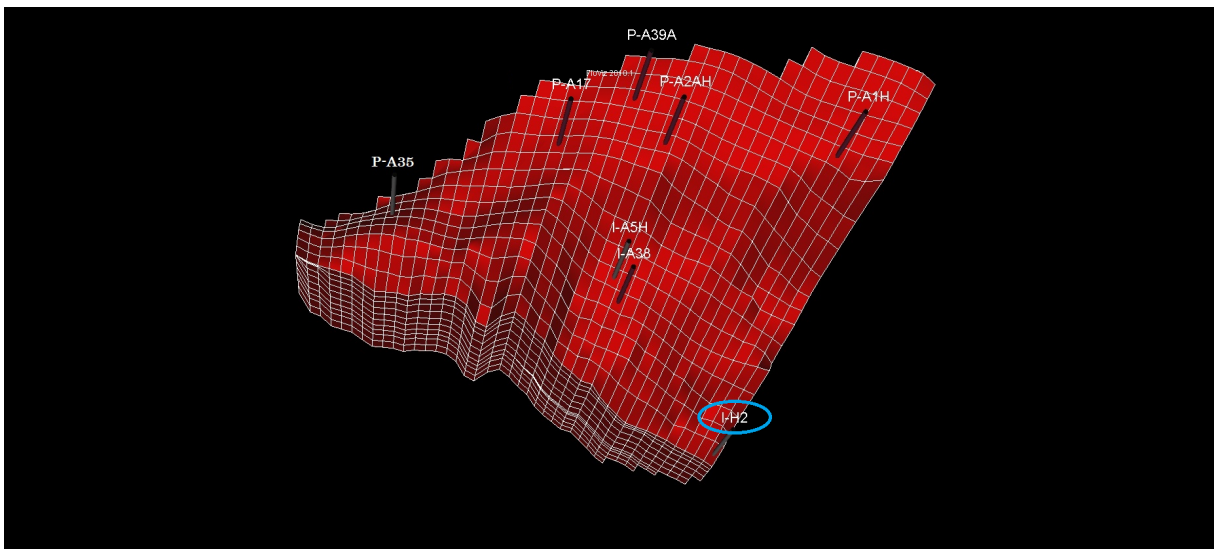


Figure A.8: Well I-H2 position ([click here to return](#))



Appendix B

Optimal Simulation Model Well Reduction

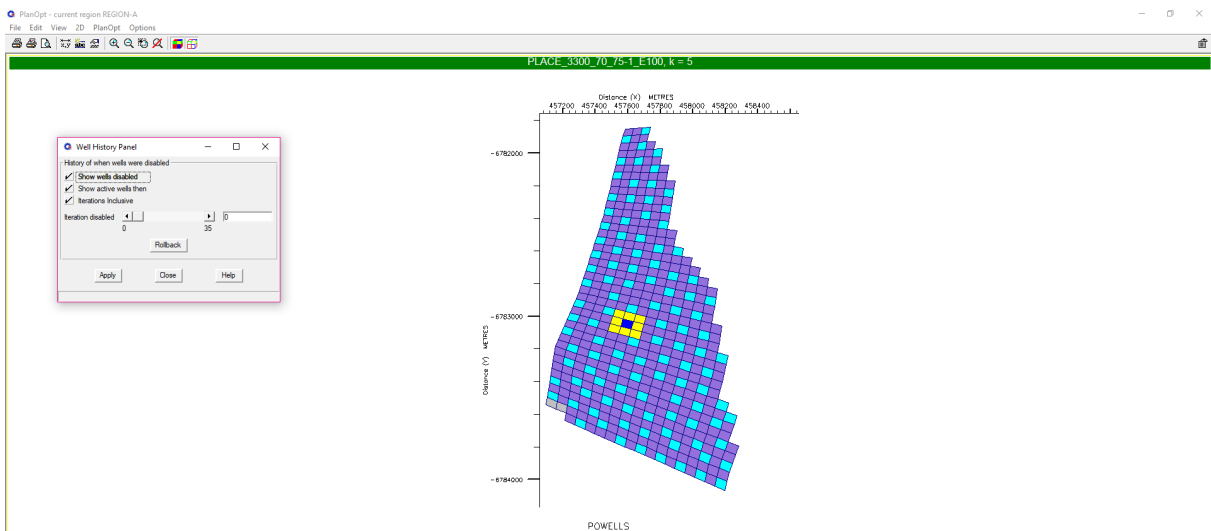


Figure B.1: Before optimization begins ([click here to return](#))

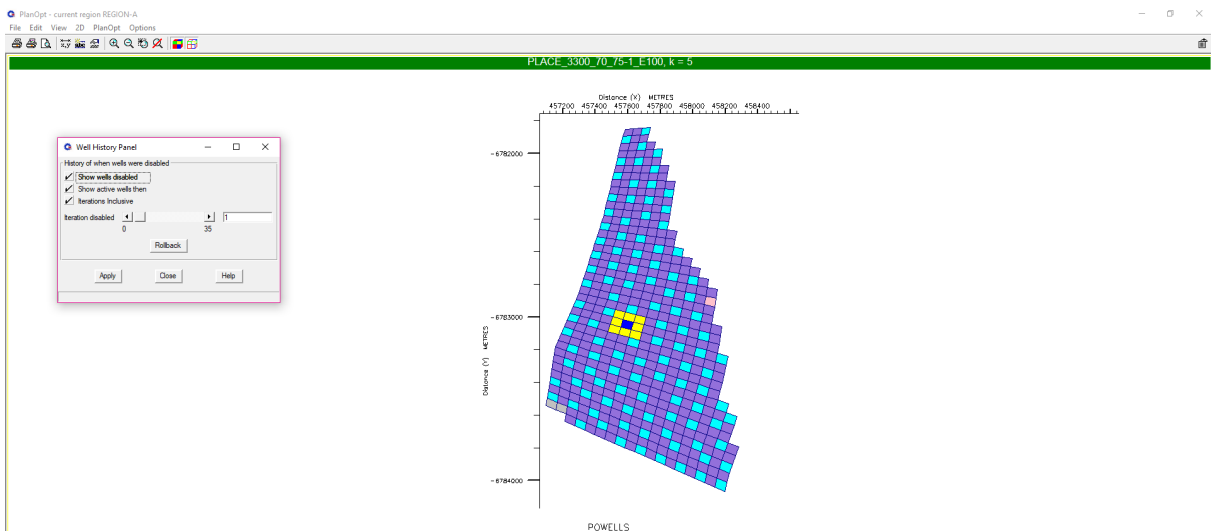


Figure B.2: Iteration No.1 ([click here to return](#))

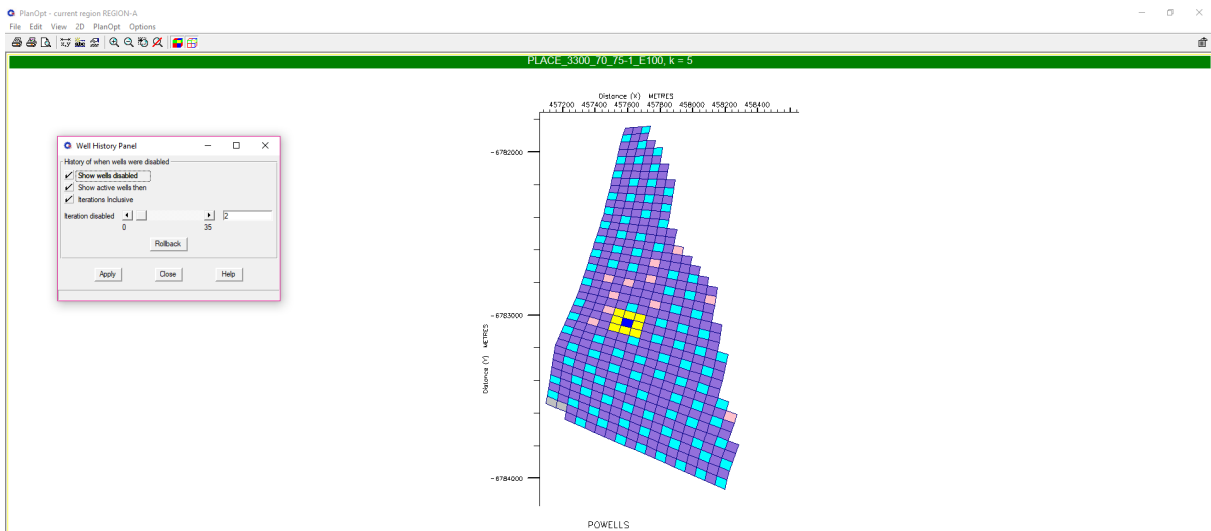


Figure B.3: Iteration No.2 ([click here to return](#))

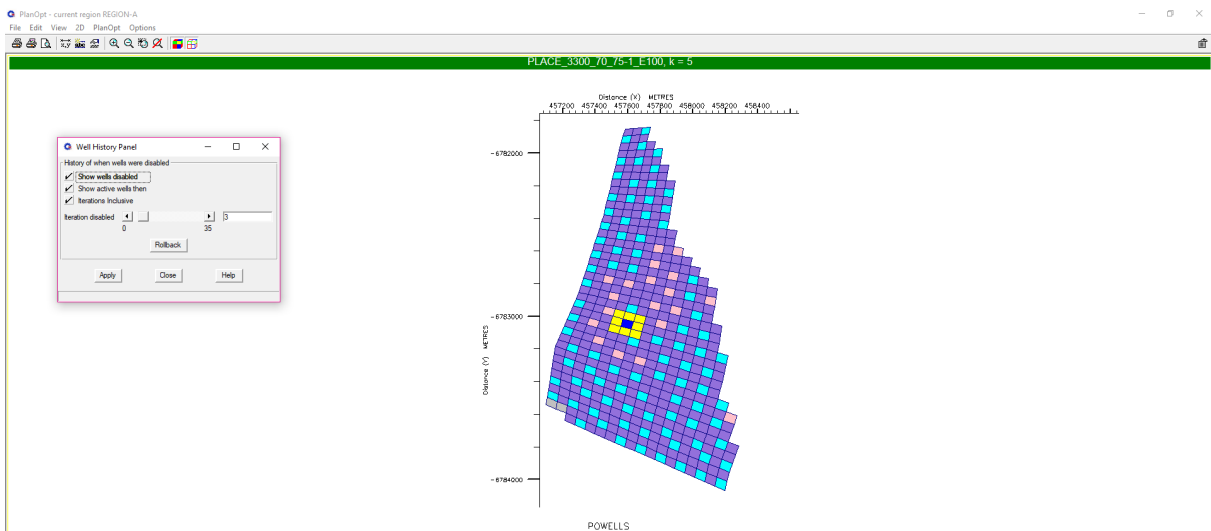


Figure B.4: Iteration No.3 ([click here to return](#))

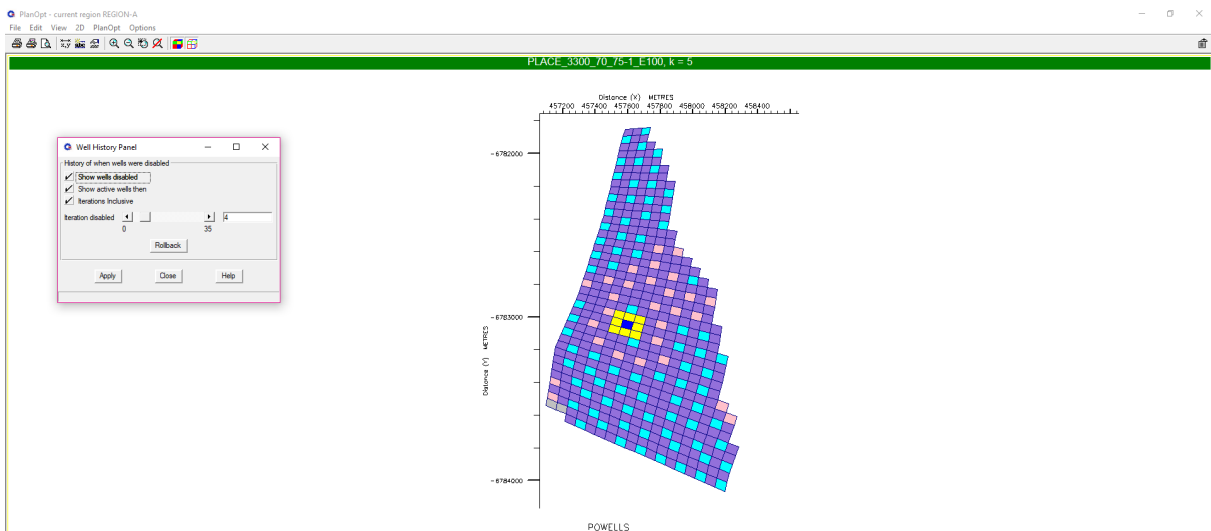


Figure B.5: Iteration No.4 ([click here to return](#))

APPENDIX B. OPTIMAL SIMULATION MODEL WELL REDUCTION

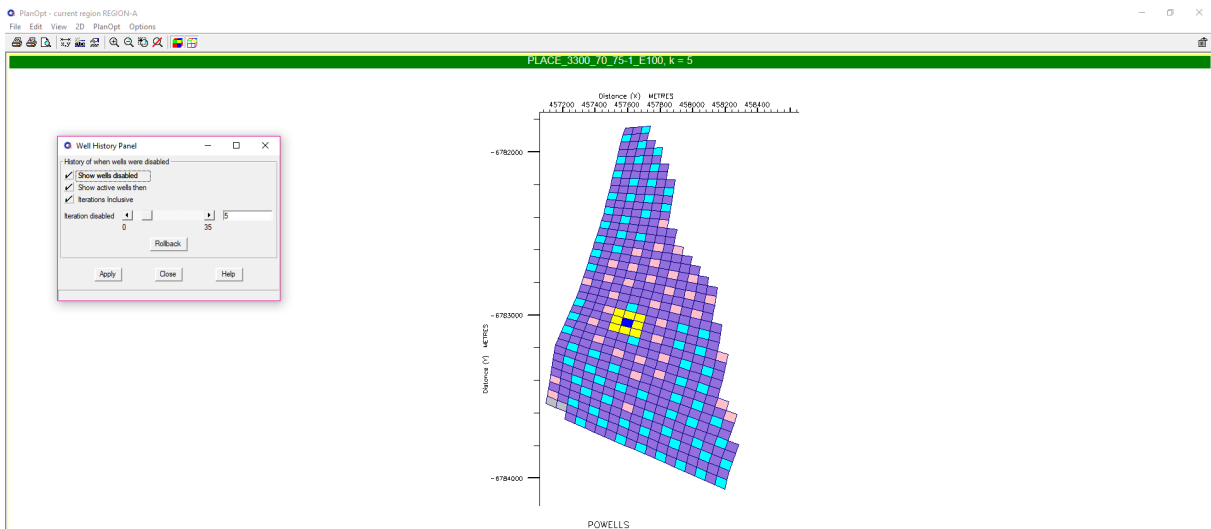


Figure B.6: Iteration No.5 ([click here to return](#))

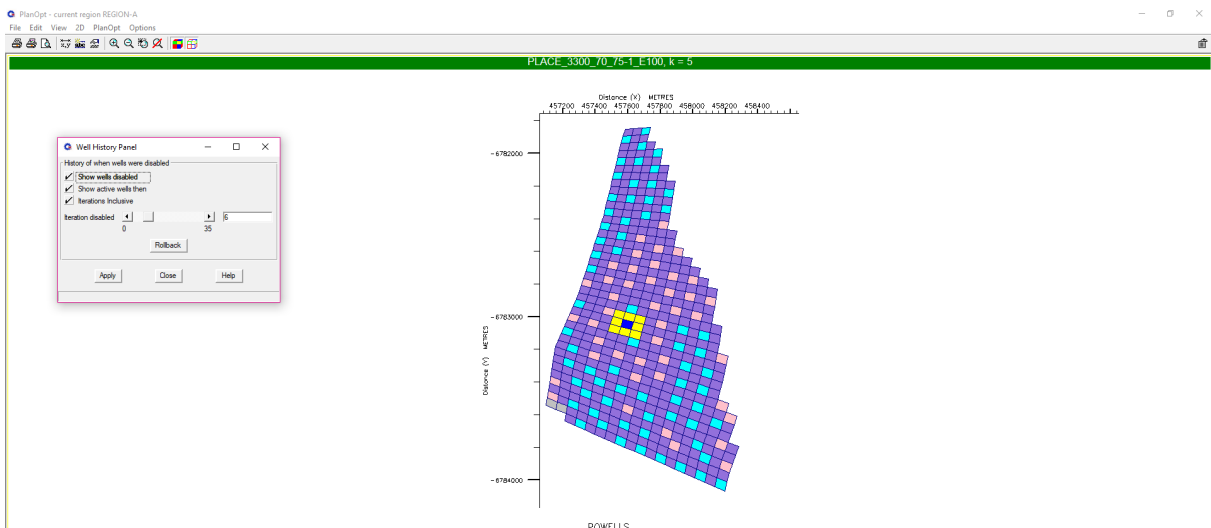


Figure B.7: Iteration No.6 ([click here to return](#))

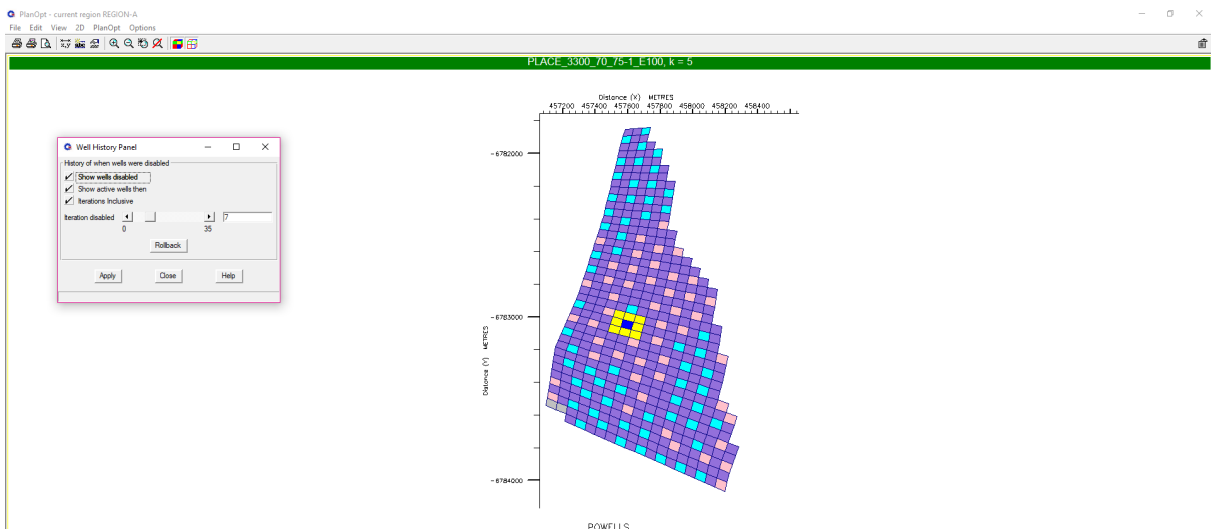


Figure B.8: Iteration No.7 ([click here to return](#))

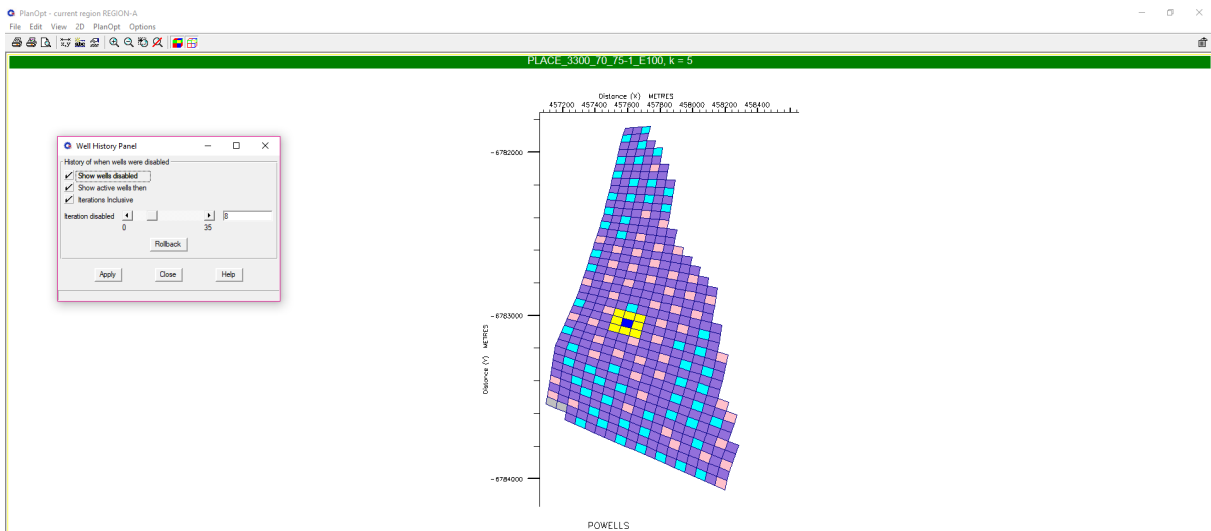


Figure B.9: Iteration No.8 ([click here to return](#))

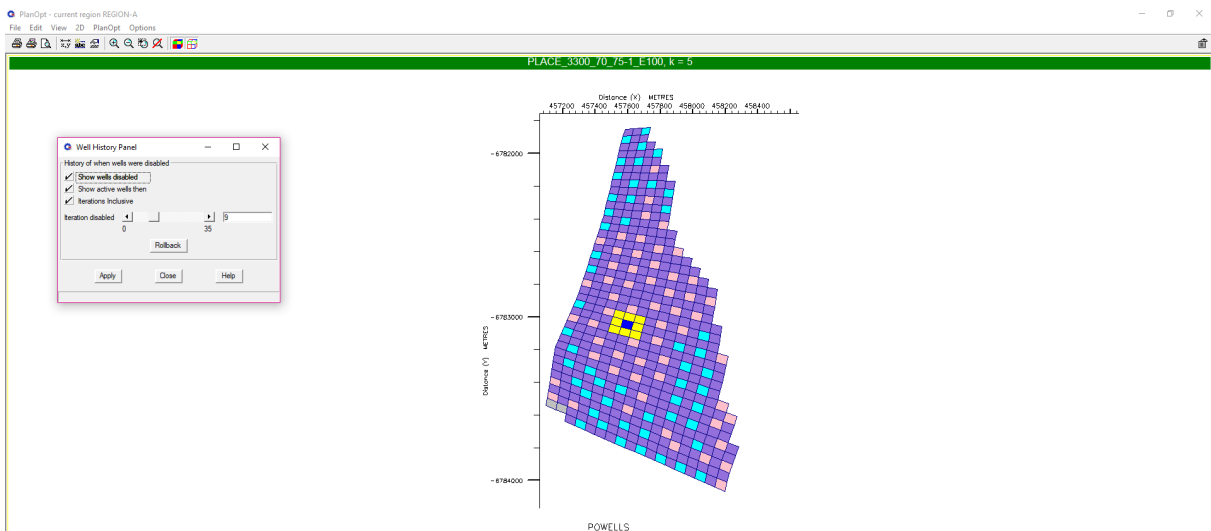


Figure B.10: Iteration No.9 ([click here to return](#))

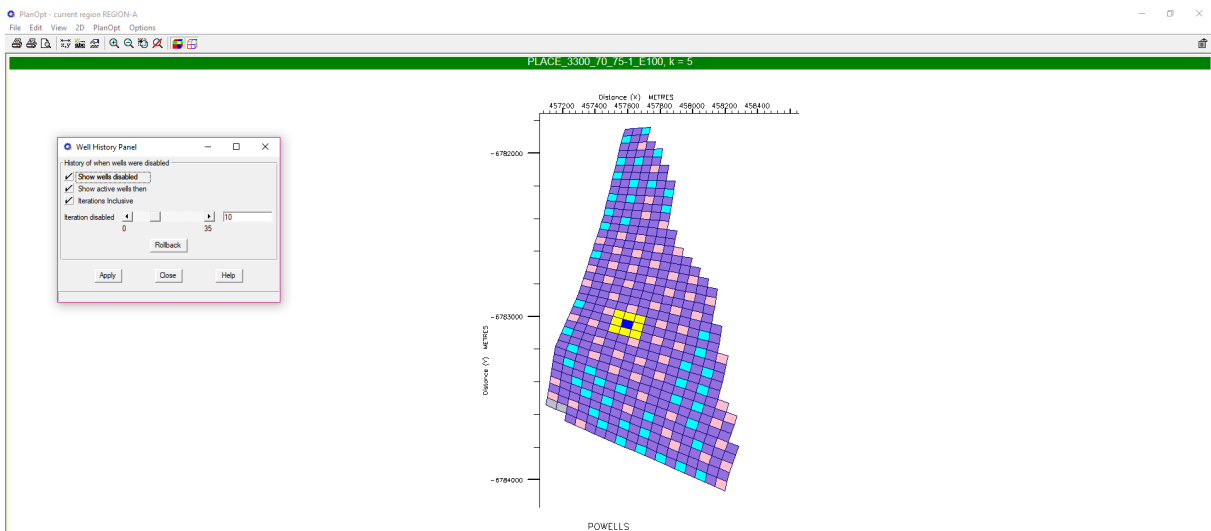


Figure B.11: Iteration No.10 ([click here to return](#))

APPENDIX B. OPTIMAL SIMULATION MODEL WELL REDUCTION

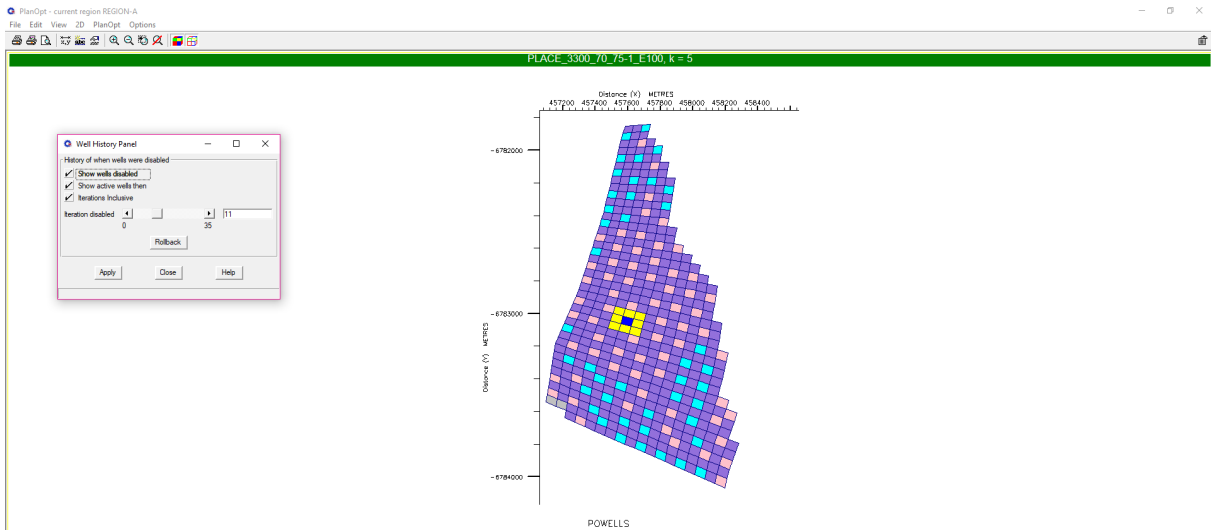


Figure B.12: Iteration No.11 ([click here to return](#))

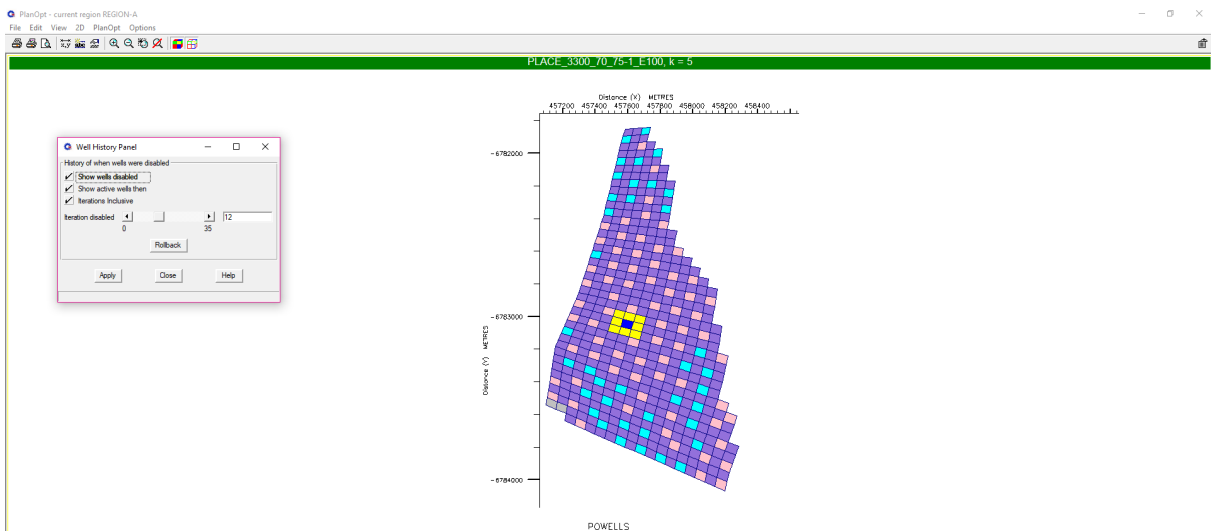


Figure B.13: Iteration No.12 ([click here to return](#))

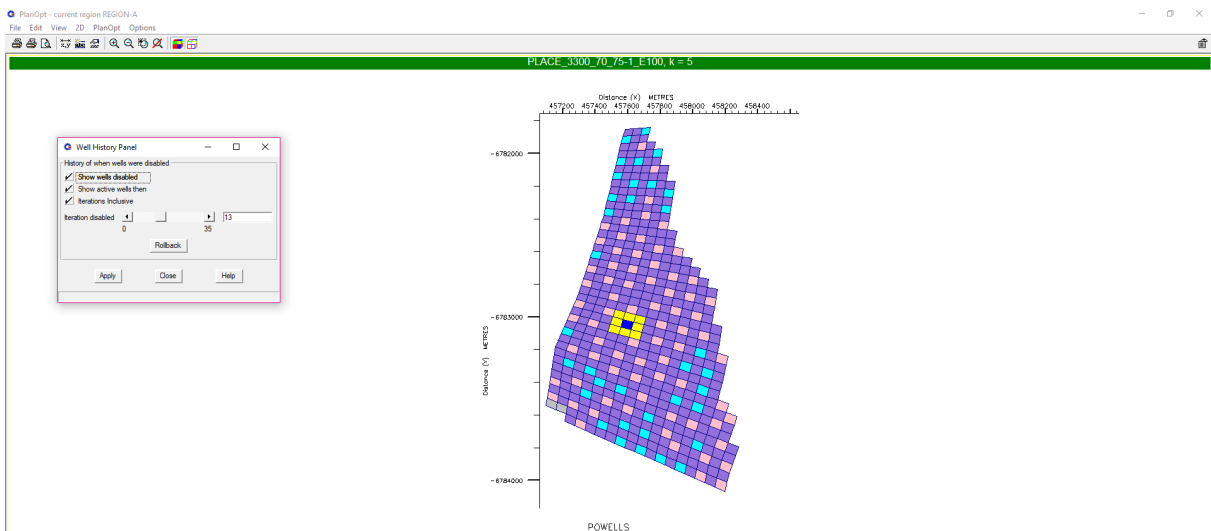


Figure B.14: Iteration No.13 ([click here to return](#))

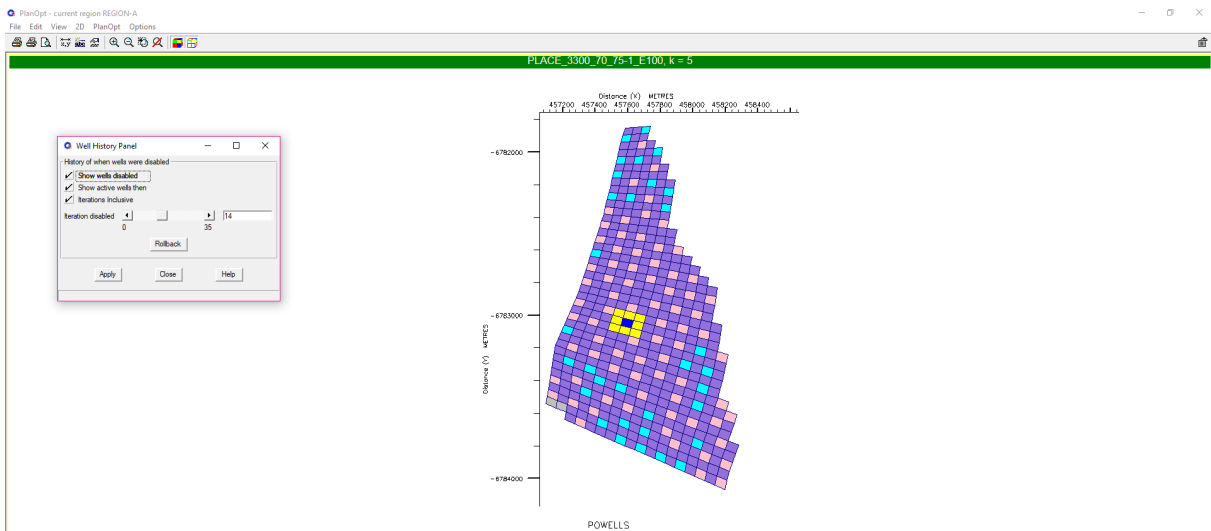


Figure B.15: Iteration No.14 ([click here to return](#))

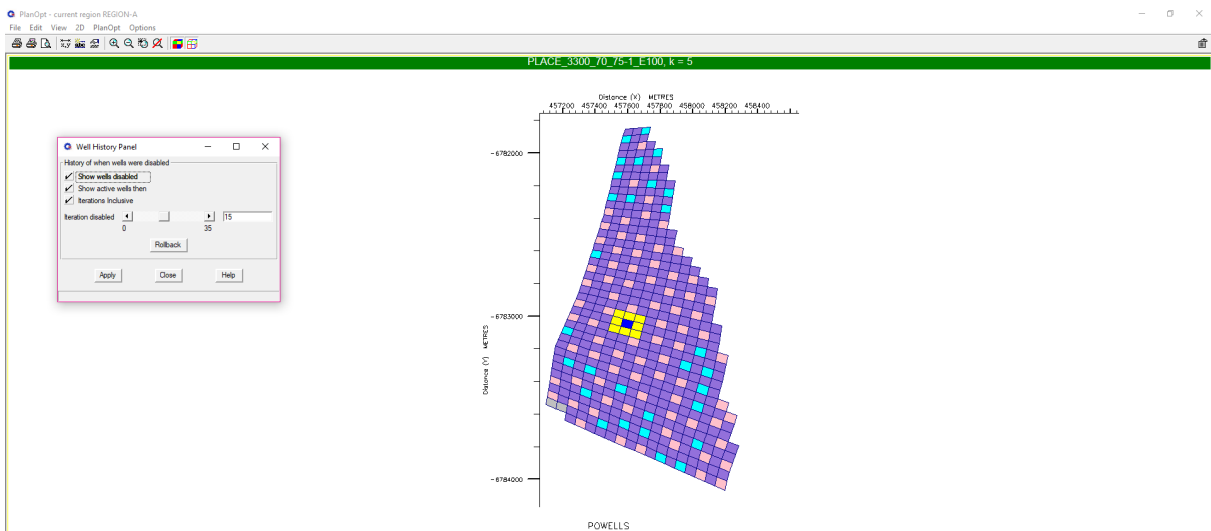


Figure B.16: Iteration No.15 ([click here to return](#))

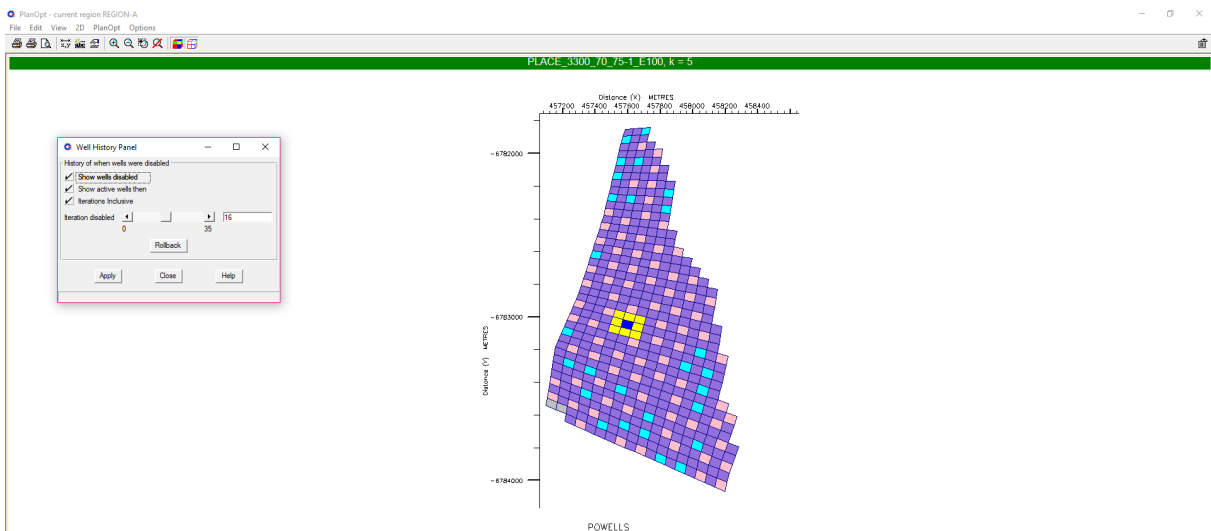


Figure B.17: Iteration No.16 ([click here to return](#))

APPENDIX B. OPTIMAL SIMULATION MODEL WELL REDUCTION

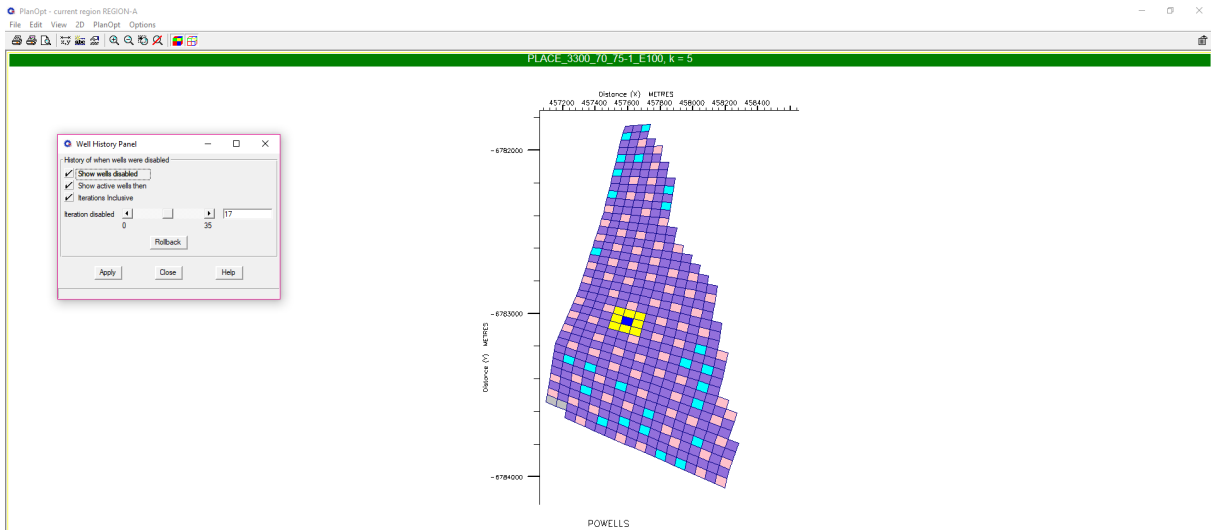


Figure B.18: Iteration No.17 ([click here to return](#))

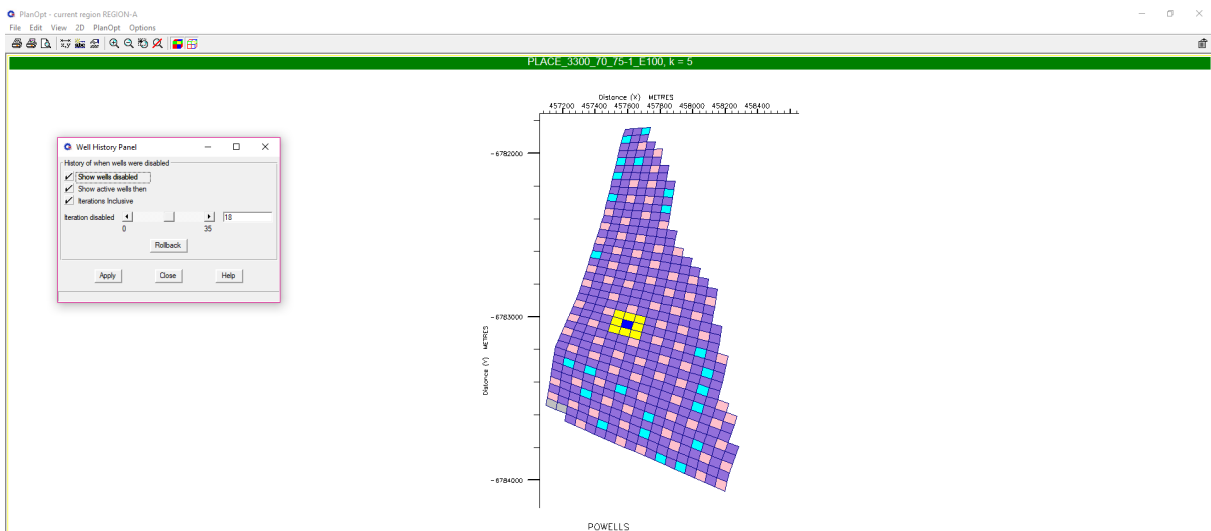


Figure B.19: Iteration No.18 ([click here to return](#))

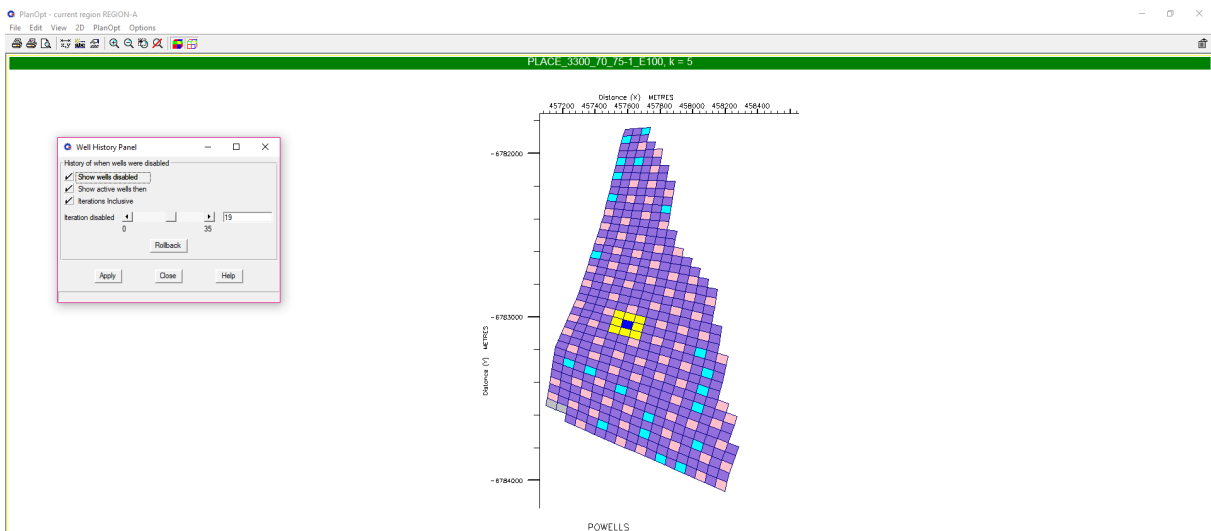


Figure B.20: Iteration No.19 ([click here to return](#))

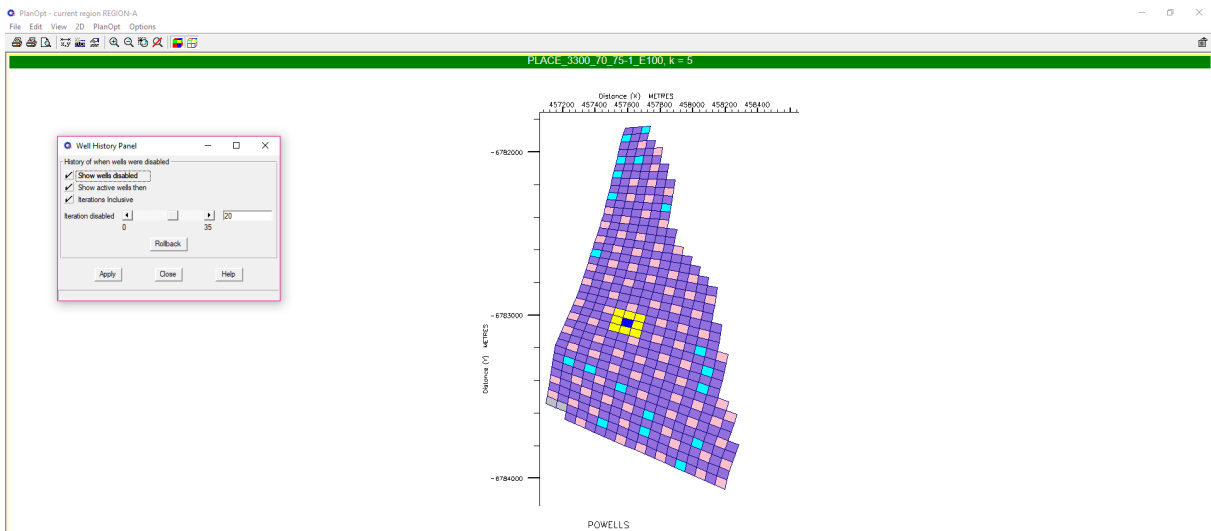


Figure B.21: Iteration No.20 ([click here to return](#))

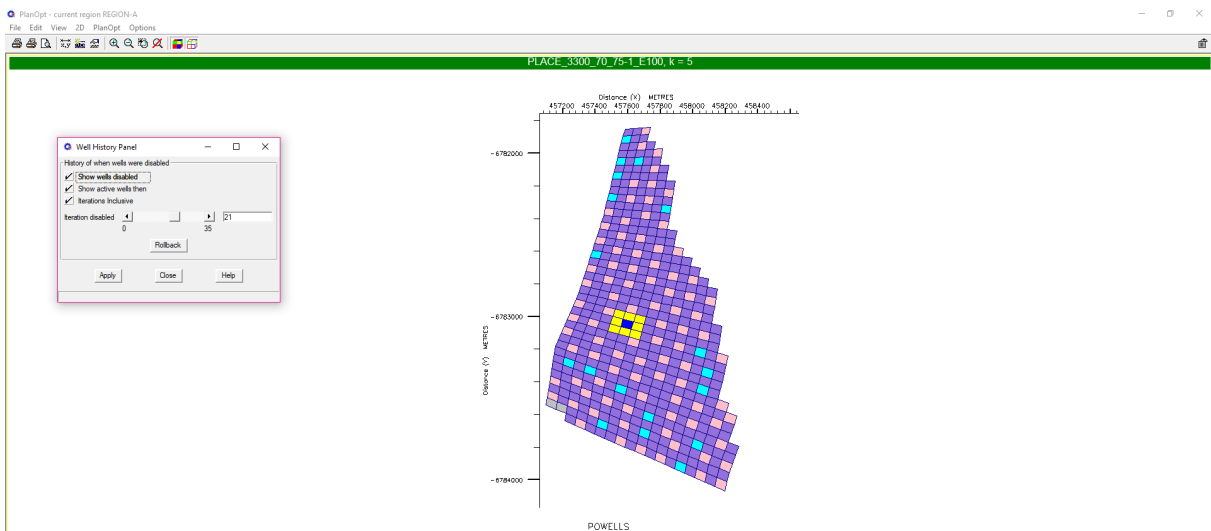


Figure B.22: Iteration No.21 ([click here to return](#))

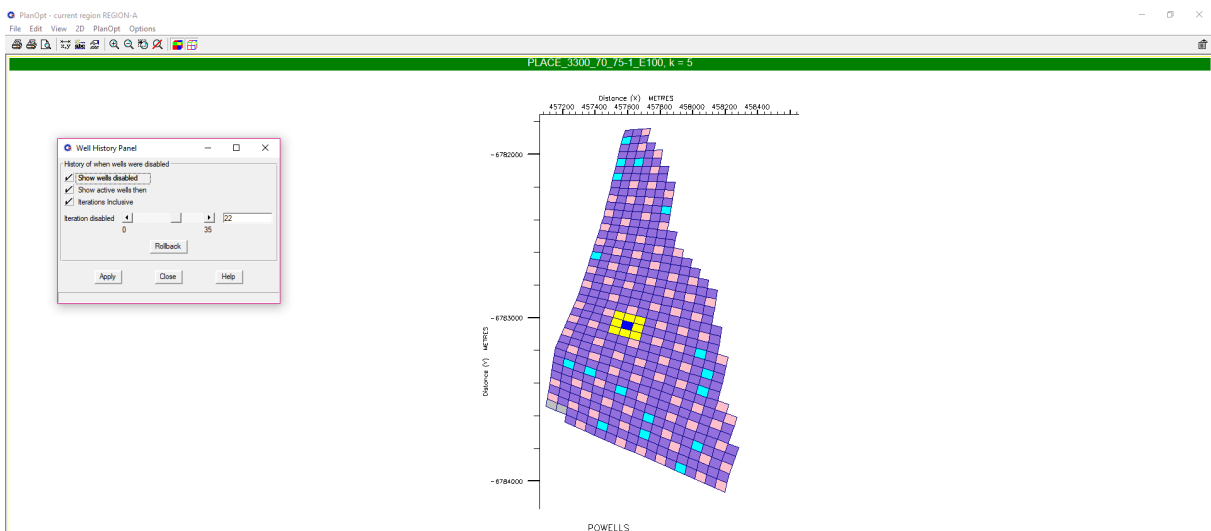


Figure B.23: Iteration No.22 ([click here to return](#))

APPENDIX B. OPTIMAL SIMULATION MODEL WELL REDUCTION

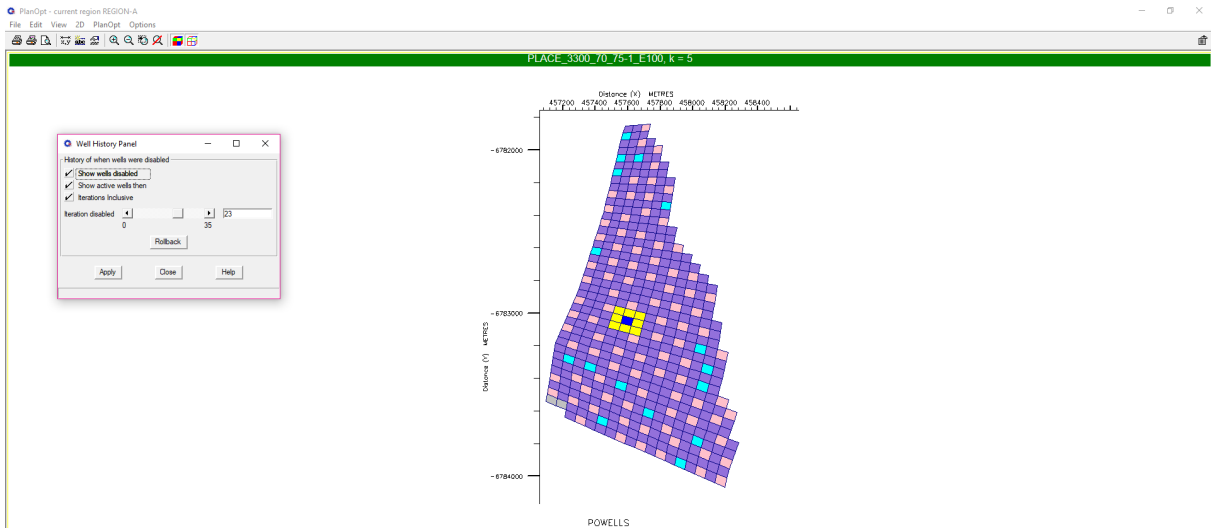


Figure B.24: Iteration No.23 ([click here to return](#))

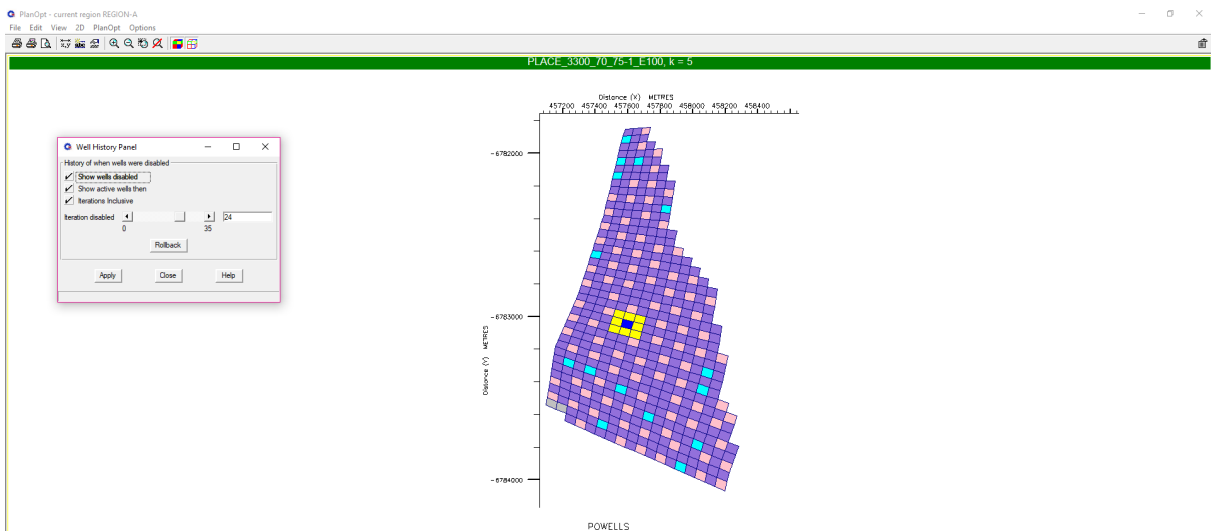


Figure B.25: Iteration No.24 ([click here to return](#))

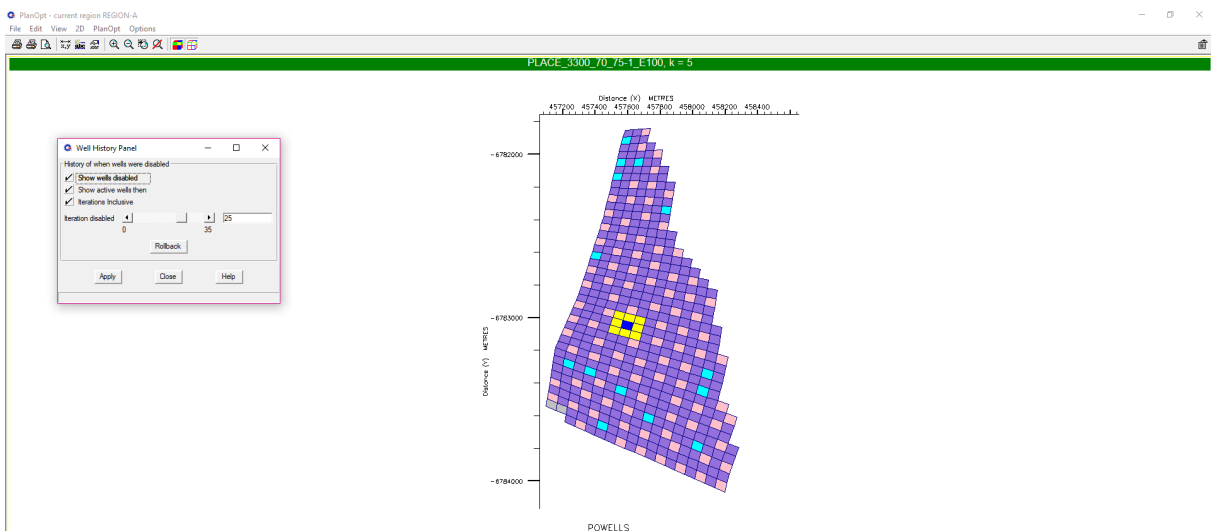


Figure B.26: Iteration No.25 ([click here to return](#))

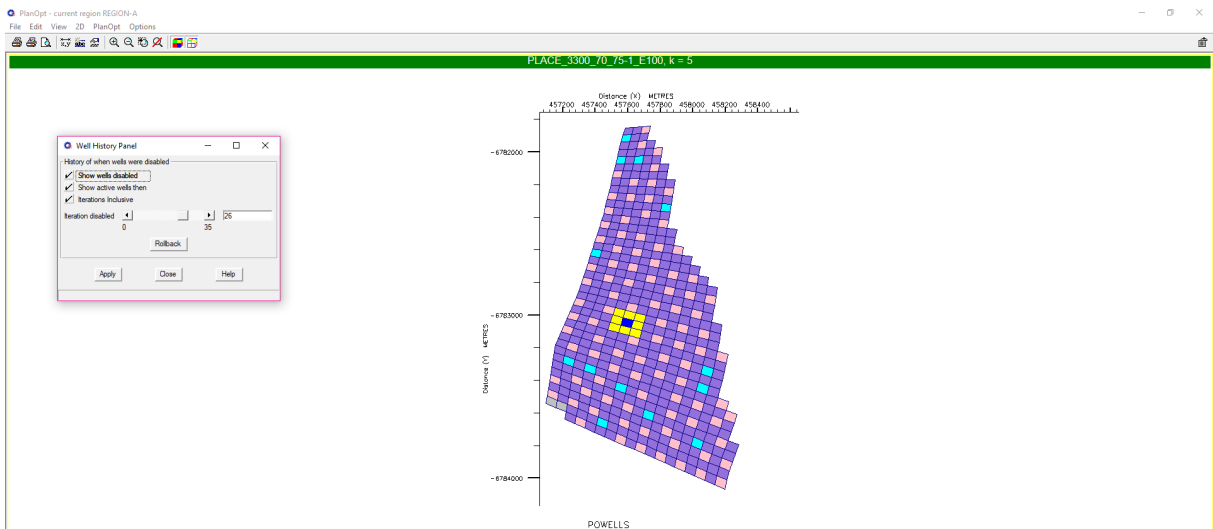


Figure B.27: Iteration No.26 ([click here to return](#))

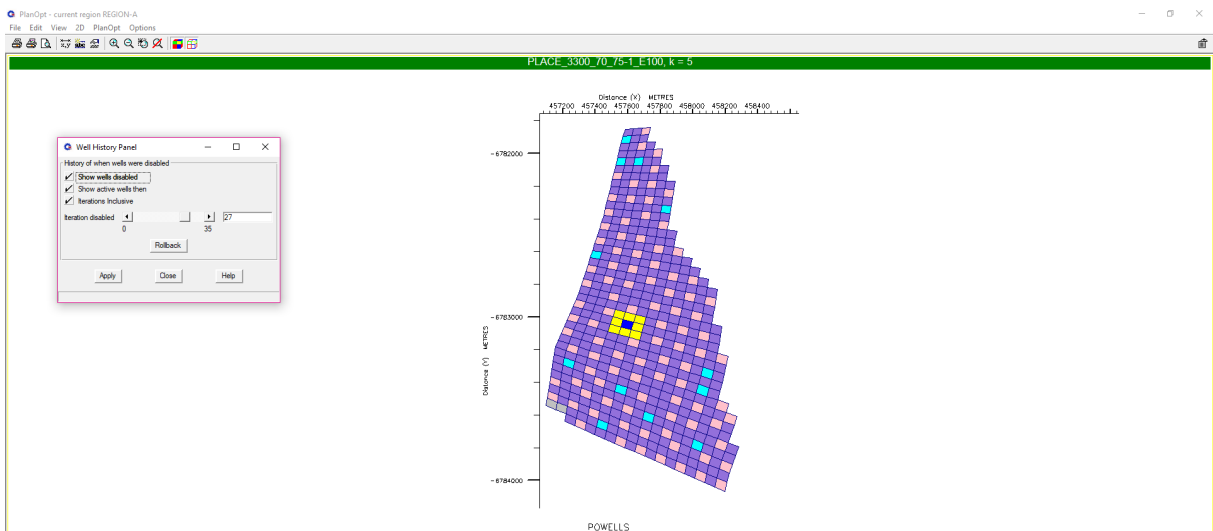


Figure B.28: Iteration No.27 ([click here to return](#))

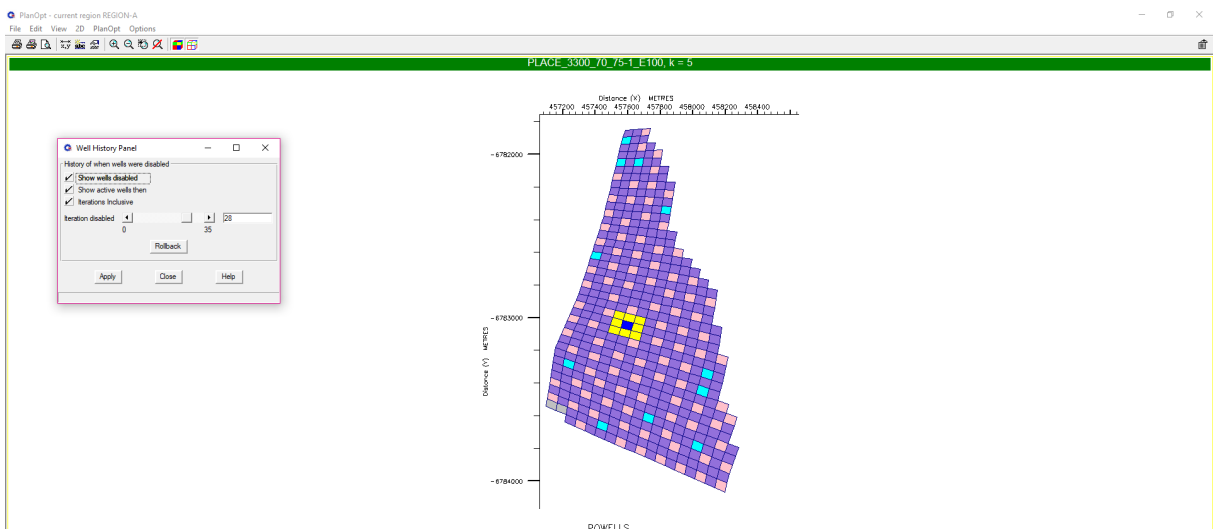


Figure B.29: Iteration No.28 ([click here to return](#))

APPENDIX B. OPTIMAL SIMULATION MODEL WELL REDUCTION

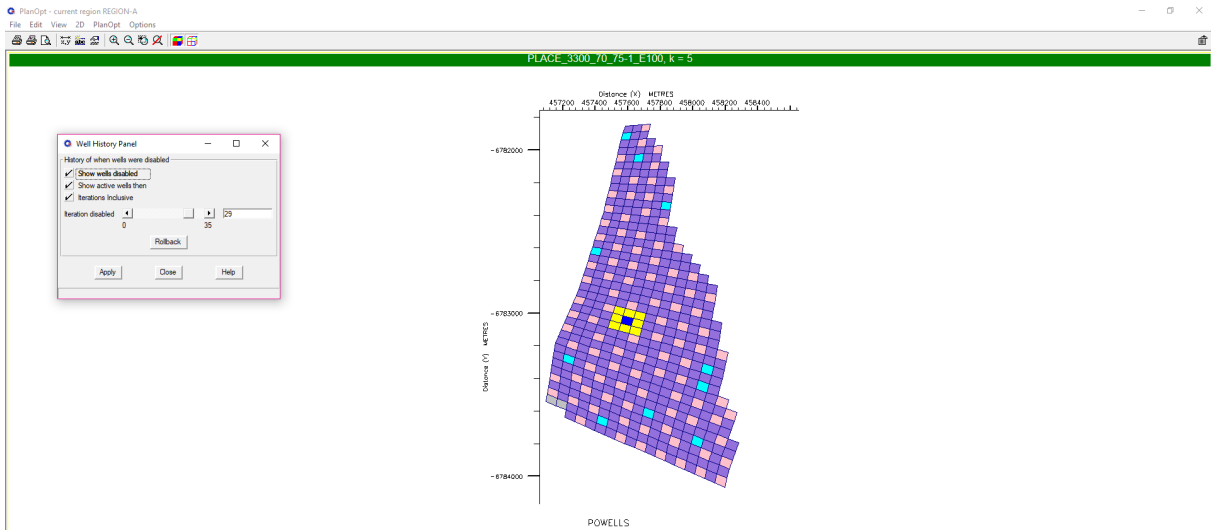


Figure B.30: Iteration No.29 ([click here to return](#))

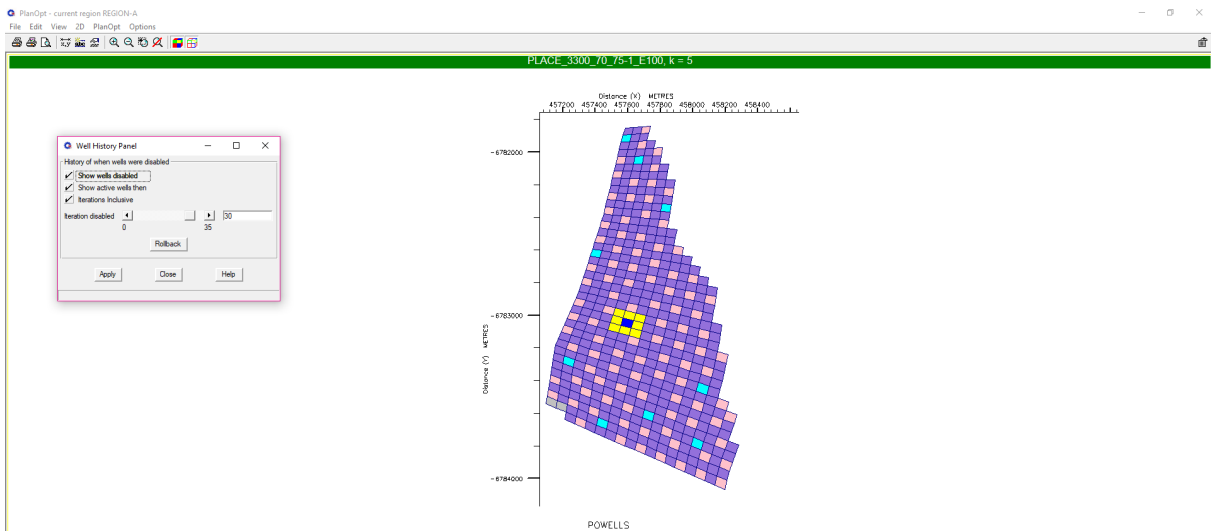


Figure B.31: Iteration No.30 ([click here to return](#))

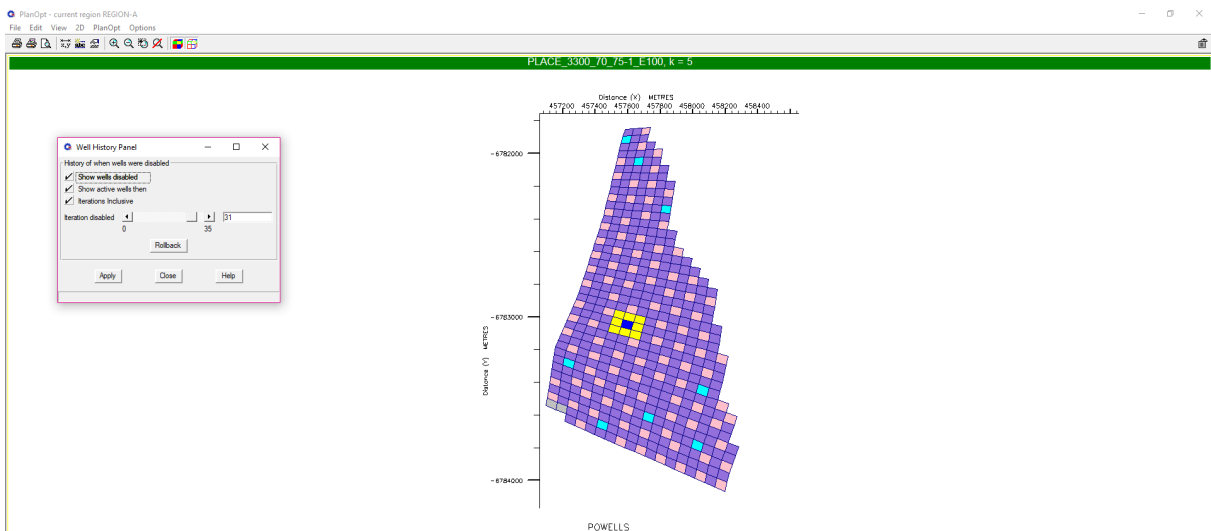


Figure B.32: Iteration No.31 ([click here to return](#))

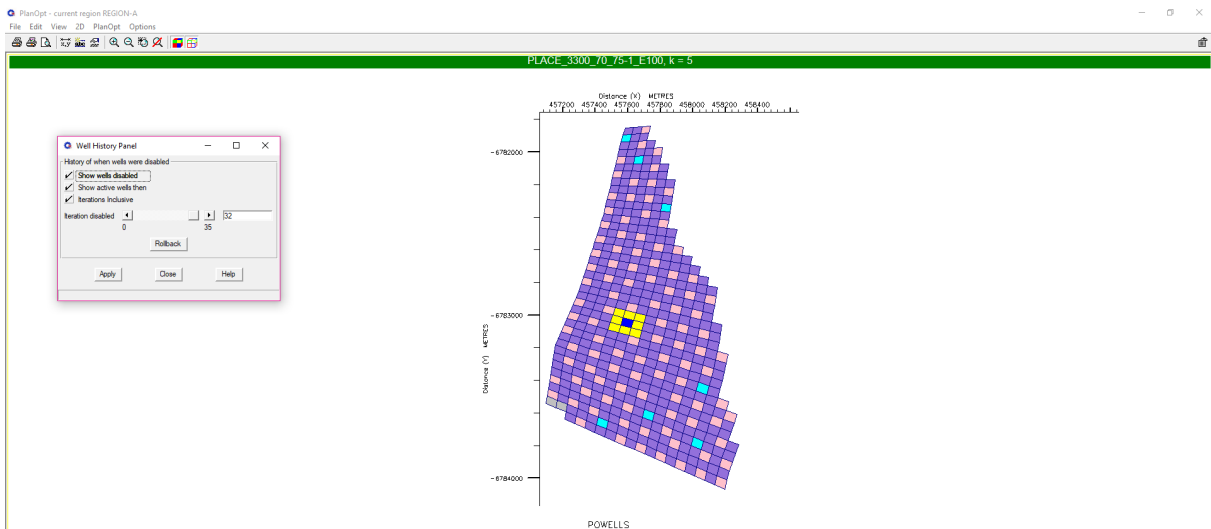


Figure B.33: Iteration No.32 ([click here to return](#))

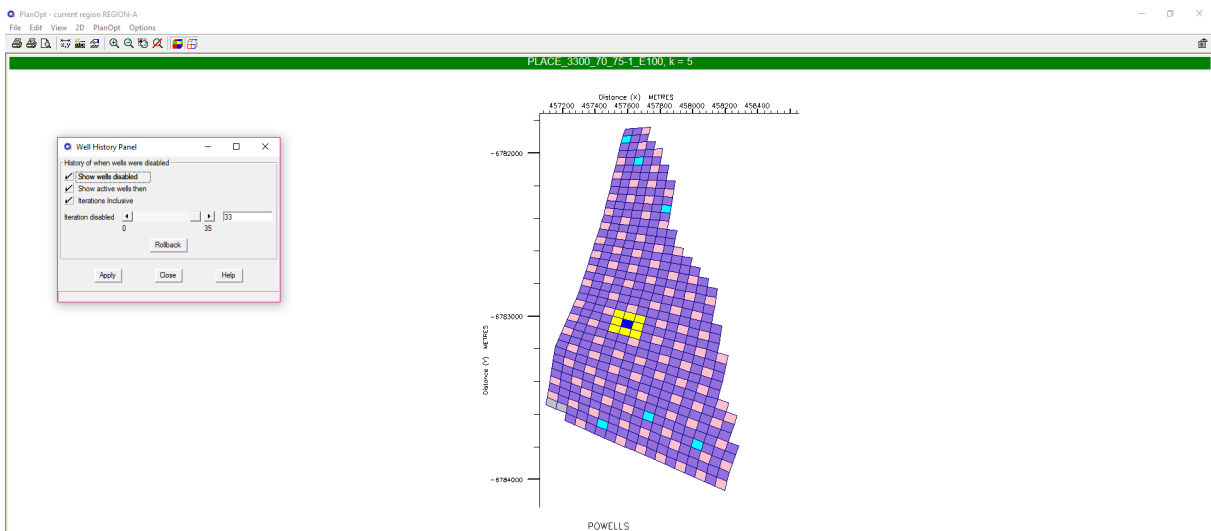


Figure B.34: Iteration No.33 ([click here to return](#))

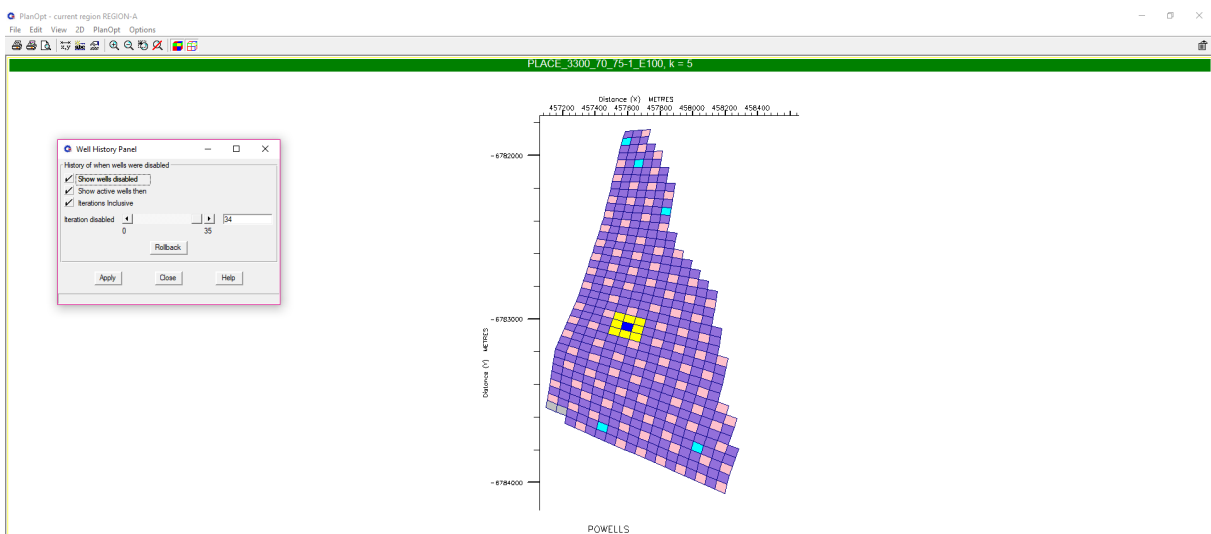


Figure B.35: Iteration No.34 ([click here to return](#))

Appendix C

Well Position on Optimal Simulation Model

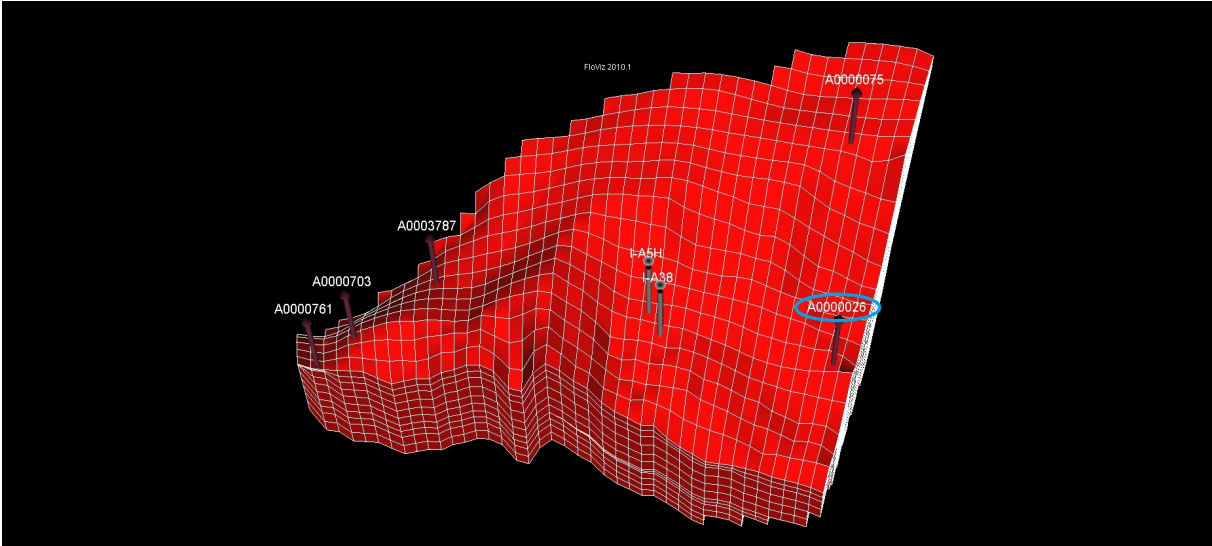


Figure C.1: Well P-A000026 position ([click here to return](#))

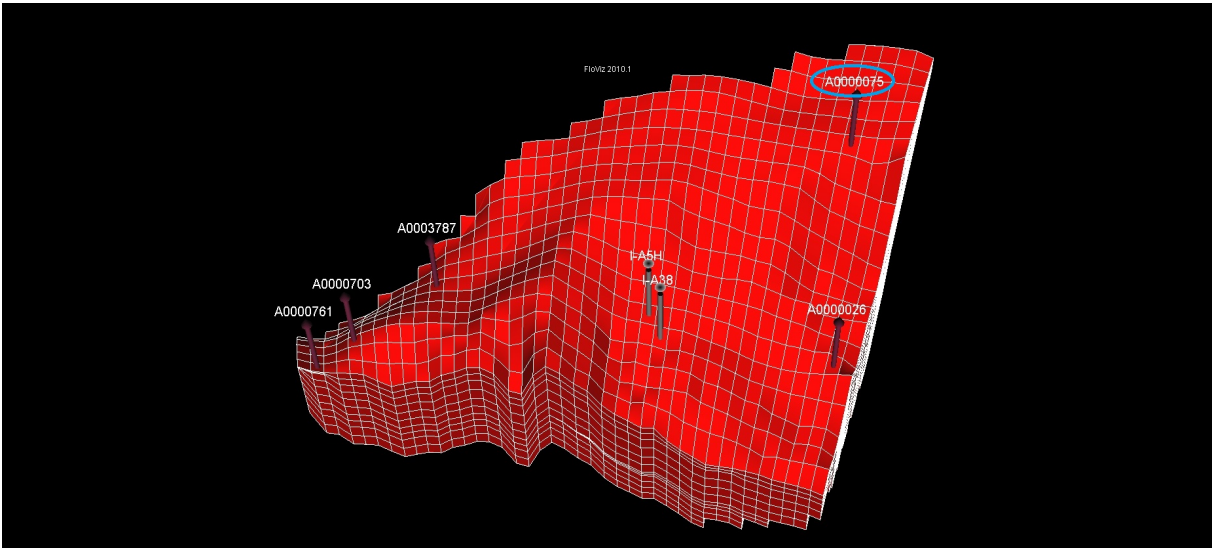


Figure C.2: Well P-A000075 position ([click here to return](#))

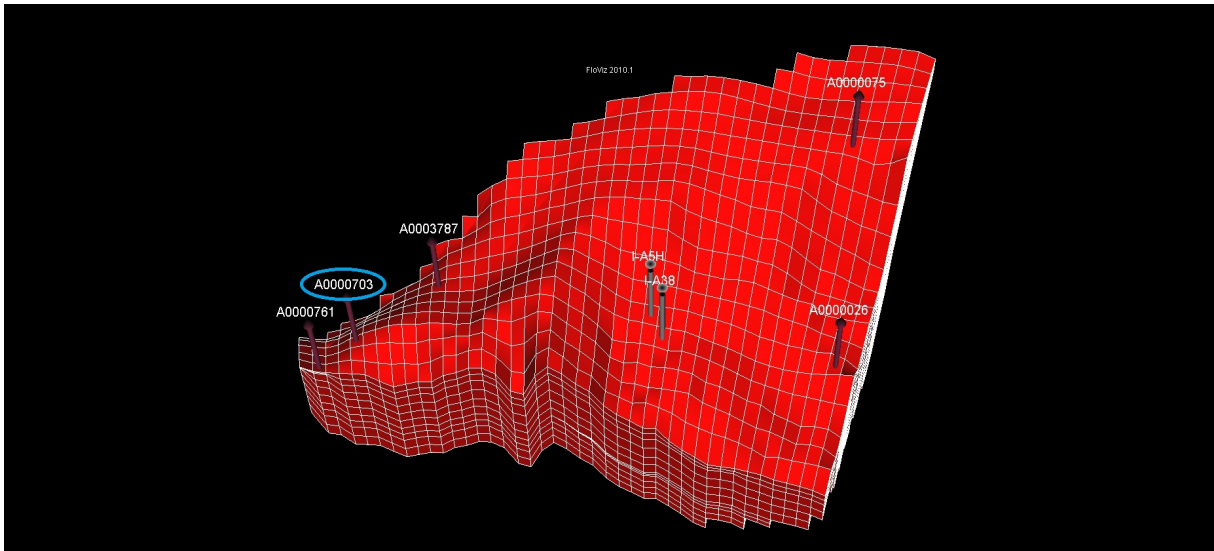


Figure C.3: Well P-A0000703 position ([click here to return](#))

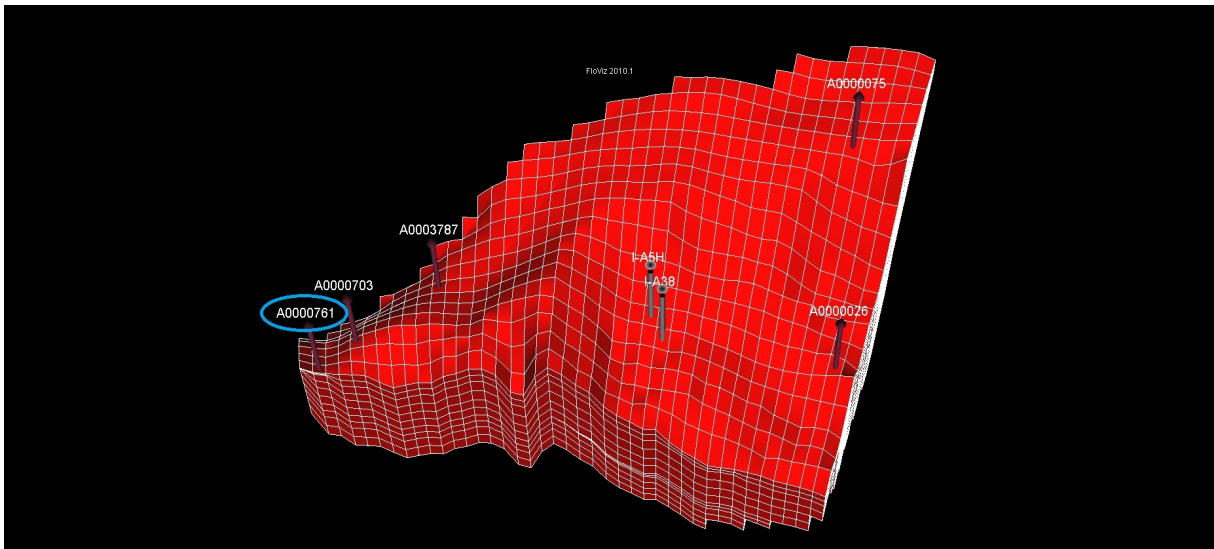


Figure C.4: Well P-A0000761 position ([click here to return](#))

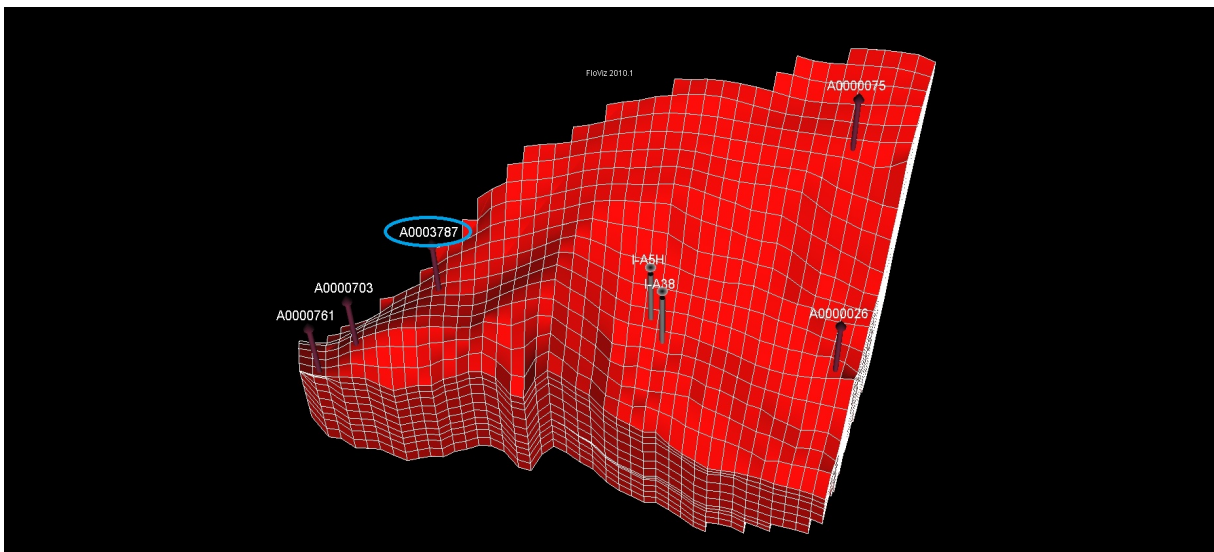


Figure C.5: Well P-A0003787 position ([click here to return](#))

Bibliography

- [1] Schlumberger, *ECLIPSE (ECLIPSE* reservoir simulation software Version 2010.1) Reference Manual*. 2010.
- [2] Schlumberger, *PlanOpt (ECLIPSE* reservoir simulation software Version 2010.1) User Guide*. 2010.
- [3] Schlumberger, *SimOpt (ECLIPSE* reservoir simulation software Version 2010.1) User Guide*. 2010.
- [4] Schlumberger, “Formulation of the Equations,” in *ECLIPSE (ECLIPSE* reservoir simulation software Version 2010.1) Technical Description*, ch. 23, pp. 341–358, 2010.
- [5] Schlumberger, “Solution of the Linear Equations,” in *ECLIPSE (ECLIPSE* reservoir simulation software Version 2010.1) Technical Description*, ch. 63, pp. 937–954, 2010.
- [6] P. Vinsome, “Orthomin, an Iterative Method for Solving Sparse Sets of Simultaneous Linear Equations,” in *4th Symposium of Numerical Simulation of Reservoir performance, 19-20 February*, (Los Angeles, California), Society of Petroleum Engineers, 1976.
- [7] J. Appleyard and I. Cheshire, “Nested Factorization,” in *SPE Reservoir Simulation Symposium, 15-18 November*, (San Francisco, California), Society of Petroleum Engineers, 1983.
- [8] S. Talukdar and R. Instefjord, “Reservoir Management of the Gullfaks Main Field,” *SPE Europec/EAGE Conference and Exhibition, Rome, Italy*, no. June 2008, pp. 9–12, 2008.
- [9] L. Feng, C. Xuejun, and Z. Fangde, “The Measurement of Crude Oil/Natural Gas/Water Flow Rates by Using Microwave Technique,” in *SPE Annual Technical Conference and Exhibition, 23-26 September*, (New Orleans, Louisiana), Society of Petroleum Engineers, 1990.